FINAL TECHNICAL REPORT

Discovering Blind Geothermal Systems in the Great Basin Region: An Integrated Geologic and Geophysical Approach for Establishing Geothermal Play Fairways: All Phases

Authors: James E. Faulds[1], Nicholas H. Hinz[1], Mark Coolbaugh[1-2], Bridget Ayling[1], Jonathan Glen[4], Jason W. Craig[1], Emma McConville[1], Drew Siler[4-7], John Queen[5], Jeff Witter[8], and Christian Hardwick[3]

Recipient: Board of Regents on behalf of the University of Nevada, Reno

Award Number: DE-EE0006731

Principal Investigator: James E. Faulds, Nevada Bureau of Mines and Geology, University of Nevada, Reno

Project Partners: *Cost-sharing partners

- [1*]Nevada Bureau of Mines and Geology, University of Nevada, Reno (James Faulds-PI, Nick Hinz, Bridget Ayling, Eli Mlawsky, Andrew Sadowski, Alan Ramelli; M.S. Students—Emma McConville and Jason Craig; undergraduate Jade Bourdeau-Hernikl)
- [2]ATLAS Geosciences, Inc. (Drs. Lisa Shevenell and Mark Coolbaugh) – Phases 1 and 2
- [3]Utah Geological Survey (Christian Hardwick, Mark Gwynn, and Rick Allis) – Phase 2
- [4]U.S. Geological Survey (Drs. Jonathan Glen and Drew Siler) – Phases 2 and 3
- [5]Hi-Q Geophysical, Inc. (Dr. John Queen) – Phases 1 and 2
- [6]Zonge International, Inc. (Chet Lide) – Phase 2
- [7]Lawrence Berkeley National Laboratory (Drs. Drew Siler, Nic Spycher) – Phases 1 and 2
- [8]Innovative Geoscience (Dr. Jeff Witter) – Phase 3

Project Period: October 1, 2014 to September 30, 2019.

DOE Project Team: Contracting Officer – Laura Merrick; Project Officer – Michael Weathers
Project Monitor – Angel Nieto

McGinness Hills Geothermal Power Plant (~150 MWe), Central Nevada:
Blind System Providing Key Motivation for Play Fairway Analysis

ACKNOWLEDGMENTS AND DISCLAIMER

Acknowledgment: This material is based upon work supported by the Department of Energy, Office of Energy Efficiency and Renewable Energy (EERE), Geothermal Technologies Offices, under Award Number DE-EE0006731. Reviews by Margaret Avery and Anthony Pivarunas improved this report.

TABLE OF CONTENTS

EXECUTIVE SUMMARY

Most geothermal resources in the Great Basin region of the Western USA are blind, meaning that they have no surface hot springs or steam vents. This makes it difficult to discover new commercial-grade systems. Finding these blind systems requires synthesis of an array of favorable geothermal characteristics. This multi-parameter integration approach to identify areas with high geothermal potential is the geothermal play fairway concept. This project integrated multiple datasets to apply the play fairway concept to a large region of the Great Basin in Nevada. It is therefore referred to as the Nevada play fairway project. This project was a strong collaborative effort between several organizations, led by the Nevada Bureau of Mines and Geology at the University of Nevada, Reno, with key support from the U.S. Geological Survey, ATLAS Geosciences, Inc., Hi-Q Geophysical, Inc., Lawrence Berkeley National Laboratory, Utah Geological Survey, and Innovative Geothermal Ltd.

In Phase 1 of this project, available data for nine geologic, geochemical, and geophysical parameters were synthesized to produce a new detailed geothermal potential map of 96,000 km^2 from west-central to eastern Nevada (Figure 1). These parameters were grouped into subsets and individually weighted (Figure 2) to delineate rankings for local permeability, intermediate permeability, regional permeability, and thermal potential, which collectively defined geothermal play fairways. The fairways correspond to the most likely locations for significant geothermal fluid flow. This initial work was aimed at reducing the risks in regional exploration and therefore facilitating discovery of new commercial-grade systems in blind settings, as well as in areas with surface expressions of geothermal activity.

Phase 2 of the project involved detailed analysis of some of the promising areas identified in Phase 1. Twenty-four highly prospective areas, including both known undeveloped systems and previously undiscovered potential blind systems, were identified for further analysis (Figures 3 and 4). After general reviews and field reconnaissance of these areas, five of the most promising sites were selected for detailed studies. Multiple techniques were employed in the detailed studies, including geologic mapping, shallow temperature surveys, gravity surveys, LIDAR, geochemical studies, seismic reflection analysis, and 3D modeling. The goal of the detailed studies was to identify specific areas with the highest likelihood for high permeability and thermal fluids, such that drill sites could be selected. Three main sets of predictive maps were generated for each detailed study area: 1) play fairway maps, 2) play fairway error maps, and 3) direct evidence maps. Local- and intermediate-scale permeability models were revised to reflect results of the detailed geologic, geophysical, and geochemical analyses.

Phase 3 of the project involved more detailed analyses and temperature-gradient (TG) drilling in southeastern Gabbs Valley and northern Granite Springs Valley (Figure 4), deemed the two most promising sites, with the goal of providing preliminary validation of the play fairway methodology. In southeastern Gabbs Valley, the collocation of a favorable structural setting (displacement transfer zone and fault intersections), Quaternary faults, intersecting and terminating gravity gradients, magnetic low, shallow (2 m) temperature anomaly, low resistivity anomaly, and promising geothermometry from nearby water wells provided evidence for a blind system. Drilling of six TG holes defined an apparent geothermal system at this locality with temperatures as high as 124°C at 152 m. This system is blind, with no surface hot springs, fumaroles, or paleo-geothermal deposits. For northern Granite Springs Valley, a favorable structural setting (termination of a major Quaternary normal fault), terminating gravity gradient, magnetic gradient, newly discovered sinter deposits, nearby warm water wells, previously drilled TG holes in the vicinity, and promising geothermometry suggest a hidden system. Drilling of six new TG holes yielded temperatures of ~96°C at ~250 m, suggesting the presence of a geothermal system.

Major lessons learned in the course of this project include: 1) initially identified sites commonly include multiple favorable structural settings at a finer scale; 2) promising sites in Cenozoic basins cannot be well-defined without detailed geophysical surveys; and 3) play fairway analysis should be refined as the exploration program vectors into the most promising sites and more detailed studies are conducted. In addition to producing copious amounts of data, this project resulted in 18 published papers, 10 abstracts, more than 45 presentations across the U.S. and abroad (including several keynote addresses), 2 Masters theses, and 9 media reports.

INTRODUCTION

Geothermal *play fairway analysis* is a concept adopted from the oil industry (e.g., Doust, 2010) aimed at reducing the risks in geothermal exploration and drilling. The geothermal play fairway concept involves integration of multiple parameters indicative of geothermal activity to identify potential areas for new development (e.g., Faulds et al., 2016a,b, 2018; Shervais et al., 2016; Forson et al., 2016; Lautze et al., 2017; Siler et al., 2017; Wannamaker et al., 2017). This includes evaluation of the favorability of known, undeveloped geothermal systems, as well as assessing the probability of a particular area for hosting a blind relatively high-temperature (>130ºC) system capable of generating electricity. Blind systems have no surface manifestations of geothermal activity, such as hot springs or steam vents (e.g., Richards and Blackwell, 2002). In this project, we have applied the play fairway methodology to 96,000 km^2 of the Great Basin region of Nevada, which encompasses an active extensional to transtensional setting within western North America (Figure 1).

The Great Basin region of Nevada and adjacent parts of neighboring states is a world-class geothermal province with nearly 1 GW of current installed capacity at power plants at ~28 geothermal systems. Although geothermal production has been trending slowly upward in recent years, all studies indicate far greater potential (30 GW) for conventional hydrothermal systems in the region (e.g. Williams et al., 2007, 2009; U.S. DOE GeoVision Report, 2019). The Great Basin lies within the Basin and Range province of western North America, a broad region of crustal extension that has been active since the Miocene (~20 to 12 million years ago). The geothermal wealth of this region can be attributed to its active extensional to transtensional setting, including the diffusion of ~20% of the Pacific-North American dextral plate motion (~1 cm/year) along the Walker Lane into extension (Blewitt et al., 2003, 2005; Faulds et al., 2004; Faulds and Henry, 2008). Accordingly, strain rates increase to the northwest across Nevada from much less than 1 mm/year near the Utah border to ~1 cm/year in the Walker Lane belt (Kreemer et al., 2012).

Most geothermal systems (>85%) in the Great Basin region, especially the relatively high-temperature systems (>130ºC), reside in four discrete types of fault interaction zones: 1) step-overs or relay ramps between overlapping normal faults; 2) horse-tailing normal fault tips or terminations, 3) fault intersections, and 4) accommodation zones, whereby oppositely dipping normal fault systems intermesh with multiple fault terminations and intersections (Curewitz and Karson, 1997; Faulds et al., 2006, 2011; Faulds and Hinz, 2015). In the transtensional western part of the Great Basin region, pull-aparts and displacement transfer zones, involving the termination of individual strike-slip faults in arrays of normal faults, also host many geothermal systems. These fault interaction zones typically contain higher densities of faults and fractures, which enhance permeability and thus provide conduits for geothermal fluids. The main segments of major normal faults are generally not conducive to geothermal activity due to periodic release of stress in major earthquakes and thick zones of gouge that inhibit permeability. Notably, most geothermal systems in the region are amagmatic and lack middle to upper crustal magma chambers as a heat source. Heat is generally provided by a high geothermal gradient associated with active regional extension and crustal thinning. It is also noteworthy that most geothermal systems in this region, especially the higher temperature systems (>130°C), are associated with normal fault systems active in the Quaternary (Bell and Ramelli, 2007, 2009).

Because most geothermal systems in the Great Basin are controlled by Quaternary normal faults, they generally reside near the margins of basins. Consequently, upwelling fluids along the faults commonly flow into permeable sediments in the subsurface and do not emanate directly along the fault. Outflow from these upwellings may therefore surface many kilometers away from the deeper source or remain entirely "blind" or hidden with no surface hot springs or steam vents (Richards and Blackwell, 2002; Coolbaugh et al., 2007). Impermeable clay caps may also develop in some systems and inhibit or preclude development of surface manifestations. Blind systems probably comprise more than 75% of the geothermal resources in this region (Coolbaugh et al., 2007), but only 40% of the known systems across the region are blind (Faulds and Hinz, 2015). Notably, most of these blind systems were discovered accidentally through drilling for agricultural wells or mineral exploration.

Thus, techniques are needed both to identify favorable structural settings that enhance permeability and to determine which areas may currently channel hydrothermal fluids, particularly since not all favorable

settings will host a viable geothermal system. The recent discovery in central Nevada of the robust geothermal system at McGinness Hills (Nordquist and Delwiche, 2013), a blind field that currently produces ~150 MW, suggests that many systems are yet to be discovered in the region. Application of play fairway methodologies can therefore significantly reduce the risks in geothermal exploration and development.

In this report, we describe the results of each phase of the Nevada play fairway project, which culminated in successful drilling of TG holes at two sites. Summaries are presented for the first two phases (or budget periods), with more detailed accounts provided in the original reports for Phases 1 and 2 (Faulds et al., 2015b, 2017b). A detailed description of the recently completed Phase 3 is then provided, including thorough accounts of individual tasks and milestones. Brief descriptions of lessons learned from this project and recommendations for future research are also provided toward the end of this report. A final section includes lists of publications, presentations, student theses, and media reports from this project.

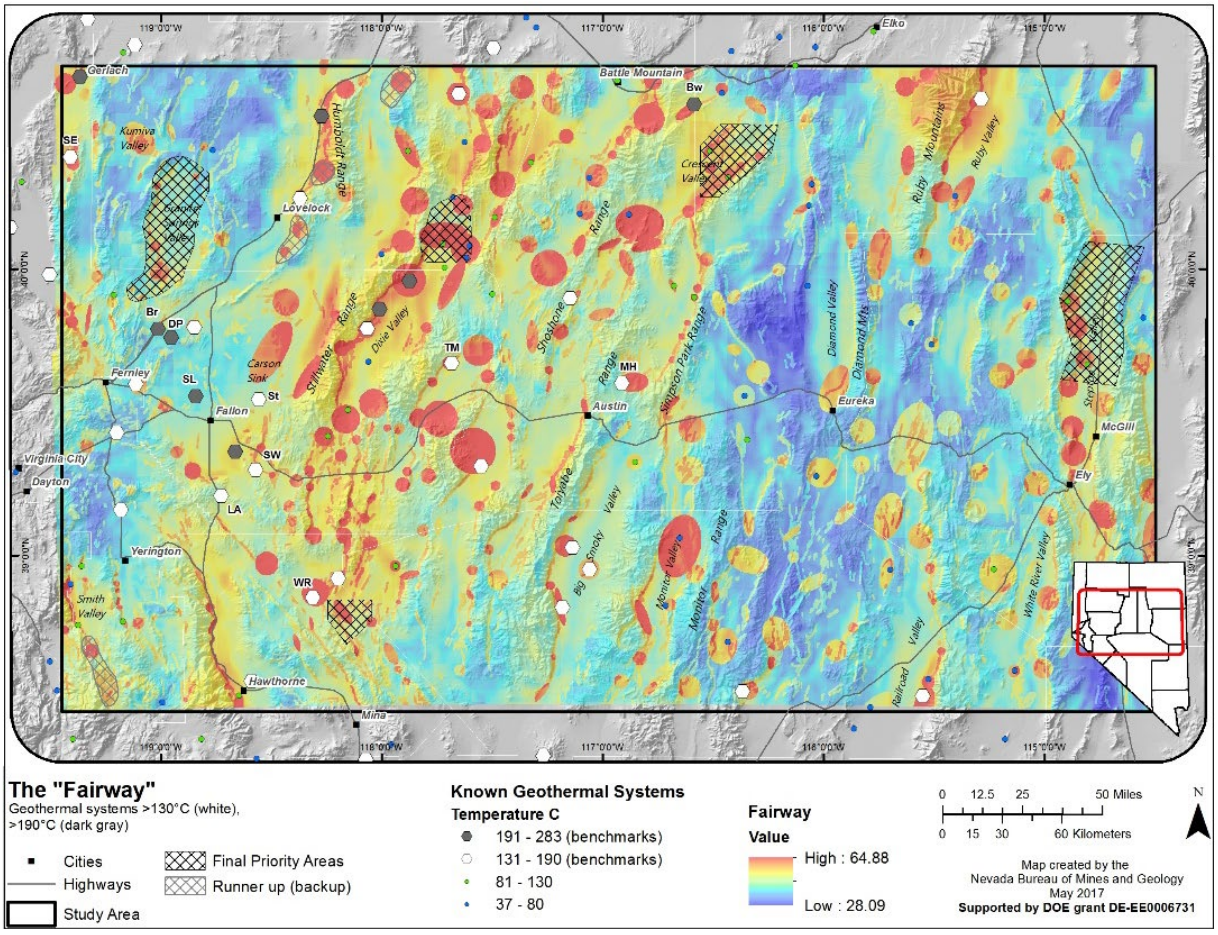

Figure 1. Geothermal play fairway map produced during Phase 1 of the Nevada play fairway project. Final down-select areas for detailed studies in Phase 2 shown by black hachures. Runner-up areas are shown by light gray hachures. From west to east across the northern tier, detailed study areas are Granite Springs Valley, Sou Hills, Crescent Valley, and Steptoe Valley. The lone area in the southern part is southeastern Gabbs Valley. From north to south, runner-up areas are Dun Glen, Lovelock Meadows, southern west flank of the Humboldt Range, and Wellington.

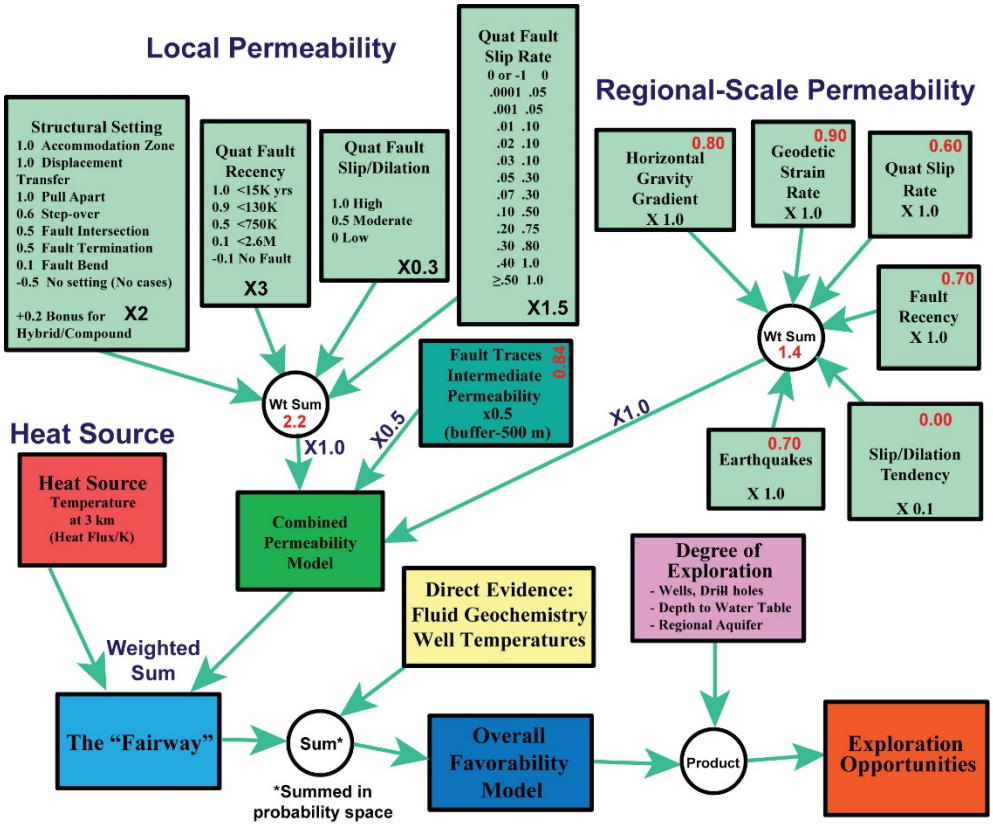

Figure 2. Nevada play fairway modeling workflow (Faulds et al., 2016). Red numbers indicate relative weights determined from weights of evidence. Black numbers indicate expert driven weights used in the analysis. In all cases, the expert driven weights took into account the statistical analyses.

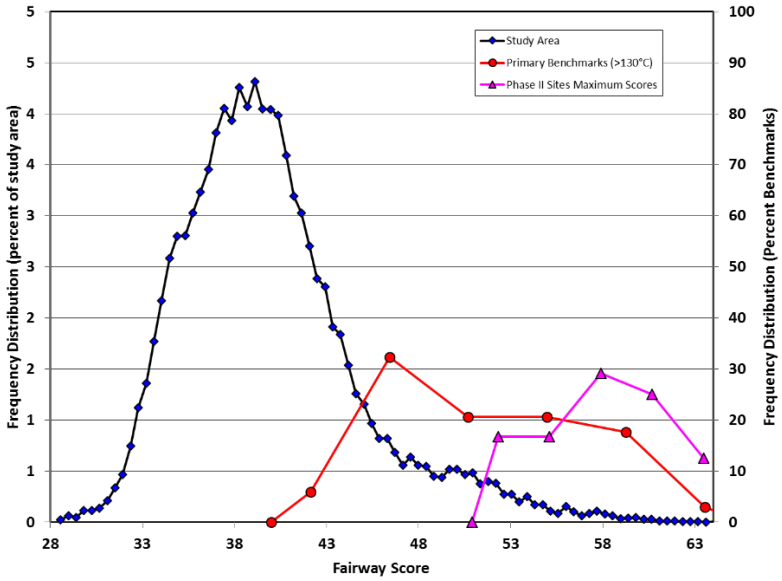

Figure 3. Distribution of play fairway scores for the primary benchmark (>130°C) systems (red) compared to scores for the study area as a whole (blue) and the maximum values within the 24 highly prospective sites selected for analysis in Phase 2 (purple) (Faulds et al., 2016).

NEVADA PLAY FAIRWAY PROJECT

The Nevada geothermal play fairway project utilized a phased approach, with three distinct phases funded under this U.S. Department of Energy, Geothermal Technologies Office award. Our primary goals in this project were to expedite the geothermal exploration process, facilitate discovery of new commercial-grade systems (>130ºC), and reduce the risks in geothermal exploration and development. The first phase involved development of the play fairway methodology and production of a regional-scale geothermal potential map of 96,000 km^2 from west-central to eastern Nevada (Figure 1) that synthesized nine geologic, geochemical, and geophysical parameters. These parameters were grouped into subsets and individually weighted to delineate rankings for local permeability, intermediate permeability, regional permeability, and heat (Figure 2), which collectively defined geothermal play fairways. The second phase included detailed studies of five particularly prospective areas identified in Phase I, as well as some refinement of the play fairway methodology. The third phase involved additional detailed analyses and temperature-gradient drilling at two of the most promising areas. Details of each phase are described below.

Phase 1 Summary (Budget Period 1)

Phase 1 focused on development of a statistically based geothermal potential map for 96,000 km^2 across the Great Basin region of Nevada (Figure 1; Faulds et al., 2015a,b, 2016a,b, c; Hinz et al., 2015). This study area was selected to include regional strain gradients and changes in composition of the underlying basement from primarily Mesozoic crystalline rocks (granitic and metamorphic rocks) in the west to dominantly Paleozoic carbonates and sediments overlying Proterozoic gneisses and granites in the east. In addition, there were 34 known areas with temperatures ≥130°C, and these localities served as benchmarks or training sites that guided our analysis. Due to the strong control of Quaternary faults on geothermal systems in the region (Blackwell et al., 1999; Richards and Blackwell, 2002; Bell and Ramelli, 2007; Faulds et al., 2006, 2011, 2013; Hinz et al., 2011, 2013, 2014, 2017), our approach emphasized fault-controlled geothermal play fairways. Nine parameters were incorporated into the regional geothermal potential map, including: 1) structural settings, 2) age of recent faulting, 3) slip rates on Quaternary faults, 4) regional-scale strain rates based on GPS geodesy, 5) slip and dilation tendency on Quaternary faults, 6) earthquake density, 7) gravity gradients, 8) temperature at 3 km depth, and 9) geochemistry from springs and wells.

As described extensively in the Phase 1 Report and other contributions (Faulds et al., 2015b, 2016a), these parameters were grouped into key subsets to define regional permeability, intermediate-scale permeability, local permeability, and regional heat, which collectively defined the geothermal play fairway (i.e., most likely locations for significant geothermal fluid flow; Figure 2). A major challenge was the determination of optimal weights for individual data types to best predict permeability and overall geothermal potential. Spatial statistical methods were combined with an expert-guided fuzzy logic scheme to determine the hierarchal weights of each parameter. The statistical methods included logistic regression and Bayesian weights-of-evidence, utilizing 34 benchmarks of known relatively high-temperature (>130ºC) geothermal systems in the region. Analyses of these parameters were also coupled with a thorough review of the degree of previous exploration, thus permitting identification of under-explored regions that are potentially ripe for development. Consequently, the fairway model was integrated with direct evidence of heat from wells and geothermometers to delineate favorability for geothermal development. Many sites in the broad study area yielded high play fairway values. Results compared favorably against the group of 34 benchmark sites, representing systems in the region with temperatures ≥130ºC (Figure 3). Fairway values range from a low of ~28 to near 65 (not normalized), with the 34 high-temperature (≥130ºC) benchmarks yielding an average of 51.4.

All major tasks (Tasks 1 through 12) and milestones for Phase 1 (BP1; Table 1) were completed on schedule. As described in detail in Faulds et al. (2015b), major tasks (Tasks 1 through 12 for the entire project) and subtasks included: 1) review and interpretation of geologic data; 2) review and interpretation of seismic reflection data; 3) review and interpretation of gravity data; 4) review and interpretation of

magnetotelluric data; 5) review and interpretation of seismologic data; 6) review and interpretation of geochemical data; 7) review and interpretation of geodetic data; 8) GIS database compilation; 9) preliminary modeling; 10) database management; 11) identify and characterize structural settings; 12) slip and dilation tendency analysis; 13) 3D geologic modeling of selected basins; 14) quantitative ranking of blind geothermal potential; 15) complete geothermal potential maps of study area; 16) identify data needs for Phase 2; and 17) final reporting and project review.

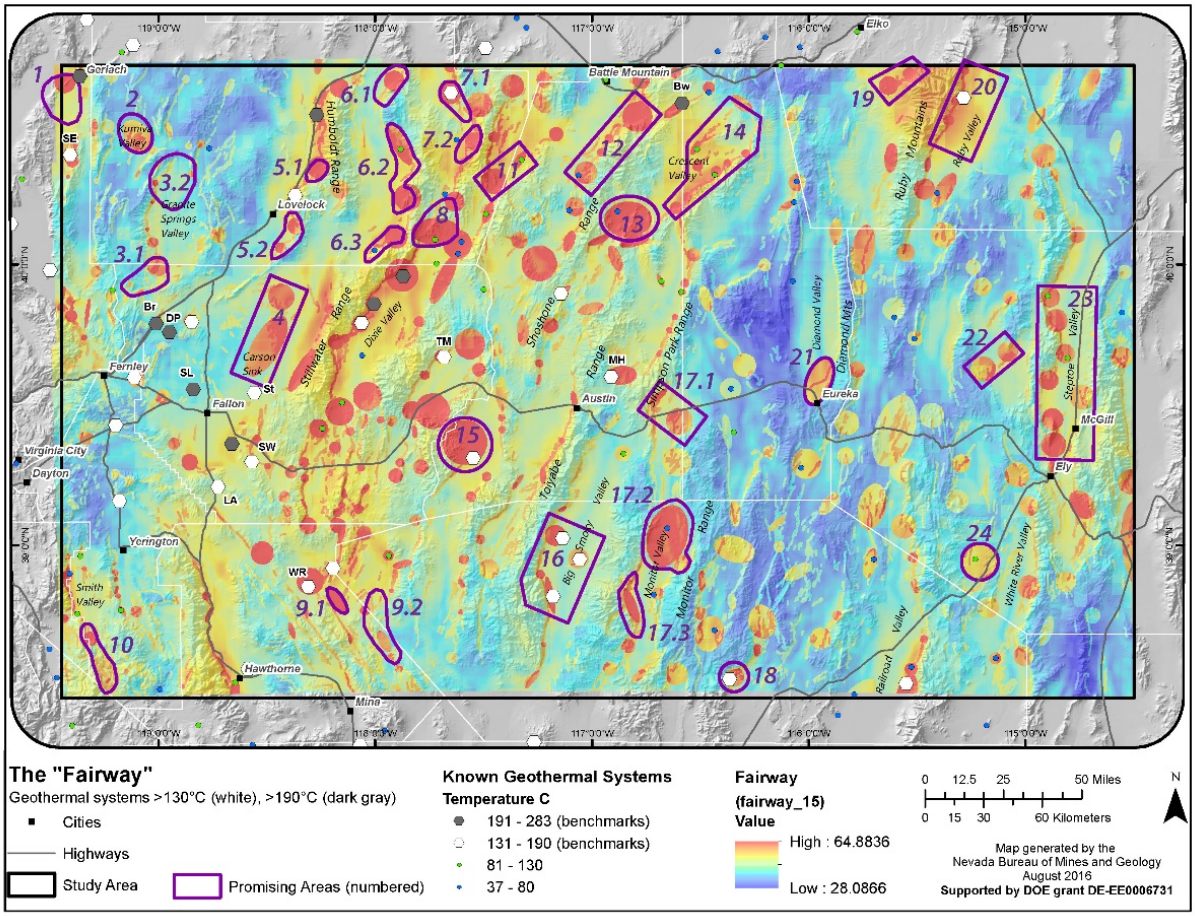

Figure 4: Highly prospective areas (purple polygons) selected for analysis in Phase 2. Numbers adjacent to the polygons refer to the following highly prospective sites: 1) northern Fox Range, 2) Kumiva Valley, 3) Granite Springs Valley with southern (3.1) and northern (3.2) portions, 4) north Carson Sink, 5) Humboldt Range-west flank, with Lovelock Meadows (5.1) and southern flank (5.2), 6) east Buena Vista Valley, with Dun Glen (6.1), Kyle Hot Springs (6.2), and New York Canyon (6.3) subareas, 7) Grass and Pleasant Valleys, with Leach Hot Springs (7.1) and Mt. Tobin (7.2) portions, 8) Sou Hills, 9) Gabbs Valley, with south Gabbs Valley (9.1) and Cedar Mountain (9.2) subareas, 10) Wellington, 11) south Buffalo Valley, 12) north Reese River Valley, 13) north Carico Valley, 14) Crescent Valley, 15) Peterson Hot Springs, 16) Big Smoky Valley, 17) Monitor Valley with north Monitor Valley (17.1), Diana's Punchbowl (17.2), and Pine Creek (17.3), 18) Hot Creek Ranch, 19) Starr Valley, 20) Ruby Valley, 21) south Diamond Valley, 22) Butte Valley, 23) Steptoe Valley, and 24) Williams Hot Springs. After an initial analysis and down-selection, five areas were chosen for detailed studies (3, 8, 9.1, 14, and 23). Abbreviations for other geothermal systems: Br, Bradys; Bw, Beowawe; DP, Desert Peak; DV, Dixie Valley; LA, Lee-Allen; MH, McGinness Hills; RV, Ruby Valley; SE, San Emidio; SL, Soda Lake; St, Stillwater; SW, Salt Wells; TM, Tungsten Mountain; WR, Wild Rose (Don Campbell).

Table 1. Milestone Summary for Budget Period 1

Recipient Name: Nevada Bureau of Mines and Geology, University of Nevada, Reno

Project Title: Discovering Blind Geothermal Systems in the Great Basin Region: An Integrated Geologic and Geophysical Approach for Establishing Geothermal Play Fairways

Task #	Task Title or Subtask Title	Milestone or Go/No Go Pt	Milestone # or Go/No-Go Pt #	Milestone Description and Decision Criteria	Milestone Verification Process	Ant. Mo.	Anticipated Qtr	Actual Qtr
1	Review and Interpretation of Geologic Data	Milestone	M1.1	Compilation of geologic maps	Maps will include lithologic data and structural data including faults and folds	3	Q1	Q3
2.1	Review and Interpretation of Seismic Reflection Data	Milestone	M2.1.1	Obtain reflection profiles from Seismic Exchange, Inc.	Purchased profiles will be submitted to NGDS	3	Q1	Q2
2.1	"	Milestone	M2.1.2	Analysis of seismic reflection profiles	Interpretation of seismic reflection profiles for 3D modeling in Task 8 and general characterization of seismic indicators of favorable structural settings	9	Q3	Q4
2.1	"	Milestone	M2.1.3	Characterization of seismic reflection indicators of favorable structural settings	List of characteristics of seismic reflection indicators of favorable structural settings	9	Q3	Q4
2.2	Review and Interpretation of Gravity Data	Milestone	M2.2.1	Compilation and analysis gravity of anomaly maps	Maps showing gravity data for Great Basin study area	3	Q1	Q2
2.2	"	Milestone	M2.2.2	Analysis of gravity data	Maps showing interpreted gravity data with inferred faults	9	Q3	Q3
2.2	"	Milestone	M2.2.3	Identify gravity signatures for favorable structural settings	List of gravity anomaly indicators of favorable structural settings	9	Q3	Q3
2.3	Review & Interpretation of Magnetotelluric Data	Milestone	M2.3.1	Compilation of MT data	MT data maps for select parts of the Great Basin study area	3	Q1	Q2
2.3	"	Milestone	M2.3.2	Analysis of MT data	Interpreted MT data and list of characteristics of MT signatures for known systems	9	Q3	Q3
2.4	Review & Interpretation of Seismologic Data	Milestone	M2.4.1	Analysis of spatial distribution of earthquakes	Maps showing earthquake distribution relative to structural setting and known geothermal systems	3	Q1	Q2
2.4	"	Milestone	M2.4.2	Characterization of seismologic character of known geothermal areas	Establish seismologic signature of known geothermal systems	6	Q2	Q3
3	Review and Interpretation of Geochemical Data	Milestone	M3.1	Compilation of geochemical data	Maps showing geochemical data for Great Basin study area	3	Q1	Q1
3	"	Milestone	M3.2	Analysis of geochemical data	Characterization of geochemical signatures of known geothermal systems and evaluate against the rest of the data for additional anomalies	6	Q2	Q2
4	Review and Interpretation of Geodetic Data	Milestone	M4.1	Compilation of geodetic data	Maps showing geodetic strain for Great Basin study area	3	Q1	Q1
4	"	Milestone	M4.2	Analysis of geodetic data	Produce list of geodetic indicators of known geothermal systems	6	Q2	Q3
4	"	Milestone	M4.3	Produce strain maps	Produce velocity gradient and strain rate maps with estimates of slip rates and styles for active faults	10	Q4	Q4
5.1	GIS Database Compilation	Milestone	M5.1	Compilation of all data into ArcGIS	Produce well organized ArcGIS data sets for study area	6	Q2	Q2/Q4
5.2	Preliminary Modeling	Milestone	M5.2	Prepare preliminary predictive model of geothermal potential	Map showing preliminary geothermal potential and data gaps	6	Q2	Q3
5.3	Database Management	Milestone	M5.3	Finalize assembled data sets at end of each quarter	Submit assembled data sets to DOE-GDR and NGDS	3, 6, 9, 12	Q1, 2, 3, 4	Q4
6	Identify and Characterize Structural Settings	Milestone	M6.1	Complete analysis of structural framework	Maps showing structures that may host blind geothermal systems	8	Q3	Q3
7	Slip and Dilation Tendency Analysis	Milestone	M7.1	Complete slip and dilation tendency analyses	Map showing slip-dilation tendency of faults for Great Basin study area	8	Q3	Q3
7	"	Milestone	M7.2	Conduct 3D slip and dilation tendency analysis for Carson Sink and Steptoe basins	Model showing slip and dilation tendency in 3D for Carson Sink and Steptoe basins	11	Q4	Q4
8	3D Geologic Modeling of Selected Basins	Milestone	M8.1	Construct 3D models of two basins	3D models constructed from geologic map data, seismic reflection profiles, and gravity data	12	Q4	Q4
9	Quantitative Ranking of Blind Geothermal Potential	Milestone	M9.1	Final rankings table and predictive maps	Database containing rankings and preliminary maps contouring geothermal potential	12	Q4	Q4
10	Complete Geothermal Potential Maps of Study Areas	Milestone	M10.1	Final geothermal potential maps	Final prediction of known and potential blind geothermal systems	12	Q4	Q4
11	Identify Data Needs for Phase II	Milestone	M11.1	Robust data sets indicating high potential, comparison with developed areas	Selection of most prospective areas for undiscovered blind geothermal systems for further study	12	Q4	Q4
12	Final Reporting and Project Review	Milestone	M12.1	Synthesis of project	Submittal of report and databases	12	Q4	Q4

Phase 2 Summary (Budget Period 2)

Phase 2 of the project focused on detailed studies of five promising areas (Faulds et al., 2017a, b). Multiple techniques, including detailed geologic mapping, Quaternary fault analysis, shallow temperature surveys, detailed gravity surveys, LIDAR in three areas, geochemical analysis of water samples, seismic reflection analysis (where available), slip and dilation tendency analysis of Quaternary faults, and 3D modeling, were employed in the detailed studies. The goal of the detailed studies was to identify specific areas with the highest likelihood for high permeability and thermal fluids, such that individual drill sites could be selected. Due to the geothermal wealth of this region, there were dozens of areas that yielded high fairway values. Thus, a major challenge in the early stages of Phase 2 was determining which areas to down-select for detailed studies. We initially chose 24 of the most promising sites for general assessment based on the play fairway values, land status, and proximity to an established electrical transmission corridor (Figure 4). We then down-selected to five sites for detailed studies through a semi-quantitative

analysis involving consideration of 1) available geological, geochemical, and geophysical data, 2) new shallow temperature and geochemical data collected in this study, 3) land status including % of area considered primary sage grouse habitat (a threatened bird species), 4) distance from an electrical transmission corridor, and 5) degree of previous exploration (Figure 5).

Due to the abundance of favorable sites in the region, we elected to include in our final selections broad geographical distribution that incorporated variations in tectonic setting (transtensional vs. extensional), strain rates, composition of basement rocks, and types of favorable structural settings. Thus, the five detailed study areas essentially span the entire region. From west to east, areas chosen for detailed study were Granite Springs Valley, southeastern Gabbs Valley, Sou Hills, Crescent Valley, and Steptoe Valley (Figure 1). The Gabbs Valley study area occupies a displacement transfer zone in west-central Nevada in a region of relatively high strain at the transition between the Walker Lane dextral shear zone (cf., Stewart, 1988; Faulds and Henry, 2008) and extensional Basin and Range province. The Walker Lane accommodates ~20% of the dextral motion between the Pacific and North American plates (e.g., Hammond et al., 2009). In contrast, Steptoe Valley lies 250 km to the east in eastern Nevada in an area of relatively low extensional strain.

As we examined each area more carefully, we found that all contain several finer-scale, favorable structural settings and thus multiple potential geothermal targets. This required a revision of the play fairway analysis within each study area to select the most highly prospective targets for drilling (Faulds et al., 2017a,b, 2018; Craig, 2018; McConville, 2018). This process permitted vectoring into the more promising locations for geothermal activity within individual areas.

All major tasks (Tasks 13 to 24) and milestones for Phase 2 (BP2; Table 2) were completed on schedule with no major variances. As described in detail in Faulds et al. (2017b), major tasks included: 1) down select for final sites for detailed study; 2) geologic studies of detailed study areas; 3) geochemical investigations; 4) shallow temperature surveys; 5) LIDAR surveys; 6) gravity surveys; 7) seismic reflection analysis; 8) slip and dilation tendency analysis; 9) 3D modeling; 10) thermal modeling of one site; 11) selection of drilling targets for Phase 3 (BP3); and 12) project reporting and project review.

Results of the detailed analyses of the five study areas are summarized below (from west to east), including application of the play fairway analysis developed in Phase 1 to the detailed study areas. Results are compared with those obtained in the more regional analysis in Phase 1, with adjustments made to the play fairway regimen to account for the more comprehensive and detailed nature of the data sets.

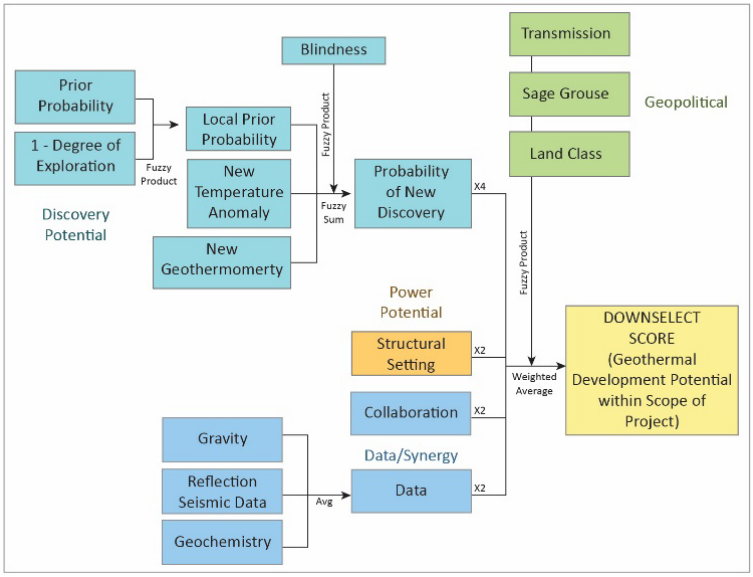

Figure 5: Flow chart showing down-selection process for selecting Phase 2 detailed study areas from prospective areas identified in Phase 1. Collaboration refers to potential for industry collaboration. Transmission relates to proximity (within ~20 km) of existing transmission corridors. Sage grouse refers to presence of sensitive habitat for a native bird species.

Table 2. Milestone Summary for Budget Period 2								
Recipient Name:	Nevada Bureau of Mines and Geology, University of Nevada, Reno							
Project Title:	Discovering Blind Geothermal Systems in the Great Basin Region: An Integrated Geologic and Geophysical Approach for Establishing Geothermal Play Fairways							
Task #	Task Title or Subtask Title	Milestone or Go/No Go Pt	Milestone # or Go/No-Go Pt #	Milestone Description and Decision Criteria	Milestone Verification Process	Ant. Mo.	Ant. Qtr	Comp. Qtr
13	Down Select to Final Sites for Detailed Study	Milestone	M13.1	Compilation of geological and geophysical data	GIS databases of available geologic maps and geophysical data sets	5	Q2	Q2
13	"	Milestone	M13.2	Select 3-5 sites for detailed studies	List of 3-5 most promising sites	5	Q2	Q2
14	Geologic Studies	Milestone	M14.1	Compilation of all available and new data	GIS databases of 3-5 sites including preexisting and new data	12	Q4	Q5
14	"	Milestone	M14.2	Detailed geologic maps	Detailed digital geologic maps showing bedrock and Quaternary units, as well as faults	15	Q5	Q6
15	Geochemical Investigations	Milestone	M15.1	Compilation of available and new geochemical data for most promising areas	GIS database of geochemical data for most promising sites	5	Q2	Q2
15	"	Milestone	M15.2	Geochemical characterization of 3-5 detaield study sites	GIS database/geochemical assessment of 3-5 detailed study areas	12	Q4	Q6
16	Shallow Temperature Surveys	Milestone	M16.1	Reconnaissance shallow-temp surveys for most promising areas	GIS database of reconnaissance shallow temperature surveys	5	Q2	Q2
16	"	Milestone	M16.2	Detailed shallow-temp surveys for 3-5 detailed study areas	GIS database of detailed shallow temperature surveys of 3-5 detailed study areas	12	Q4	Q6
17	LiDAR Surveys	Milestone	M17.1	New LiDAR acquired for some of the 3-5 detailed study sites	GIS databse of new LiDAR data for some of the 3-5 detailed study areas	9	Q3	Q5
17	"	Milestone	M17.2	Interpretations of new LiDAR data	GIS database of interpreted LiDAR and incorporation into geologic maps	13	Q5	Q6
18	Gravity Surveys	Milestone	M18.1	Compilation and analysis of available gravity data in some of the most promising areas	Maps showing gravity data for some of the most promising sites	5	Q2	Q2
18	"	Milestone	M18.2	Acquisition and processing of new gravity data in 3-5 detailed study areas	GIS database and maps showing interpreted gravity data with inferred faults	12	Q4	Q6
19	Seismic Reflection Analysis	Milestone	M19.1	Obtain reflection profiles from Seismic Exchange, Inc. for some of the detailed study areas	Amended license with Seismic Exchange, Inc., permitting interpretation of newly purchased profiles	6	Q2	Q3
19	"	Milestone	M19.2	Interpretation of seismic reflection profiles	GIS database of interpreted profiles and time to depth conversions	12	Q4	Q6
20	Slip and Dilation Tendency Analysis	Milestone	M20.1	Complete slip and dilation tendency analyses of 3-5 detailed study areas	Digital map showing slip-dilation tendency of faults for detailed study areas	13	Q5	Q6
20	"	Milestone	M20.2	Conduct 3D slip and dilation tendency analysis for those detailed study areas modeled in 3D	Model showing slip and dilation tendency in 3D for some of the detailed study areas	15	Q5	Q6
21	3D Modeling	Milestone	M21.1	Construct 3D models for some of the 3-5 detailed study sites	3D models constructed from geologic map data, seismic reflection profiles, and gravity data for some of the sites studied in detail (~3 sites)	15	Q5	Q6
22	Thermal Modeling	Milestone	M22.1	Complete thermal modeling of some of the detailed study sites in eastern Nevada	Digital thermal models of some of the detailed study sites	11	Q4	Q6
23	Selection of Drilling Targets for BP3	Milestone	M23.1	Selection of promising drilling targets for geothermal reservoirs at the 3-5 detailed study areas	Digital maps showing locations of promising drilling targets for 3-5 detailed study areas	16	Q6	Q6
24	Final Reporting and Project Review	Milestone	M24.1	Synthesis of project	Submittal of report and databases	17	Q6	Q6

Granite Springs Valley

The Granite Springs Valley study area lies in the Basin and Range province of northwestern Nevada (Figures 1 and 6). No hot springs or steam vents occur in the area. Favorable structural settings, including the terminations of a major range-front fault and a broad accommodation zone, resulted in high play fairway scores in Phase 1. Our analysis in Phase 2 involved: 1) detailed mapping of Quaternary faults and ~50 km^2 of bedrock in the eastern Truckee Range, 2) reconnaissance mapping of >200 km^2, 3) a new gravity survey totaling 415 stations, 5) acquisition of LIDAR for 215 km^2 in the southwest part of Granite Springs Valley, 6) a shallow temperature survey (55 stations), 7) interpretation of nine seismic reflection profiles (144 km), 8) slip and dilation tendency analysis, and 9) geochemical analyses of 34 water samples (Faulds et al., 2017b and appendices therein; Faulds et al., 2019).

The structural framework is dominated by a major east-dipping Quaternary normal fault (Sahwave fault), (slip rates of ~0.1-0.3 mm/yr), on the western margin of Granite Springs Valley. Granite Springs Valley is a large W-tilted, ~2-km-deep half graben in the hanging wall of the Sahwave fault, as evidenced by seismic reflection data. This fault breaks into multiple splays as it terminates in the northwest and

southwest parts of the basin. The east-dipping fault system gives way southward in the southern part of the basin to mainly west-dipping normal faults in a broad accommodation zone in the eastern Truckee Range (Figure 6E). A system of west-dipping Quaternary normal faults also extends southward from the west flank of the Seven Troughs Range and continues into the northeast part of the basin, where it terminates directly east of Adobe Flat, as evidenced by a prominent NNE-trending gravity gradient and gravity high (Figure 6D). Isolated exposures of Oligocene tuff and shallow (~100 m) Mesozoic basement (based on well data) confirms this basement high.

Geologic and geophysical data indicate six favorable structural settings conducive for geothermal activity in the study area (Figure 6D). From north to south, these include: 1) the horse-tailing northern termination of the Sahwave fault in the northwest part of the basin; 2) the southern termination of the west-dipping normal fault zone extending south from the west flank of the Seven Troughs Range into the northeast part of the basin directly east of Adobe Flat (Figures 6 and 7); 3) a major step-over in the Sahwave fault in the southwest part of the basin; 4) the horse-tailing southern end of the Sahwave fault in the southwest part of the basin; 5) the northern termination of a major west-dipping normal fault zone in the eastern Truckee Range; and 6) fault intersections along the north end of Fireball Ridge. Potential host rocks in these areas include highly fractured Mesozoic granite and Miocene volcanic rocks along and proximal to arrays of closely-spaced normal faults.

Notably, we discovered Quaternary sinter, silicified sands, and travertine deposits at the favorable setting (#2 above) directly east of Adobe Flat (Figures 6D and 7). This area also corresponds to a low-resistivity anomaly extending from shallow levels (127 m) to >4 km depth (Figure 6A-C). The sinter and silicified sands suggest temperatures of >180ºC. Additionally, two hydrophreatic explosion craters are found in the horse-tailing termination of a W-dipping normal fault zone in the eastern Truckee Range (#5 favorable setting noted above). NNE-striking normal faults have the highest slip and dilation tendency. Thus, many faults in study area are well oriented for slip and dilation, including the fault splays in the Adobe Flat area.

Past geothermal exploration included widespread TG drilling (Figure 6E) in the 1970s-1980s generally to depths of <200 m. Previous exploration had focused on the north end of Fireball Ridge, the southwest part of the basin, and Adobe Flat area (Desormier, 1985; Ormat, unpublished; Hulen, 2007; Benoit, 2008). However, no comprehensive analysis of potential geothermal resources had previously been conducted in the area.

Considering the lack of hot springs and fumaroles, previously drilled wells provide the only direct evidence of geothermal activity in the area. The most focused previous work was conducted in the Fireball Ridge area, where >20 TG holes defined an ENE-trending, ~5-km-long thermal anomaly (~10-14ºF/100 ft; Desormier, 1985). Slightly elevated thermal gradients also mark the southwest part of Granite Springs Valley. However, the Adobe Flat area contains the maximum thermal anomaly in the area, as defined by several TG holes (Benoit, 2008).

Thirty-four water analyses were available, including 11 historical, 15 new gray literature sources, and 8 new samples (see Appendix B in Faulds et al., 2017b). Most of the waters in the area are cool (<25°C), although 3 shallow water wells in the northern part of the basin have reported bottom-hole temperatures between 30 and 41°C, and 3 gradient wells in this same area have bottom-hole temperatures of 63.8, 73.7 and 89.7°C (Well AV-ST-1) at 200, 260 and 550 m depth, respectively. One analysis from a water well in the Adobe Flat area has the highest geothermometer temperature (160°C from the quartz) in the study area. The high geothermal gradient (140°C/km) and geothermometry in this area together with the Quaternary sinter deposits 3 km to the north warranted further investigation. However, 2-m temperature surveys throughout the area (55 stations) did not show any significant thermal anomalies, although the extremely wet winter of 2017 may have suppressed temperatures.

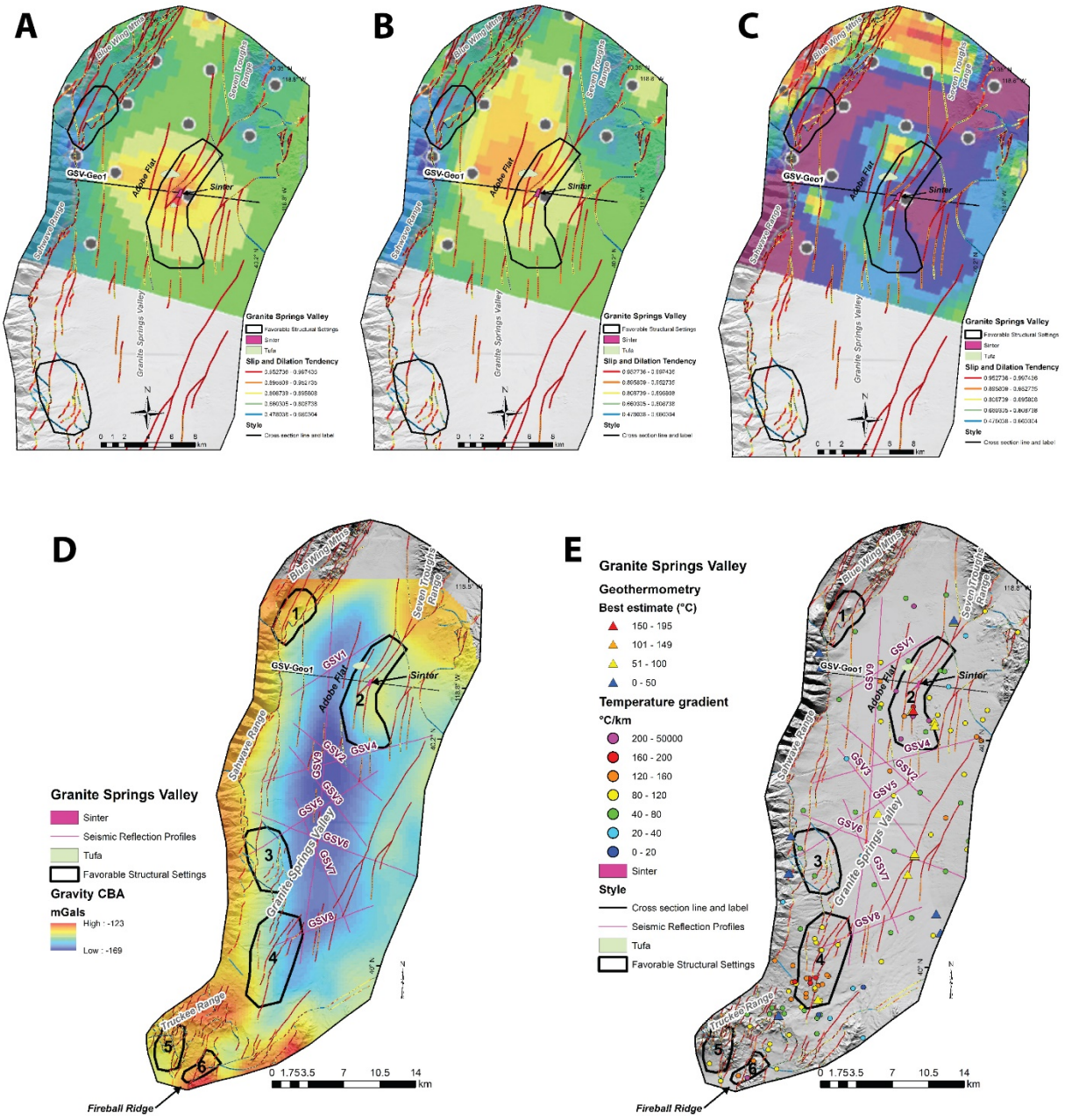

Figure 6. Granite Springs Valley study area. Favorable structural settings are outlined in black, with setting #2 the highest priority in this area. A. Slip and dilation tendency and MT data slice (Wannamaker et al., 2019) at 0.127 km; note the low resistivity co-located with the sinter deposit. B. Slip and dilation tendency with a low resistivity anomaly at 0.565 km. C. Low-resistivity anomaly at 4.77 km. D. Complete Bouguer gravity anomaly. E. TG and geothermometry data and location of seismic reflection profiles (purple lines) and geologic cross section. Cross section GSV-Geo1 shown in Figure 7.

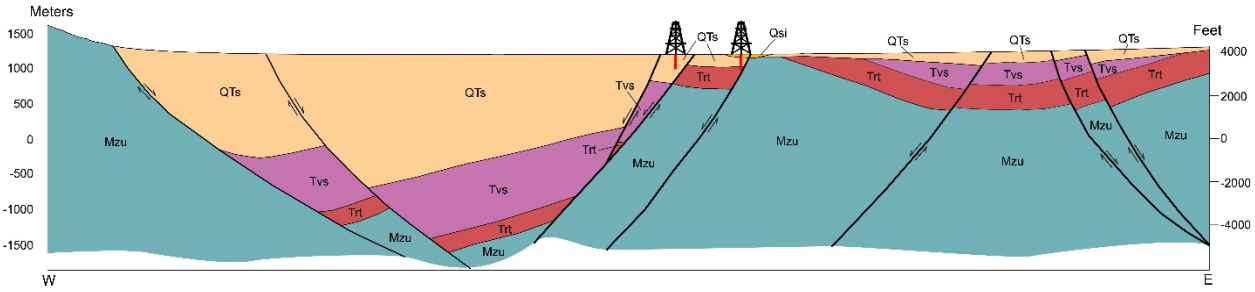

Figure 7. E-W cross section in northern Granite Springs Valley through Adobe Flat area, showing W-tilted half graben of the Granite Springs basin and W-dipping normal fault zone on the east side of basin that controls recent hydrothermal activity (sinter deposition). See Figure 6 for location (GSV-Geo-1). Derricks indicate approximate locations of TG drilling sites in Phase 3. Qsi, silica sinter; QTs-late Miocene to Quaternary basin-fill sediments; Tvs, Miocene volcanic and sedimentary rocks; Trt, Oligocene ash-flow tuffs; Mzu, Mesozoic granitic and metamorphic rocks.

Southeastern Gabbs Valley

The southeastern Gabbs Valley study area (Figures 1 and 4) is a complex structural basin situated at the intersection of a major NW-striking, Quaternary dextral fault in the Walker Lane (Petrified Springs fault) and NNE-striking Quaternary normal faults. It occupies a "displacement transfer zone", whereby the major dextral fault terminates in an array of normal faults. Some geothermal exploration had occurred in northern Gabbs Valley ~15 km north of the study area (Payne et al., 2011; Payne, 2013), but no previous exploration had taken pace in southeastern Gabbs Valley. Within the study area, there are no surface expressions (springs or fumaroles) of a geothermal system. Our analysis of the area in Phase 2 included: 1) new detailed mapping of ~180 km^2, including Quaternary fault analysis aided by partial LIDAR coverage, 2) a 2-m temperature survey (124 stations), 3) geochemical analyses of 20 water samples, and 4) a new gravity survey totaling 274 stations (Figure 8; see Faulds et al., 2017b and appendices therein; Craig et al., 2017; Craig, 2018; Faulds et al., 2018).

Geologic and geophysical data indicate five favorable structural settings (Figure 8C), including a broad displacement transfer zone, fault intersections, and one small releasing bend. Potential host rocks for a geothermal reservoir include highly fractured Cretaceous granitoids, Triassic metasedimentary rocks, and Miocene ash-flow tuffs along and proximal to faults. Slip and dilation tendency analyses indicate that NNE-striking normal faults have the highest slip and dilation tendency. Thus, many faults are well oriented for slip and dilation (Figure 8C).

Twenty water analyses were available in the study area (Faulds et al., 2017b), including historical (11), new gray literature sources (5), and new samples (4). The available geochemical data are mainly from wells, with four new analyses from irrigation wells at the Diamond A Ranch. Traditional geothermometers, a mixing model (Shevenell and Coolbaugh, 2011), and GeoT multicomponent equilibria modeling (Spycher, pers. comm., 2017) were utilized to estimate subsurface temperatures of thermal fluids from the ranch. The mixing model (Figure 9) and GeoT (Figure 10) indicate subsurface temperatures of ~140°C and 130°C, respectively.

A possible source area for the fluids sampled at the ranch was detected by the shallow temperature survey (124 stations) with thermal anomalies found in a discrete 7 km^2 area 2.7 to 6.7 km south-southeast of the ranch. Highest temperatures recorded are 32°C, averaging 5°C above background. The combination of high geothermometer temperatures from wells at the ranch and a nearby up-gradient 2-m temperature anomaly in a favorable structural setting suggest a new blind system that could be power-capable.

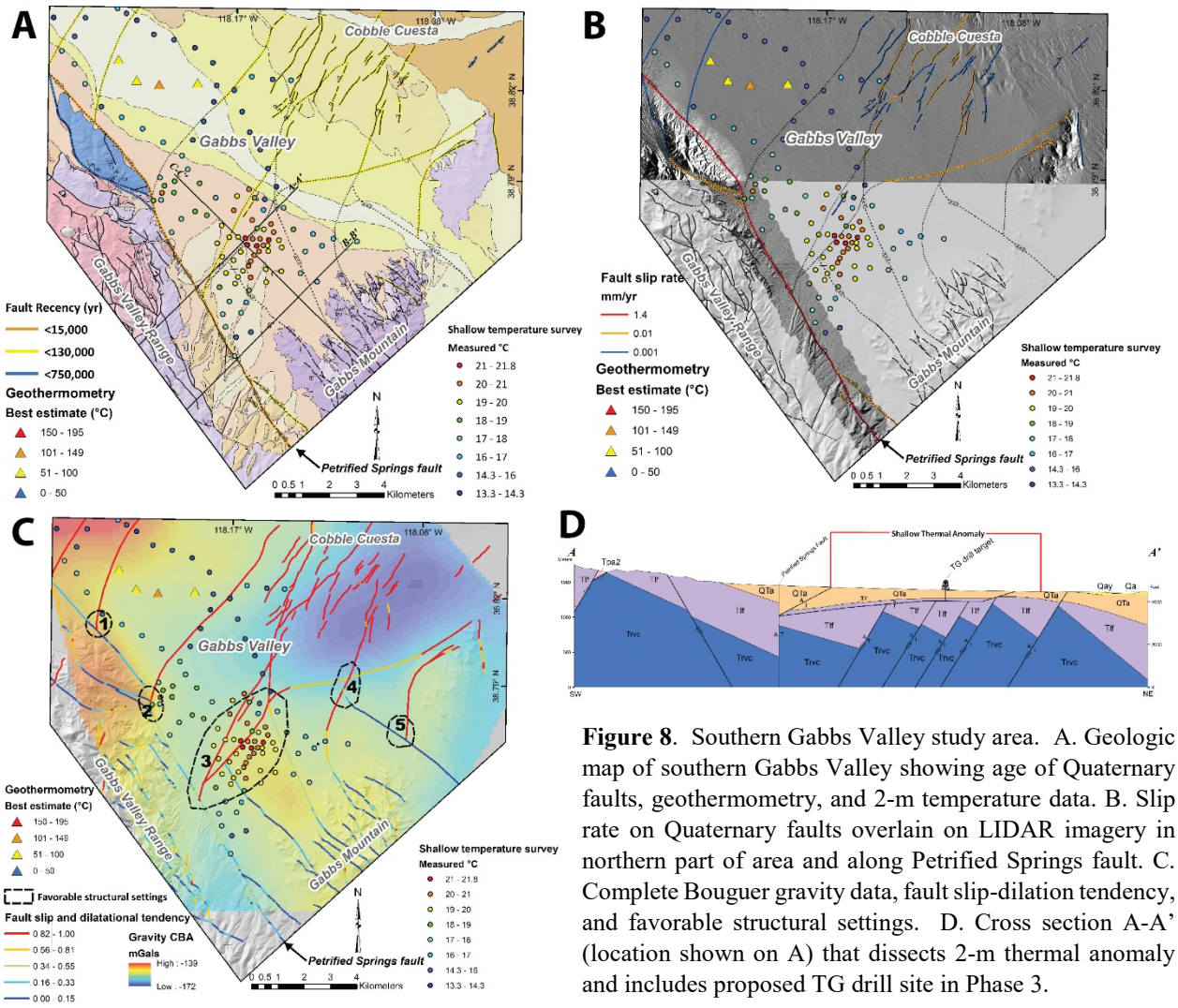

Figure 8. Southern Gabbs Valley study area. A. Geologic map of southern Gabbs Valley showing age of Quaternary faults, geothermometry, and 2-m temperature data. B. Slip rate on Quaternary faults overlain on LIDAR imagery in northern part of area and along Petrified Springs fault. C. Complete Bouguer gravity data, fault slip-dilation tendency, and favorable structural settings. D. Cross section A-A' (location shown on A) that dissects 2-m thermal anomaly and includes proposed TG drill site in Phase 3.

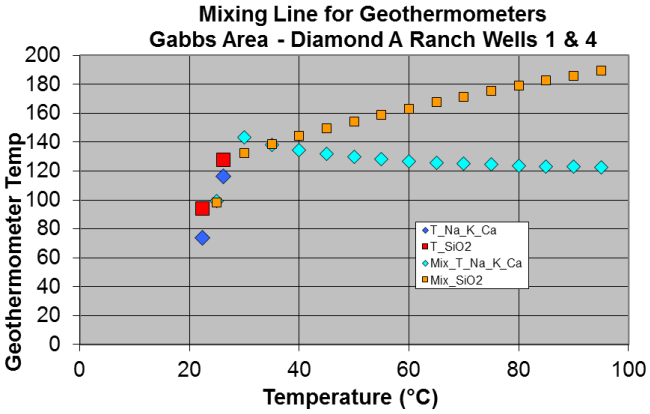

Figure 9. Mixing model (Shevenell and Coolbaugh, 2011) for wells 1 and 4 at the Diamond A Ranch in Gabbs Valley. Cross over of calculated SiO_2 and Na-K-Ca occurs at approximately 139°C.

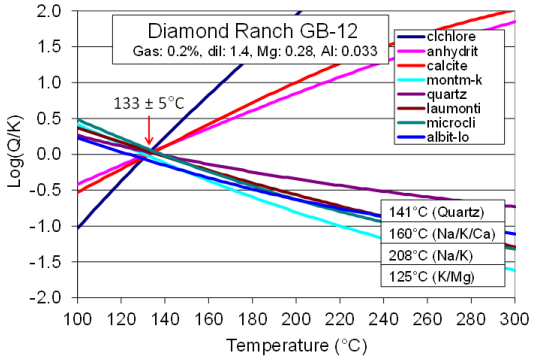

Figure 10. GeoT multicomponent chemical equilibria model results (Spycher, pers. comm., May 2017). The modeled minerals attain equilibria under the modeled conditions for Well 1 (22.4°C) at 133 ± 5°C, suggesting last temperature of equilibration near 135°C.

Sou Hills

The Sou Hills study area (Figure 1) includes the northernmost part of Dixie Valley and a series of low ridges (the Sou Hills) that form an interbasinal high between Dixie Valley on the south and Pleasant Valley on the north (Figure 11). Thermal areas occur at Seven Devils Hot Springs (57-76.7°C) and the McCoy Spring area (46°C). Our analysis of the area included: 1) new detailed mapping of ~60 km^2, 2) reconnaissance mapping of >200 km^2, 3) analysis of abundant Quaternary faults, 4) new detailed logging of 4 wells (~2,000 m) and integration of ~5,500 m of existing logs from 9 other wells, 5) a new gravity survey totaling 355 stations, 6) acquisition of 290 km^2 of LIDAR, 7) a shallow temperature survey (82 stations), 8) interpretation of 7 seismic reflection profiles, 9) slip and dilation tendency analysis, 10) geochemical analyses of 23 water samples, and 11) preliminary 3D modeling (Faulds et al., 2017b and appendices therein; Faulds et al., 2020b).

The structural framework of the Sou Hills is dominated by an accommodation zone (Fonseca, 1988) between a) the west-dipping Quaternary fault zone that bounds Pleasant Valley on the east and ruptured in 1915 in a M7.2 earthquake (Wallace, 1984), and b) the east-dipping Quaternary fault zone that bounds Dixie Valley on the west that has also experienced historic ruptures (Caskey et al., 1996). As such, the area is characterized by multiple, closely-spaced, west- and east-dipping normal faults. Seismic reflection and gravity data indicate an extensional anticline in northernmost Dixie Valley directly south of the Sou Hills (Figures 11 and 12; Faulds et al., 2020b). The anticline marks a zone of multiple intersecting, oppositely dipping normal faults. Quaternary faults in the Sou Hills have ruptured in the past 15 to 130 ka and have slip rates ranging from 0.01 to 0.3 mm/yr.

The geologic and geophysical data indicate five discrete, favorable structural settings for geothermal activity in the Sou Hills area (Figure 11B; Faulds et al., 2020b). From north to south, these include: 1) a broad ~5 km wide step-over in the west-dipping Pleasant Valley fault zone between the Sou Hills and Tobin Range; 2) a narrow ~1 km wide, step-over and relay ramp along a southern strand of the Pleasant Valley fault zone; 3) a small graben between oppositely dipping normal faults in the western part of the Sou Hills; 4) a major fault intersection between the east-dipping Dixie Valley range-front fault and an oblique-slip east-striking fault bounding the Sou Hills on the south; and 5) the extensional anticline in northernmost Dixie Valley. NNE-striking normal faults have the highest slip and dilation tendency. Thus, many of the normal faults in the study area are well oriented for slip and dilation, including faults in each of the favorable structural settings.

Past geothermal exploration in the Sou Hills includes several TG wells, though none showed any appreciable anomalies. However, nearly all wells were drilled outside the favorable structural settings (Figure 11B-C). One previously undocumented warm well (29°C) was found in this study at the Sou Ranch in the axial part of the extensional anticline, but we could not obtain a sample due to a malfunctioning pivot pump.

Twenty-three geochemical water analyses include 20 historical and 3 new samples collected in this study. Prior to this study, Seven Devils Hot Springs and McCoy Spring were the two known thermal areas in the Sou Hills. Seven Devils is a localized cluster of ~7 northerly trending hot springs and associated travertine mounds in the southernmost Sou Hills. These hot springs reside directly north of the extensional anticline. Relatively low subsurface temperatures of 85°C for Seven Devils and 55°C for McCoy are suggested by the chalcedony, Na-K-Ca, Mg-corr and K/Mg geothermometers. However, estimates by Spycher (LBNL) using GeoT (Spycher et al., 2016) suggest temperatures as high as 160°C in both systems, although a considerable amount of fluid reconstruction implies significant uncertainties. One additional sample was modeled for the Paris Well at the Draper Ranch in the northern part of the area. The chalcedony, Na-K-Ca, Mg-corr and K/Mg geothermometers indicated temperatures of 55-60°C, but GeoT analysis yielded 160°C with high uncertainty. Thus, both previously known systems and the newly identified Draper Ranch area may have power-capable temperatures at depth.

A total of 82 two-meter temperature stations was acquired in the area and did not reveal any appreciable thermal anomalies. However, much higher than average winter precipitation in 2017 may have suppressed shallow thermal expression of geothermal upwellings. Further, relatively low water tables in elevated parts of the Sou Hills may result in little expression of thermal anomalies at such shallow levels.

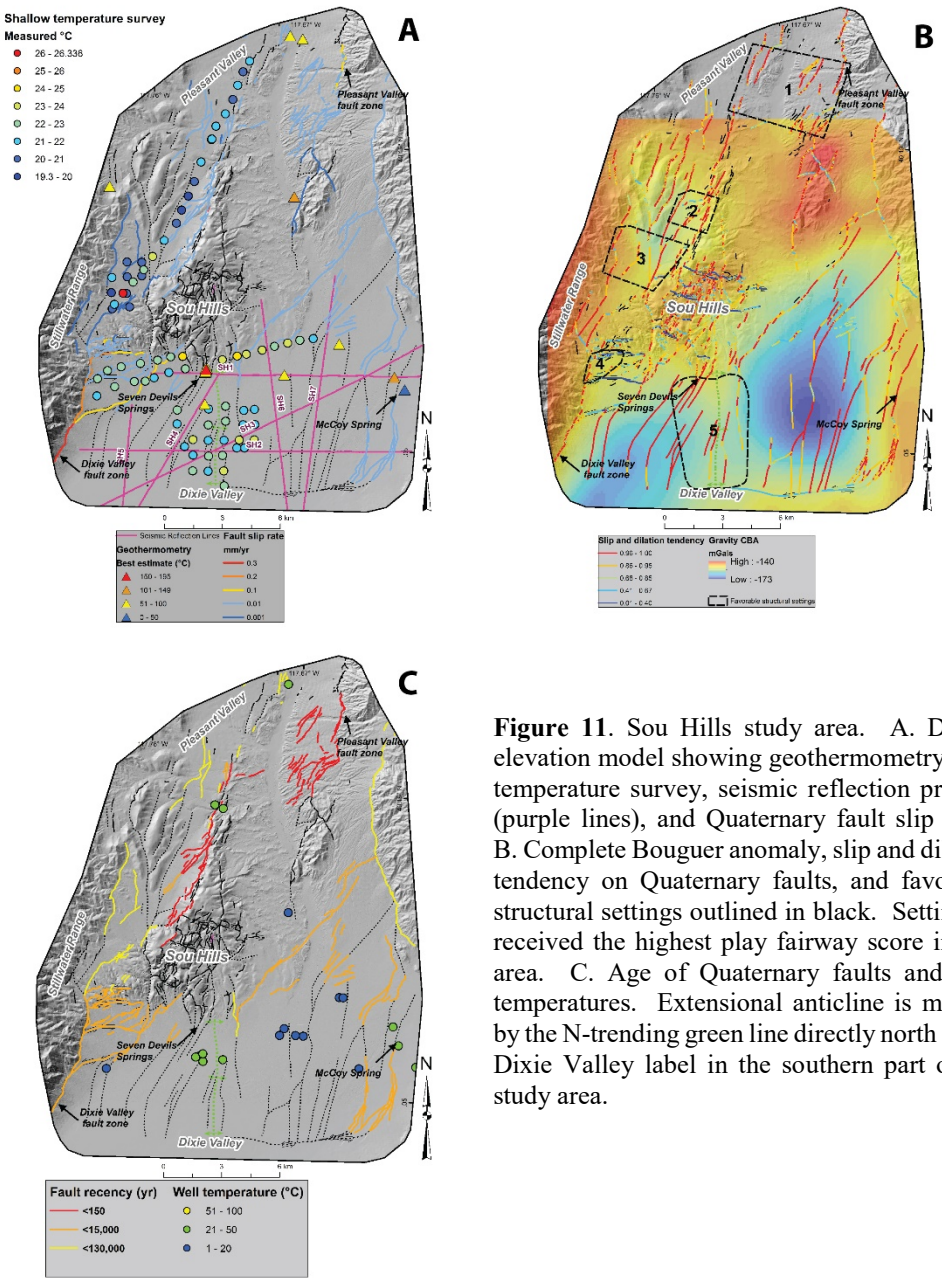

Figure 11. Sou Hills study area. A. Digital elevation model showing geothermometry, 2-m temperature survey, seismic reflection profiles (purple lines), and Quaternary fault slip rates. B. Complete Bouguer anomaly, slip and dilation tendency on Quaternary faults, and favorable structural settings outlined in black. Setting #5 received the highest play fairway score in this area. C. Age of Quaternary faults and well temperatures. Extensional anticline is marked by the N-trending green line directly north of the Dixie Valley label in the southern part of the study area.

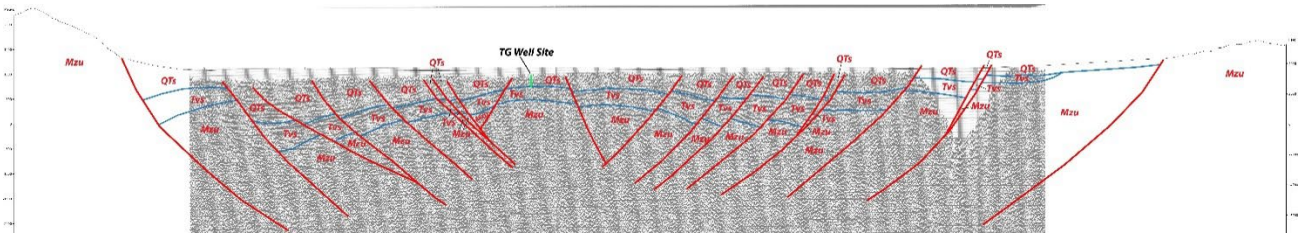

Figure 12. E-W-trending seismic reflection profile SH2 looking north and imaging anticlinal accommodation zone in the northernmost part of Dixie Valley. Location shown on Figure 11A. Proposed TG well site shown by bright green line. QTs-late Miocene to Quaternary basin-fill sediments; Tvs, Miocene-Oligocene volcanic and sedimentary rocks; Mzu, Mesozoic granitic and metamorphic rocks.

Crescent Valley

The Crescent Valley study area is a composite late Cenozoic basin in north-central Nevada that includes the Dry Hills and northern flank of the Cortez Mountains (Figures 1 and 13). Hot springs are present at both Dann Ranch along the Cortez Mountains and Hot Springs Point at the south end of the Dry Hills. Our studies included: 1) detailed Quaternary fault mapping of ~500 km^2, 2) slip and dilation tendency analysis, 3) new detailed logging of 4 wells (2,638 m) and integration of ~20 km of existing logs from 39 wells, 4) integration of 22 TG wells, 5) a new gravity survey of 236 stations merged with ~3,000 legacy stations, 6) a shallow temperature survey (31 stations), 8) interpretation of 4 seismic reflection profiles, and 9) geochemical analyses of 23 water samples (Faulds et al., 2017b and appendices therein; McConville et al., 2017; McConville, 2018).

The structural framework of Crescent Valley is dominated by a composite east-tilted half graben bounded on the east by the northwest-dipping Crescent fault (Figures 13 and 14). Four discrete right step-overs (relay ramps) occur along the Crescent fault. One of these step-overs encompasses Dann Hot Springs, which has a surface temperature of 87ºC and silica geothermometry of ~180ºC. Silica sinter mantles alluvial fan deposits directly north of the hot spring. The Dry Hills in northern Crescent Valley is a horst block bounded by oppositely dipping normal faults. Hot Springs Point is located at the southwest tip of the Dry Hills at a complex fault intersection. A major NNW-striking, west-dipping intrabasinal fault continues southward from Hot Springs Point to the Cortez Mountains front, where it terminates against the Crescent fault. Gravity, seismic reflection data, and depth to basement estimates (Watt et al., 2007; McConville, 2018) indicate that the Crescent basin deepens from ~0.7 km in the northeast to ~5 km in the southwest portion of the study area. The most active Quaternary fault in the area is the Crescent fault, which ruptured during one Holocene event, with surface offset >4 m (Friedrich et al., 2004). The long term slip rate of this fault is ~0.2 mm/yr (Figure 13A). Faults bounding the Dry Hills on the northwest have slip rates of ~0.1 mm/yr (Wesnousky et al., 2005). NNE-striking normal faults have the highest slip and dilation tendency, with a maximum on normal faults striking N26ºE. Thus, many of the normal faults in the Crescent Valley study area are well oriented for slip and dilation, including faults in each of the structural target areas.

The geologic and geophysical data suggest nine favorable structural settings capable of hosting geothermal fluids in the Crescent Valley area (Figure 13). These include a major fault intersection and three discrete step-overs along the Crescent fault, two fault intersections in the central part of the Dry Hills, a major fault intersection along the northwest flank of the Dry Hills, a fault intersection near Hot Springs Point, and an intrabasinal fault intersection to the south of Hot Springs Point.

The Crescent Valley study area contains two known thermal systems. Hot Springs Point in the central part of the valley includes 10 known springs with temperatures between 41.2 and 60.8°C. The Dann Ranch area hosts the highest temperature springs (89.4°C) and wells (125.5°C) known in the study area. Ormat was exploring this area for potential power production during the final stages of this project.

Thirty-one water analyses include historical (8), company files (15-US Geothermal [now Ormat]), and new samples collected in this study (8 sites). Although the Hot Springs Point area indicates relatively low temperatures with traditional geothermometers (~90-100°C with chalcedony and K/Mg geothermometers), temperatures in excess of 180°C (possibly 200°C) are indicated in the Dann Ranch area. The Dann Ranch and Hot Springs Point areas appear to be separate systems. A 2-m temperature survey with 31 stations did not reveal a shallow temperature anomaly in the southern and central parts of the basin, although the very wet winter of 2017 may have resulted in cooler temperatures at 2 m depth.

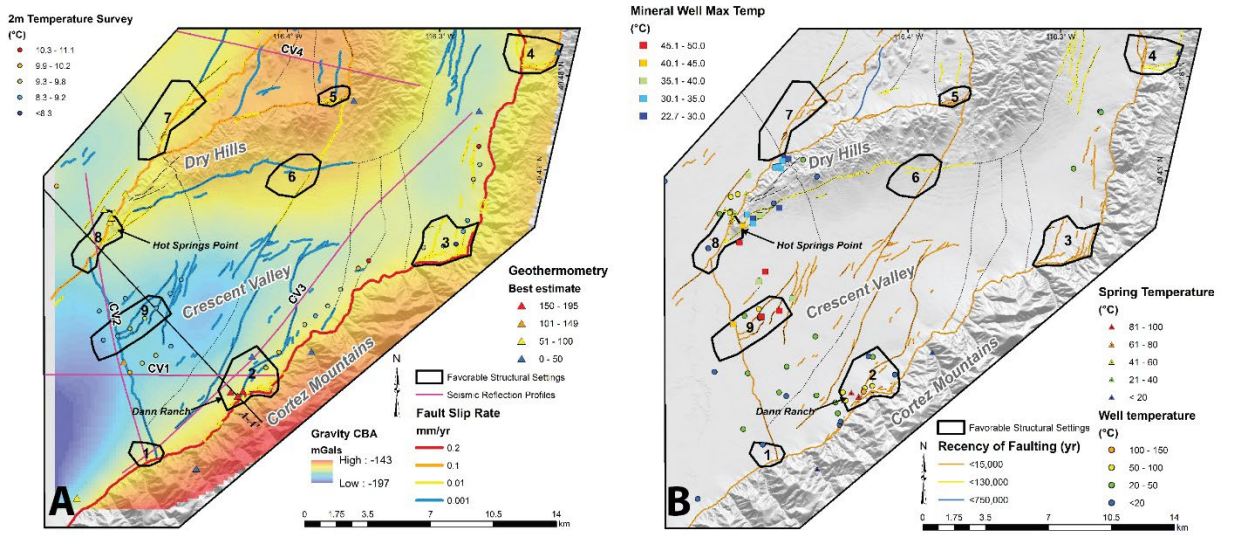

Figure 13. Crescent Valley study area (see Figure 1 for location). A. Generalized map showing complete Bouguer gravity anomaly, Quaternary fault slip rates, geothermometry, results of 2-m temperature survey, and seismic reflection profiles (purple lines). Favorable structural settings are outlined in black. Setting #2 received the highest play fairway score in this area. B. Map showing spring and well temperatures, as well as age (recency) of Quaternary faults.

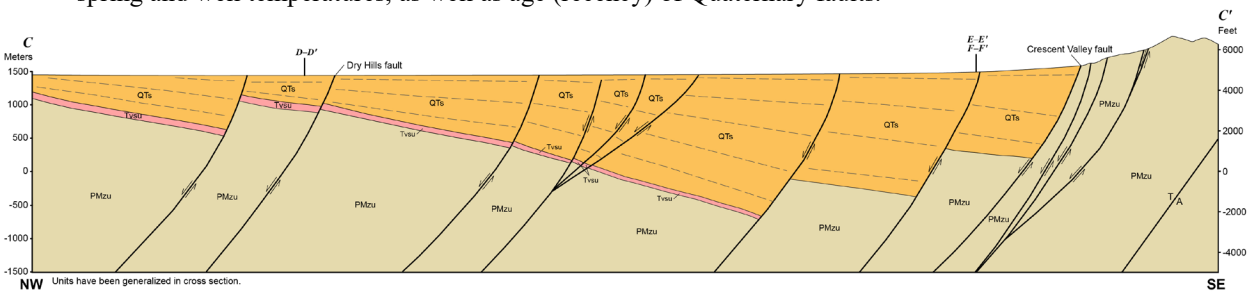

Figure 14. NW-SE cross section (see Figure 13 for location) through the Hot Spring Point and Dann Ranch geothermal areas in Crescent Valley (from McConville, 2018). Proposed drilling sites are discussed in McConville (2018). QTs-late Miocene to Quaternary basin-fill sediments; Tvsu, Miocene-Oligocene volcanic and sedimentary rocks; MPzu is Mesozoic-Paleozoic basement undivided.

Steptoe Valley

The Steptoe Valley study area is an elongate north-trending late Cenozoic west-tilted half graben in eastern Nevada (Figure 1). The Phase 2 study area boundaries (Figure 15) were selected to include several highly favorable areas identified in Phase 1 and also areas with substantial available subsurface data, including, oil and gas exploration wells, geothermal exploration wells, and 2D seismic profiles. New gravity stations (278 total) were collected, principally along seismic lines to facilitate depth to basement modeling for better control. Cuttings from eight oil and gas wells were analyzed to provide stratigraphic control in interpreting the 2D seismic reflection lines. New field mapping was also conducted along much of the range-front fault system on the west side of the basin and merged with existing mapping of the bedrock (Fritz, 1968; Hose et al., 1976) to produce a new geologic map of the study area. A 3D geologic map of the entire study area was constructed from the geologic map, drill-hole, and 2D seismic line data. Forty samples of well cuttings from key stratigraphic units were analyzed for thermal conductivity. Existing temperature data, the new thermal conductivity measurements, and the 3D geologic model were used to develop a new heat flow model for the entire study area (see Faulds et al., 2017b and appendices therein; Hinz et al., 2020).

Steptoe Valley contains two hot springs, both associated with normal fault step-overs (Hinz et al., 2020). Monte Neva Hot Springs is associated with a 0.28 km^2 travertine spring mound. No other surficial

geothermal features have been observed in Steptoe Valley. Hunt Oil Company drilled ~50 TG holes and two deep geothermal wells in the basin in the 1970s (Chovanec, 2003). A few of the TG holes recorded elevated temperature gradients and lost circulation zones, but the temperature gradients in the two deep geothermal wells and most TG wells were largely conductive. Ultimately, no major resource was encountered, which demonstrates the importance of conducting play fairway analysis prior to drilling. Despite this previous work, much of the basin has not been explored, including key structural target areas.

Late Cenozoic extension was accommodated by a system of N- to NE-striking, dominantly east-dipping normal faults. These normal faults include the range-front fault along the west side of the basin as well as numerous intrabasinal faults. The range-front fault makes a broad, 15-km, hard-linked, left step between the Monte Neva and Cherry Creek Hot Springs areas. Quaternary fault scarps mark most of the trace of the range-front fault system. A few additional Quaternary fault scarps with short lengths were identified along the intrabasinal faults. The most recent fault rupture is late Pleistocene (Koehler and Wesnousky, 2011). Slip rates for all major singular strands of the range-front fault are 0.03 mm/yr.

Lithologic logs from 25 wells, geologic map data, 16 cross-sections including data from 14 seismic reflection profiles (Figure 16), and depth to basement modeled from gravity data were synthesized into a 3D geologic map of the Steptoe Valley study area (Figure 17). The Steptoe 3D map contains three stratigraphic units: undivided basement, Tertiary volcanic rocks, and Quaternary/Tertiary sediments. The 3D model reveals the anatomy of the basin, including a broad, gently west-tilted half graben bounded by a major moderately east-dipping range-front on the west and cut by several, relatively minor northerly striking intrabasinal faults. The 3D geologic map constrains the geometry of several structural discontinuities that may be important sites of permeability and fluid flow. Monte Neva Hot Springs occupies a ~2.5 km-wide left-step in the range-front fault (Figures 15 and 17). Several additional steps and bends occur farther north, including one associated with the Cherry Creek hot springs.

For slip and dilation tendency analysis, we assumed a normal faulting stress regime with a minimum horizontal stress (Shmin) direction of 117°, both of which are consistent with regional trends (Hickman et al., 1997; Hickman and Davatzes, 2010). Under these stress conditions 60°-dipping NNE-striking faults have the highest slip tendency, whereas more steeply-dipping NNE-striking faults have the highest dilation tendency (Figure 17C). The predominantly NNE- striking fault system in Steptoe Valley is generally well oriented for both slip and dilation, including at both Monte Neva and Cherry Creek hot springs.

Twelve favorable structural settings were defined from the new 2D and 3D geologic maps (Hinz et al., 2020). These include seven normal fault step-overs and five fault intersections. The largest and most complex favorable settings include the step-over associated with Monte Neva Hot Springs and a second step-over southwest of Monte Neva. Another key step-over associated with Cherry Creek Hot Springs is just 200 m wide, only slightly narrower than the step-over associated with Bradys Hot Springs (Faulds et al., 2010, 2017b; Siler et al., 2016b). All three step-overs lack continuous Quaternary scarps, indicating that these structures are acting as key arrest zones during earthquake ruptures and may reside in areas of elevated coulomb stresses (e.g., Siler et al., 2018).

Steptoe Valley has been one of the primary focus areas for studies of geothermal resources in deep sedimentary basins, with elevated temperatures initially documented during oil and gas well drilling (Allis, et al., 2011, 2012, 2015; Kirby, 2012; Allis and Moore, 2014; Gwynn et al., 2014). These studies suggest large, untapped geothermal resources within stratigraphic horizons at depth in Cenozoic basins in eastern Nevada and western Utah, including this portion of Steptoe Valley. These studies show a high heat flow of 90 to 100 mW/m^2 corresponding to temperatures of 170 to 230°C at ~3 km depth. Notably, Sandia National Laboratories was funded in 2020 by the DOE Geothermal Technologies Office to further analyze the potential for sedimentary hosted geothermal systems in Steptoe Valley. Data acquired in this play fairway project provides an important foundation for that study.

Nineteen water analyses are available in the study area, including 17 historical samples and one sample each from gray literature and this study. The Monte Neva Hot Spring area has the hottest surface discharge of fluids in the area at 79°C. Deep wells in this area have measured bottom-hole temperatures of 198-200°C at 3,306-3566 m depth (Hunt geothermal 74-23 and Shell #1 wells). However, none of these have available chemistry data, and all have conductive temperature profiles. Traditional geothermometers

suggest relatively low temperatures for Monte Neva near the discharge temperature, but GeoT modeling (Spycher, pers. comm., May 2017) indicates subsurface temperatures of 180°C (Figure 18). Similar GeoT modeling of Cherry Creek and Well 37-23 show a grouping of minerals at equilibria at 136±5°C and 174±3°C, respectively. Power-capable geothermal systems are thus possible at all three areas (Monte Neva, Cherry Creek, and area of Hunt wells), although the higher temperatures (>180°C) are likely at ≥3 km depths based on conductive temperature gradients of the Hunt wells averaging ~60°C/km. Results at Cherry Creek suggest a higher level, intermediate system that could exploit a lower temperature (~135°C) resource.

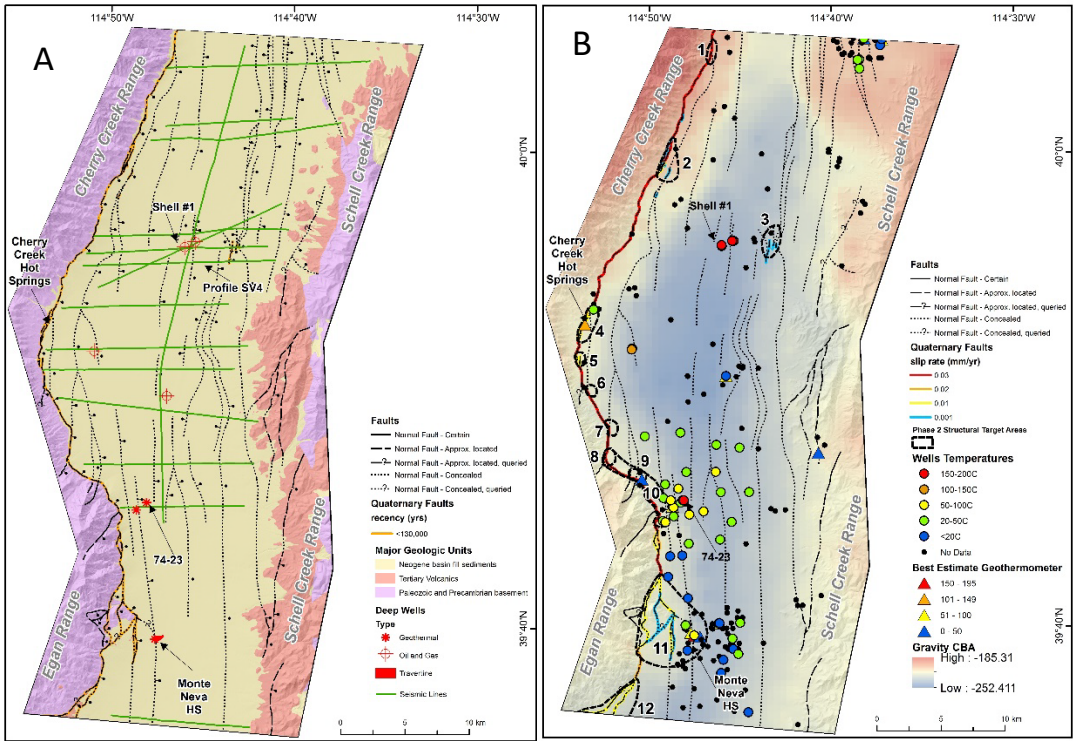

Figure 15. A. Geologic map of the Steptoe Valley study area with simplified geologic units, and Quaternary faults attributed by fault recency. Also shown are the seismic profiles (purple lines). B. Fault map of the study area with Quaternary faults attributed by slip rate on a hillshade with a transparent overlay of the CBA gravity model. Favorable structural settings are outlined in black.

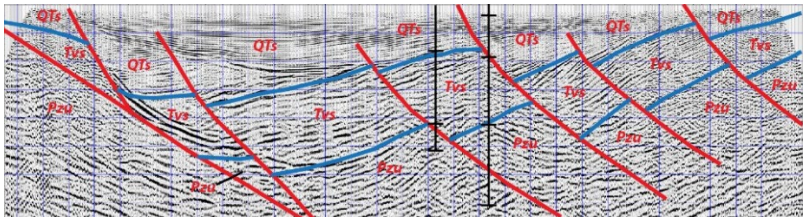

Figure 16. E-W (looking north), interpreted seismic reflection profile (SV4) with local well control. Pzu, Paleozoic sedimentary rocks; other unit names same as in Figure 12. Location in Figure 15A.

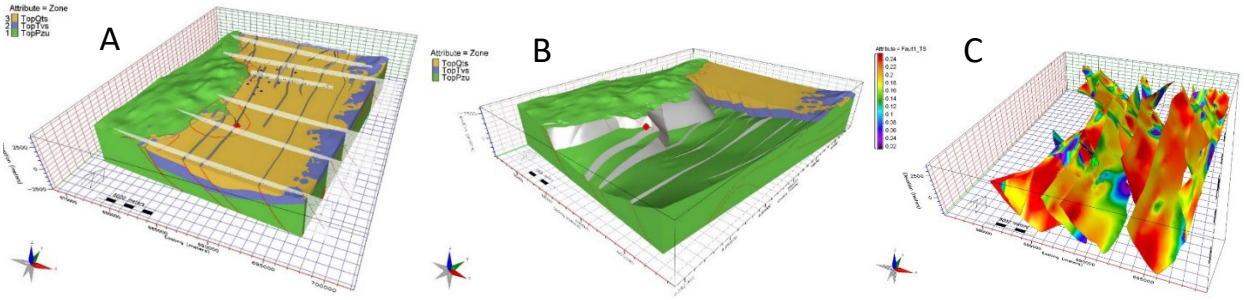

Figure 17. Perspective views of a portion of the Steptoe 3D geologic map looking NNW (A) and NW (B), and a perspective view of slip tendency calculated along faults in Steptoe 3D geologic map looking NNW (C). Several of the seismic reflection profiles and 2D geologic cross-sections that were used to constrain the 3D geologic relationships are shown protruding from the 3D map on left. Lithologic units, undivided Paleozoic basement (Pzu), Tertiary volcanics (Tv), and Neogene sedimentary rocks (QTs) are shown in green, blue, and yellow respectively. Faults are shown as gray planes and as red lines in section view. Blue dots indicate the location of downhole lithologic data used to constrain 3D geologic relationships. Monte Neva Hot Springs is shown with the red dot at a left step-over between a relatively large-offset interbasinal fault and the range-front fault. Favorable steps and bends in the range-front fault system are circled in red.

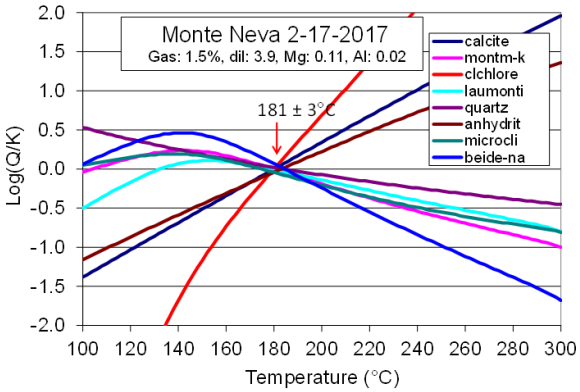

Figure 18. GeoT multicomponent chemical equilibria model results (Spycher, pers. comm., May 2017). The modeled minerals attain equilibria under the modeled conditions for the Monte Neva Hot Springs 2017 sample (78.2°C) at 181 ± 3°C, suggesting the last temperature of equilibration near 180°C.

Refined Play Fairway Analysis

Detailed play fairway maps were generated for each of the five study areas using the exploration data obtained during Phase 2 studies (Faulds et al., 2017a,b). These new data were integrated with the existing Phase 1 database. The general methodologies for producing regional predictive maps in Phase 1 (Faulds et al., 2015b) were followed in building detailed predictive maps in Phase 2. The regional-scale permeability and heat models of Phase 1 remained unchanged, with the exception of the Steptoe Valley heat model. In contrast, the local- and intermediate-scale permeability models were revised and updated to reflect results of detailed geologic mapping and geophysical and geochemical surveys. A number of adaptations and improvements were employed in the models to accommodate new types of data and additional structural attributes into the local permeability models. As described in detail by Faulds et al. (2017b), these changes included: 1) inclusion of a structural settings quality factor to model the strength or quality of structural settings; 2) magnetotelluric (MT) data (where present), whereby low-resistivity anomalies enhanced the structural quality factor due to their potential affiliation with clay caps and/or fluid flow at depth (e.g.,

Ussher, 2000; Cumming, 2009; Wannamaker et al., 2013, 2017); 3) replacing the regional temperature model used in Phase 1 with a more detailed temperature model at 1250 m below sea level but for only Steptoe Valley; 4) two-meter temperature anomalies, which were converted to "degrees above background" (DAB) (e.g. Sladek and Coolbaugh, 2013) and related to a probability of occurrence of a 130°C geothermal system; and 5) presence of paleogeothermal features, such as sinter/silica-cemented sands and explosion craters with probabilities estimated based on type and extent of deposit.

Three main sets of predictive maps were generated: 1) play fairway maps, 2) play fairway error maps, and 3) direct evidence maps. The fairway maps highlight areas of geothermal favorability based on fundamental underlying geologic, geophysical, and geochemical data, whereas the direct evidence maps highlight areas of favorability based on "direct observations" of geothermal features, such as temperature anomalies, fluid geothermometer temperatures, temperature gradients, or the presence of surface geothermal features such as silica-cemented sands or sinter. In Phase 1, the fairway and direct evidence maps were combined to produce overall "favorability" maps. This was not done in Phase 2. Instead, it was found that because of the widely differing types of data employed in fairway and direct evidence maps, it was more informative to compare the results of both maps side by side to facilitate visualization of one or more conceptual models of 3D fluid flow.

The fairway models of the five detailed areas have scores similar to those in the original Phase 1 model. The major difference between the detailed Phase 2 models and the Phase 1 regional model is that locations of higher favorability are more accurately shown in the Phase 2 models and at a higher level of detail, as exemplified for Gabbs and Granite Springs Valleys (Figures 19A-B and 20A-B). An error analysis shows that all potential targets of interest have a statistically significant anomalous fairway score, as measured by the difference between the local score and the average score, divided by the estimated error (Figures 19C and 20D). We note that fairway scores above ~45 indicate relatively high potential (Figure 3). Direct evidence maps are also more detailed than in Phase 1, because of the much greater availability of input data. This is most obvious for southeastern Gabbs Valley (Figure 21), where very little direct evidence was available in Phase 1, and where Phase 2 data strongly suggest a previously unknown geothermal system. Examples from the other detailed studies area are described and illustrated in Faulds et al. (2017b).

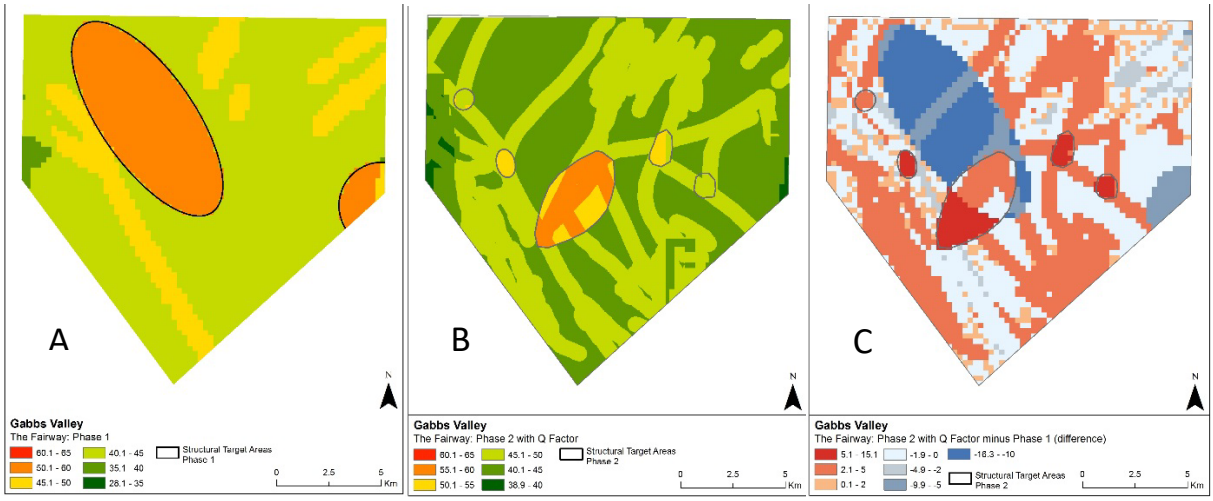

Figure 19. Comparison of Phase 1 and 2 fairway Phase 1 fairway analysis for southeastern Gabbs Valley. Phase 1 fairway results (A). Phase 2 fairway results with structural setting quality factor (B). Difference between the Phase 2 and Phase 1 fairway results (C) with positive numbers equal to increase of fairway score from Phase 1 to Phase 2, and negative numbers equal to decrease in fairway score from Phase 1 to Phase 2.

Significant differences between Phases 1 and 2 in the play fairway analysis are particularly strong for those study areas containing large late Cenozoic basins. New geophysical data in these areas afforded discovery of previously unrecognized intrabasinal, favorable structural settings, as exemplified in the

Adobe Flat area of Granite Springs Valley and in the central part of southeastern Gabbs Valley. These findings epitomize the importance of the detailed studies in refining exploration targets in such areas. Considering that nearly half of the Great Basin region is covered by basins, this also demonstrates the broad applicability of such detailed studies, as well as the large untapped potential for commercial-grade geothermal systems in many of these basins.

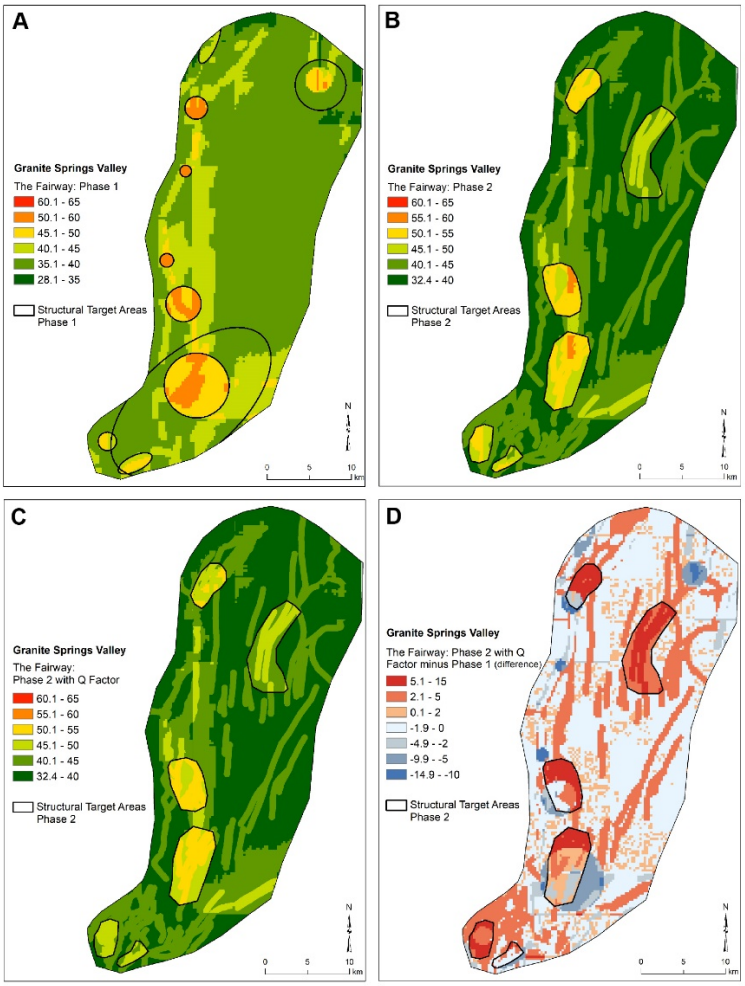

Figure 20: Comparison of Phase 1 and 2 fairway analysis for Granite Springs Valley. A. Phase 1 fairway results. B. Phase 2 fairway results calculated the same as in Phase 1. C. Fairway score from Phase 2 calculated with structural setting quality factor. D. Difference between the Phase 2 and Phase 1 fairway results with positive numbers equal to increase of fairway score from Phase 1 to Phase 2, and negative numbers equal to decrease in fairway score from Phase 1 to Phase 2.

It is important to reiterate that a primary difference between Phase 1 and 2 of this project is that the regional analysis of Phase 1 recognized relatively broad, favorable structural settings or clusters of settings in particular areas (Figure 1). As is typical in any regional exploration program, it is difficult in the early stages to parse out the detailed characteristics of a particular area to select the most favorable targets for drilling. Upon more detailed analysis of individual areas in Phase 2, it became apparent that nearly all study areas contained multiple favorable structural settings. This presented the immediate challenge of applying our play fairway methodology at a finer scale to efficiently model the geothermal potential of each of the favorable settings within a particular study area. The detailed geological, geochemical, and geophysical investigations afforded such an analysis. Ultimately, we utilized the play fairway score to compare favorable settings in each of the study areas to one another and rank such areas to select the most promising

sites for drilling. Thus, we found that our play fairway methodology was very adaptable to the natural evolution of an exploration program as it progresses from a regional analysis and vectors into the most promising prospects that present the lowest risk for development.

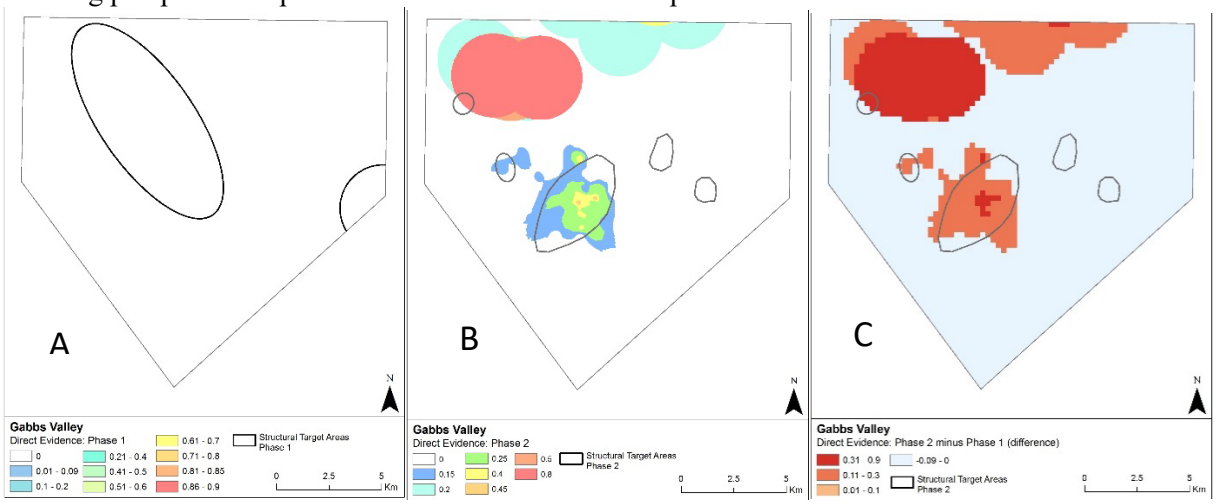

Figure 21. Comparison of Phase 1 (A) and Phase 2 (B) direct evidence grid layers for Gabbs Valley. Difference between the Phase 2 and Phase 1 direct evidence modeling grid layer (C) with positive numbers equal to increase of fairway score from Phase 1 to Phase 2.

To fully test the viability of our methodology on potential blind geothermal systems, we prioritized the primary sites in southeastern Gabbs Valley and northern Granite Springs Valley for TG drilling in Phase 3. These two sites represent newly discovered, potential blind geothermal systems, with direct evidence suggesting temperatures >130ºC. A key feature for these two sites is the blind nature of the potential geothermal systems, whereas the other three detailed study areas all contain some surface hot springs. In addition, both sites have favorable land status (BLM with no unusual restrictions) and are easily accessible.

Phase 3 Summary (Budget Period 3)

Phase 3 of the project involved more detailed geophysical analyses and TG drilling in southeastern Gabbs Valley and northern Granite Springs Valley (Figure 1), deemed the two most promising sites. As described above, southeastern Gabbs Valley occupies a broad displacement transfer zone proximal to a terminating dextral fault within the Walker Lane, and Granite Springs Valley contains several terminations of major Quaternary normal faults, fault step-overs, and a major accommodation zone. The primary goal of Phase 3 was to test the play fairway methodology with TG drilling. The more detailed geophysical analyses included additional gravity and new magnetic and magnetotelluric (MT) surveys. The additional gravity work and new magnetic work better defined the probable location of subsurface faults. The magnetic and MT surveys helped to define possible areas of alteration and fluid flow in the subsurface.

In southeastern Gabbs Valley, the extent of multiple favorable structural settings identified in Phase 2 (Figure 8C) were further refined in Phase 3 on the basis of acquisition of additional geophysical and geological data (Figure 22). One area (A in Figure 22) was particularly promising based on the collocation of Quaternary faults, intersecting and terminating gravity gradients suggesting multiple fault intersections, magnetic low, shallow (2 m) temperature anomaly, low resistivity anomaly, and promising geothermometry from nearby water wells (Figure 23; Craig, 2018; Faulds et al., 2018; Craig et al., in prep). Drilling of six temperature-gradient holes defined an apparent geothermal system at this locality with temperatures as high as 124°C at 152 m (Figure 24), with the highest temperatures in the central part of the collocated geophysical and shallow temperature anomalies. Bottom-hole temperatures fall off rapidly to the north and more gradually to the south. At ~150 m depth, the thermal anomaly is at least ~2 km long in a north-south extent and probably at least 1 km wide from east to west. This system is completely blind, with no surface hot springs, fumaroles, or paleo-geothermal deposits.

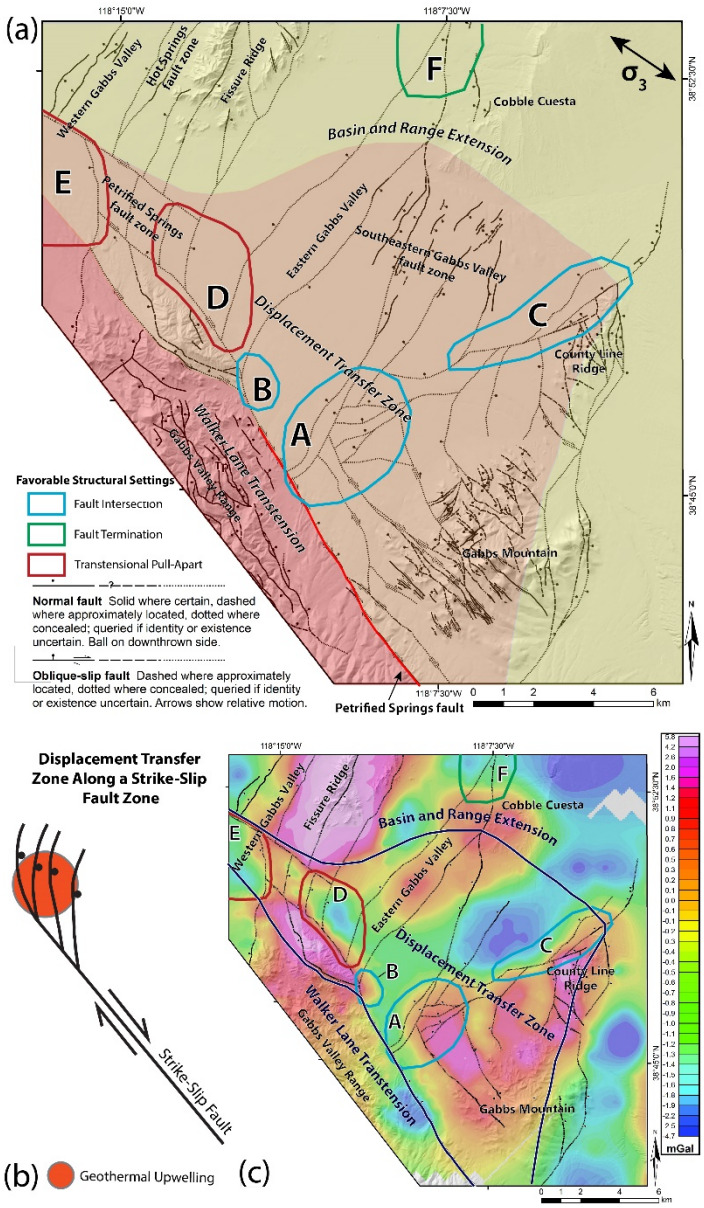

Figure 22. Southeastern Gabbs Valley displacement transfer zone (from Craig et al., in prep). **(a)** Structural domains of the area shaded to illustrate the spatial distributions of faulting: Walker Lane dextral shear in red, displacement transfer zone in orange, and Basin and Range extension shown in yellow. The surficial trace of the Petrified Springs fault is shown as a red line. Individual favorable structural settings are shown as color-coded polygons based on structural setting type: fault intersections are blue, fault terminations are green, and transtensional pull-aparts are red. Lettered polygons are areas identified as favorable structural settings referenced in text. The orientation of the minimum principal stress direction, σ_3, is shown for reference as black line with bi-directional arrows in the upper right hand corner. **(b)** Schematic diagram of a displacement transfer zone whereby a strike-slip fault terminates into a splay of normal faults (modified from Faulds and Hinz, 2015). A hypothetical area of structurally controlled geothermal upwelling is shown as a red ellipse. **(c)** Simplified fault map overlain on gravity data with favorable structural settings. Boundaries of structural domains shown as dark blue lines.

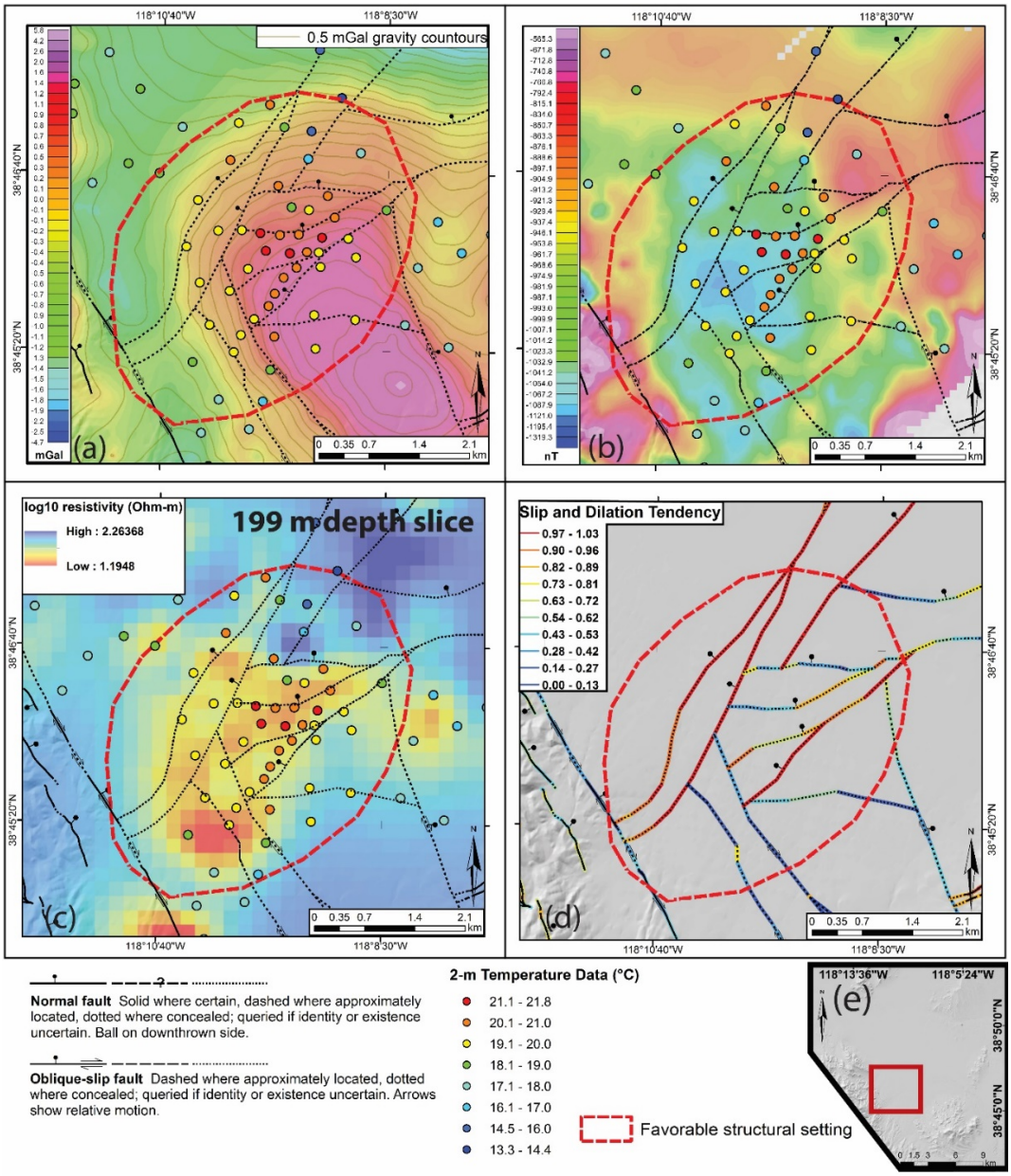

Figure 23. Collocated intersecting gravity gradients, magnetic-low, low-resistivity, 2-m temperature anomaly, and favorably oriented faults for slip and dilation. Faults are shown as black lines (except in d). 2-m temperature stations are shown as colored circles with warmer colors indicating higher measured temperatures (°C). Area of the favorable structural setting shown as red dashed polygon. All maps are overlain on DEM hillshade. **(a)** Residual isostatic gravity map with warmer colors indicating higher relative gravity values. Brown lines are 0.5 mGal gravity contours. **(b)** Reduced to pole magnetic map of study area. Warmer colors indicate relatively higher magnetic values (nT) than cooler colors. **(c)** 199 m MT resistivity depth slice. Warmer colors indicate areas with lower resistivity values (Ohm-m). **(d)** Slip and dilatation tendency analyses. Faults are colored based on slip and dilation tendency values with warmer colors indicating high slip and dilation tendency. **(e)** General study area showing location of maps as red polygon.

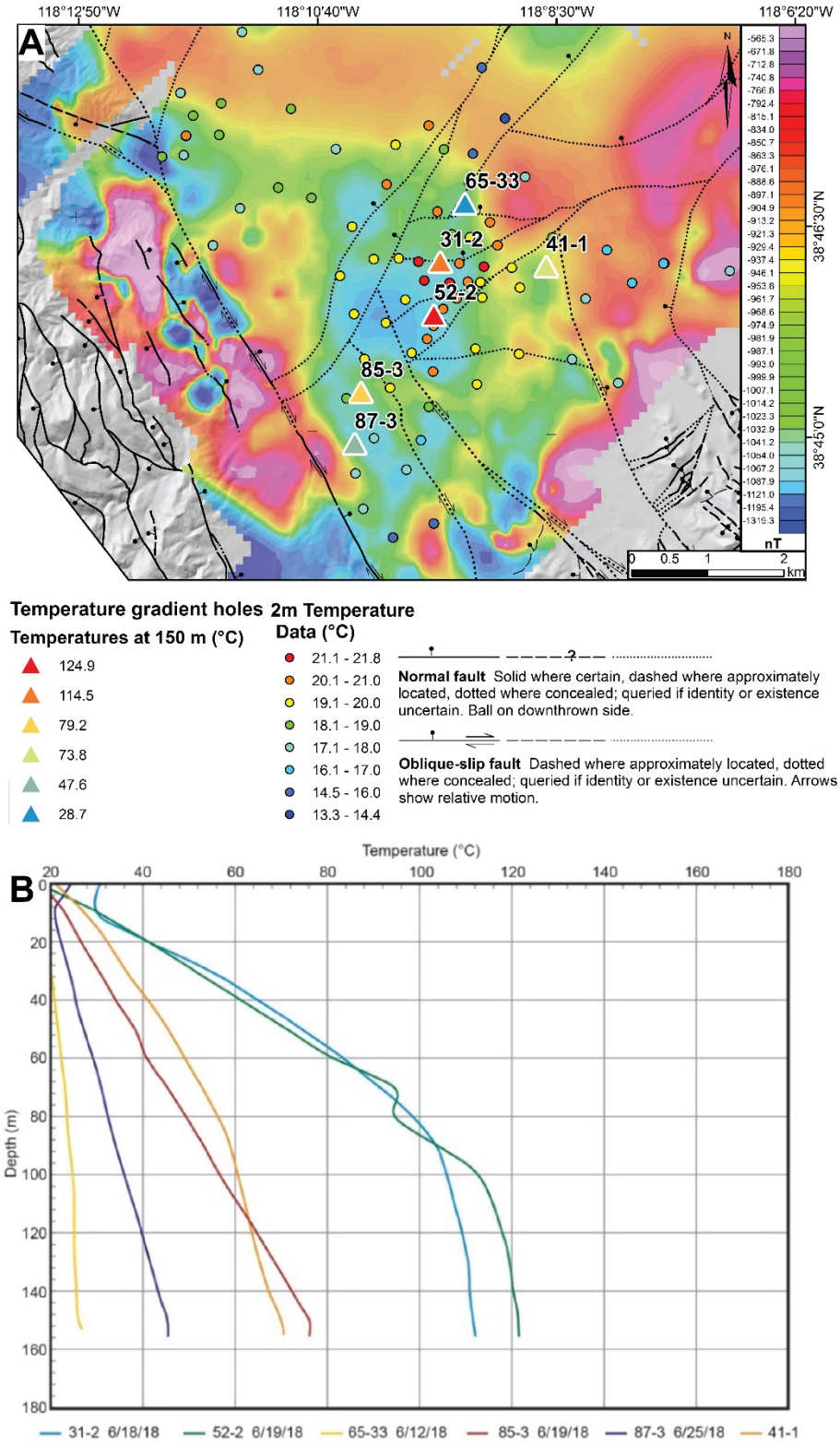

Figure 24: A. Reduced to pole magnetic map showing locations of TG holes. Warmer colors indicate relatively higher magnetic values (nT) than cooler colors. Note the low magnetic anomaly collocated with the warmer wells. **B.** Data from temperature-gradient holes in southeastern Gabbs Valley. The two hot wells are collocated with the shallow temperature anomaly, intersecting and terminating gravity gradients, magnetic low, and low-resistivity anomaly.

For Granite Springs Valley, we chose the Adobe Flat area in the northern reaches (area #2 in Figure 6D, E) for more detailed analyses and subsequent drilling in Phase 3 due to a combination of geologic, geophysical, geochemical, and practical matters (e.g., land status and accessibility). This area contains a favorable structural setting (termination of a major Quaternary normal fault), terminating gravity gradient, magnetic gradient, newly discovered late Pleistocene sinter deposits, nearby warm water wells, nearby warm previously drilled temperature-gradient holes (Benoit, 2008), and promising geothermometry from water samples collected with GeoProbe drilling (Figure 6 and 25). The collocation of all of these features suggests a hidden geothermal system. The area is also easily accessible and resides on public land. Drilling of six new temperature-gradient holes yielded temperatures of up to ~96°C at ~240 m (Figures 25B and 26), suggesting the presence of a blind geothermal system. Well 42-2 has an essentially isothermal gradient from ~150 to 250 m, and well 54-2 shows an isothermal gradient from ~110 to 152 m (Figure 26). These isothermal gradients suggest a convective heat source and upwelling in that area, which is proximal to the largest, observed sinter deposits. The nearby 76-2 well has a conductive temperature gradient to 250 m depth, suggesting that it may be more distal to upwelling geothermal fluids. We therefore suspect that a major upwelling lies in the vicinity of wells 42-2 and 54-2 proximal to sinter deposits and within a zone of intersecting faults and a possible step-over within a broader horse-tailing fault termination. The sinter deposits imply subsurface temperature of more than 180°C.

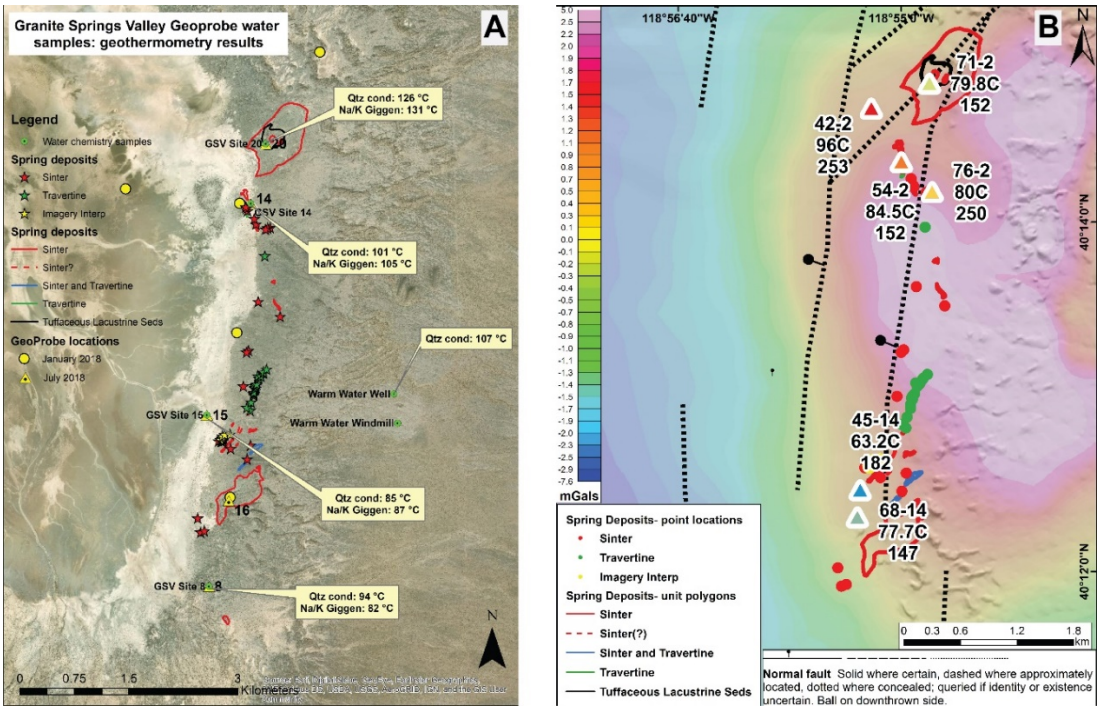

Figure 25: A. Locations of and geothermometry results from GeoProbe holes overlain on Google Earth image. B. Locations and bottom-hole temperatures of TG wells overlain on isostatic residual gravity data and interpreted faults. Well locations are marked by triangles, with warmer colors indicating higher bottom-hole temperatures. From top to bottom, numbers adjacent to wells are well number, bottom-hole temperature, and depth in meters. The distribution of sinter and travertine is also shown in both A and B.

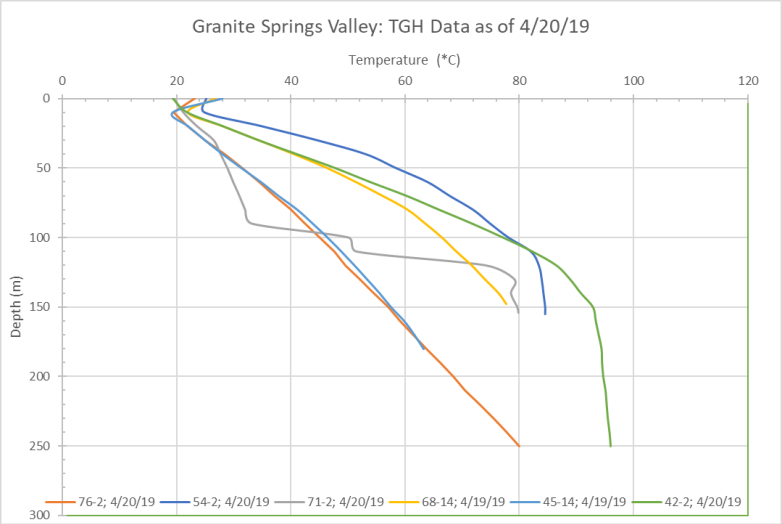

Figure 26: Temperature gradient data from six new temperature-gradient holes drilled in 2018-2019 in northern Granite Springs Valley. Locations of wells are shown in Figure 25B.

Major Tasks: Phase 3

The first 24 tasks were completed in Phases 1 and 2 (BP1-BP2) on schedule and with no significant variances, as described above and in greater detail in Faulds et al. (2015b, 2017b). All major tasks (Tasks 25 to 33) and milestones were also completed for Phase 3 (BP3; Table 3). Major tasks included: 1) permitting of GeoProbe and TG wells; 2) GeoProbe drilling; 3) TG drilling; 4) geochemical analyses; 5) potential field geophysical surveys, as well as additional geological investigations; 6) MT surveys; 7) 3D modeling; 8) conceptual models and resource capacity estimates; and 9) final reporting and project review. In contrast to the first two phases, however, there were some delays and variances. These resulted from the lack of suitability of some sites for GeoProbe drilling, unanticipated expenses and delays in both managing and conducting drilling (e.g., equipment issues and a government shutdown), and the time intensive nature of managing a drilling program and fully integrating results with other datasets. Despite some delays and minor variances, all major tasks and milestones were accomplished.

The section below describes the accomplished tasks for Phase 3 (Budget Period 3, Table 3), including some of the challenges. Phase 3 focused on detailed studies and drilling in southeastern Gabbs Valley and northern Granite Springs Valley but also included some additional work in Crescent Valley. The accomplishments for each task are described separately for each of these sites.

Task 25.0. Permitting: Permitting requests for detailed geophysical investigations (gravity, magnetics, and MT) and both GeoProbe and TG drilling will be submitted for at least two areas, with southern Gabbs Valley and northern Granite Springs Valley selected as priority areas. The permitting requires approval from the BLM field office with jurisdiction over the area. In addition, the approval process for drilling requires a technical review of the drilling plan/program by the Nevada Division of Minerals (NDOM).

Gabbs Valley: All permitting requirements were completed for southeastern Gabbs Valley for TG drilling with no major variances. GeoProbe drilling was not conducted due to the relatively deep water table and presence of coarse alluvium. Milestone 25.1 (Table 3) was completed on schedule. Major accomplishments include the following:

- **Geophysical Investigations**: Casual use permits for the detailed geophysical investigations were obtained for southeastern Gabbs Valley.
- **GeoProbe Drilling**:
    - Selected drilling locations and performed necessary GIS work.

- Submitted Notice of Intent (NOI) to Carson City BLM office.
- Received signed CatEX for Gabbs Valley GeoProbe work.
- Notified NDOM of intent to perform work and submitted all necessary documents. Permits were approved.
- Coordinated with Nevada Exploration, Inc. to perform probe work-mob and secured tentative mobilization dates.
- TG drill data suggested that water table was too low (60-80 m deep) for the GeoProbe rig, so mobilization was canceled.
- Further explored option of using Nevada Exploration's reverse circulation air drilling rig to reach water table and obtain a clean water sample for geothermometry, but presence of coarse alluvium precluded this option.

- **TG Drilling**:
  - Selected wellhead locations and performed necessary GIS work.
  - NOI submitted to BLM.
  - Received CatEX for TG drilling.
  - NEPA review submitted and accepted by DOE.
  - Worked with NDOM to issue permits and API #s.
  - Drilling commenced on May 25, 2018 and was completed in June 2018. Six holes were drilled.
  - Filed all completion reports with drilling information with NDOM and BLM.
  - P&A of all TG holes was completed on June 5, 2019.

Table 3. Milestone Summary for Budget Period 3

Recipient Name: Nevada Bureau of Mines and Geology, University of Nevada, Reno

Project Title: Discovering Blind Geothermal Systems in the Great Basin Region: An Integrated Geologic and Geophysical Approach for Establishing Geothermal Play Fairways

Task #	Task Title or Subtask Title	Milestone or Go/No Go Pt	Milestone # or Go/No-Go Pt #	Milestone Description and Decision Criteria	Milestone Verification Process	Ant. Mo.	Ant. Qtr	Comp. Qtr
25	Permitting of Drilling Sites	Milestone	M25.1	Permits for drilling at 2-4 sites	Completed permits for drilling Geoprobe and/or TG wells at 2-4 sites	2	Q1	Q5
26	Geoprobe Drilling	Milestone	M26.1	Drilling of Geoprobe boreholes	Completed drilling of as many as 6 boreholes each at 2-3 sites	5	Q2	Q4
26	"	Milestone	M26.2	Evaluation of Results of Geoprobe Drilling	Interpretation of results of Geoprobe drilling at 2-3 sites	6	Q2	Q4
27	Temperature-Gradient Drilling	Milestone	M27.1	Drilling of TG holes	Completed drilling of as many as 5 TG wells in 2-3 sites	12	Q4	Q6
27	"	Milestone	M27.2	Temperature logs of TG wells	Completed temperature profiles in GIS database of TG wells	12	Q4	Q8
27	"	Milestone	27.3	Evaluation of Results of TG Drilling	Interpretation of results of TG drilling at 2-3 sites	12	Q4	Q8
28	Geochemical Analyses	Milestone	M28.1	Acquisition of new Geochemical Data from Geoprobe Boreholes	Completed geochemical analyses in GIS database for Geoprobe boreholes	9	Q3	Q4
28	"	Milestone	M28.2	Geochemical characterization of 2-3 sites	GIS database/geochemical assessment of 2-3 study areas	12	Q4	Q6
29	Potential Field Geophysical Surveys	Milestone	M29.1	Acquisition and Processing of New Ground Magnetic Data	GIS database of ground magnetic data for two study areas	4	Q2	Q3
29	"	Milestone	M29.2	Interpretation of Ground Magnetic Data	Completed interpretations of new magnetic data with maps showing data in GIS database	6	Q2	Q5
29	"	Milestone	M29.3	Acquisition and Processing of New Gravity Data	GIS database of new detailed gravity data for two sites	4	Q2	Q3
29	"	Milestone	M29.4	Forward/Inverse Modeling of Gravity Data	GIS database of forward and inverse modeling of gravity for two sites, including 3D inversion of gravity data	12	Q4	Q7
29	"	Milestone	M29.5	Interpretation of Gravity Data	GIS database and maps showing interpreted gravity data with inferred faults	12	Q4	Q6
30	Magnetotelluric Surveys	Milestone	M30.1	Acquisition of new MT Data	GIS database of new MT data for two sites	3	Q1	Q3
30	"	Milestone	M30.2	Interpretation of new MT Data	Digital map showing slip-dilation tendency of faults for detailed study areas	6	Q2	Q6
31	3D Modeling	Milestone	M31.1	Construct new 3D models for 2-3 sites	3D models constructed from geologic map data and geophysical data for some of the sites studied in detail (~2-3 sites)	15	Q5	Q8
32	Conceptual Models and Resource Capacity Estimates	Milestone	M32.1	Revised Conceptual Models	Revised conceptual structural and stratigraphic models for potential geothermal systems for 2-4 sites	17	Q6	Q8
32	"	Milestone	M32.2	Resource Capacity Estimates	Quantitative resource capacity estimates integrating geologic, geophysical, and geochemical data sets	17	Q6	Q8
33	Final Reporting and Project Review	Milestone	M33.1	Synthesis of Project into Final Report and Presentation	Submittal of report and databases	18	Q6	Q10

Granite Springs Valley: All permitting requirements were completed for northern Granite Springs Valley for both GeoProbe and TG drilling with no major variances. Milestone 25.1 was completed on schedule. Major accomplishments include the following:

- **Geophysical Investigations**: Casual use permits for the detailed geophysical investigations were obtained for northern Granite Springs Valley.
- **GeoProbe Drilling**:
  - Finalized permits with Winnemucca BLM office and received signed CatEX.
  - Coordinated with NDOM to issue permits/API #s.
  - Mobilized/supervised HEATC LLC for GeoProbe drilling in January 2018 and subsequent P&A. Clean water samples were not obtained.
  - Coordinated with Nevada Exploration, Inc. to organize next GeoProbe mobilization to Granite Springs Valley.
  - Submitted new NOI to Winnemucca BLM office to perform additional GeoProbe work in Granite Springs Valley in order to obtain clean water samples.
  - Notified NDOM of intent to perform additional GeoProbe work and obtained required permits.
  - Additional GeoProbe work was completed by Nevada Exploration, Inc. in July 2018.
- **TG Drilling**:
  - TG drill locations were selected in July 2018 after final GeoProbe work was completed.
  - Visited location for road and proposed well-site reconnaissance to assess feasibility of TGH rig access; slightly modified planned drilling sites based on these findings.
  - Permitted all new TG hole locations with NDOM and BLM; received signed CatEX from BLM.
  - NEPA requirements completed and approved by DOE.
  - Coordinated access to well for drilling water with local rancher.
  - Mobilization began on October 29, 2018. Initial drilling was slowed by equipment problems and then delayed by ~2 months due to government shutdown. TG drilling was then slowed by wet winter weather. Six holes were completed in February 2019.
  - Filed all completion reports with drilling information with NDOM and BLM.
  - P&A reports were submitted to NDOM for all locations.
  - P&A was to be completed in March 2020 after final temperature logs were obtained in January 2020. However, P&A has been delayed by the COVID-19 pandemic.

Task 26.0. GeoProbe Drilling: Planned GeoProbe borings include six 100-200 ft (31-62 m) in up to three of the Phase 2 detailed study areas, with southern Gabbs and northern Granite Springs Valleys as priority. GeoProbe drilling involves installation of temporary boreholes that allow temperature measurement and collection of water samples using GeoProbe technology (to be conducted by a subcontractor). GeoProbe will be used to obtain rapid, cost-efficient shallow temperatures and water samples at each site to help refine drilling targets for more costly TG wells. Each boring will be evaluated as it is drilled, allowing flexibility to alter locations and boring depths to accommodate specific conditions. Thus, the depths and number of borings may vary somewhat to accommodate the best use of available budget for the particular conditions.

Milestones **26.1** (drilling of up to six GeoProbe boreholes) and **26.2** (evaluation of GeoProbe results) were completed for Granite Springs Valley (Table 3). However, local conditions precluded GeoProbe drilling at Gabbs Valley.

Gabbs Valley: GeoProbe drilling was not conducted in southeastern Gabbs Valley due to the relatively deep water table and presence of coarse alluvium. Funding did not allow for consideration of a third site. The lack of GeoProbe drilling at Gabbs Valley precluded acquisition of water samples for geothermometry analyses.

Granite Springs Valley: Ten shallow GeoProbe holes were drilled in northern Granite Springs Valley in January and July of 2018 to a maximum depth of ~50 m (Table 4; Figure 27). The primary goal of the GeoProbe efforts was to collect water samples for chemical analysis, identify chemical characteristics of subsurface fluids in the vicinity, and estimate possible reservoir equilibration temperatures using geothermometry relationships. GeoProbe drilling in Granite Springs Valley was focused in the vicinity of the most widespread sinter deposits in the southern and northern parts of the area (Figure 27).

The initial GeoProbe set up used to probe five holes in January 2018 was not able to penetrate any deeper than 30 m (with the exception of GSV-11 in the middle of the playa). Water samples were retrieved from some of these holes, but we were not able to filter them sufficiently for water chemistry analysis. A second more-powerful GeoProbe setup, with improved water sampling capability, was conducted by Nevada Exploration, Inc., and used to probe five additional holes in July 2018. This campaign was successful in obtaining four water samples. These samples still contained a high suspended load but were able to be filtered in preparation for water chemistry analysis.

The probe holes were logged immediately after the maximum probe depth was reached (i.e., the probe could not go any deeper due to intersecting either a dense clay layer or hard barrier such as cobbles or bedrock). Five holes were logged fully, and a point temperature measurement was collected in GSV-11 at total depth. The highest temperature of 46°C was recorded in GSV-14 at ~50 m depth (Figure 28). The coolest temperatures were encountered in GSV-1 and GSV-11. Logs collected in GSV-14 and GSV-20 show the influence of summer air temperatures, as indicated by the increasing temperature toward the surface to ~25°C.

The GeoProbe temperature data show some differences in their shallow profiles when compared to the data obtained from the deeper TG holes (Figure 29). This may partly reflect differences in hole location, as some of the GeoProbe and TG holes were purposefully located close together but may be separated by 10's of meters in some cases. One example is the temperature log in GeoProbe hole GSV-6 in the southern focus area. This demonstrates a steeper geothermal gradient that is substantially higher than TG well 68-14, which is immediately adjacent. It is not clear whether this reflects anomalous frictional heating of the probe hole during penetration, or is a real thermal feature of the subsurface in this area. This area warrants further investigation, given the presence of a large paleo-sinter deposit at this location.

Task 27.0. Temperature-Gradient (TG) Drilling: TG wells will be drilled using information obtained from the GeoProbe results to refine drill locations. This drilling will be carried out by the USGS and will be funded directly by the DOE. UNR will provide onsite technical assistance during the drilling, including 1) logging of cuttings, 2) review of drilling progress and results, 3) input to DOE, BLM, and other UNR team members (not on site), and 4) determining next steps in drilling program depending on results, permitting framework, and input from the USGS and DOE. The initial results will be evaluated to determine if deeper or shallower TG wells would best define the geothermal system. Unanticipated findings will be incorporated into the decision-making process to maximize the information obtained with available budgets. Temperature logs will be run in the gradient wells immediately after completion and three additional times thereafter to assure that temperatures have equilibrated. As many as five 500-750 ft (150-230 m) TG wells are planned at two sites.

Go/No-Go: Prior to mobilization for drilling, UNR will submit a complete permit package and updated NEPA questionnaire and associated data for review by DOE. USGS will not mobilize to any study area or begin any fieldwork until DOE completes environmental reviews and provides written authorization to proceed. These conditions were met and the go/no-go decision point was satisfied.

The budget permitted drilling of six TG holes at both southeastern Gabbs Valley and northern Granite Springs Valley. **Milestones 27.1** (Drilling of as many as five TG wells 500-750 ft (150-230 m) deep at 2-4 sites), **27.2** (Completion of temperature logs of TG wells), and **27.3** (Evaluation of results of TG drilling) were completed for both southeastern Gabbs Valley and northern Granite Springs Valley (Table 3). Results and interpretations are described below.

Table 4: GeoProbe Holes, Granite Springs Valley

Probe ID	Date	TG measurement collected?	Clean water sample collected?
GSV-1	Jan-18	Y	N
GSV-3	Jan-18	N	N
GSV-4	Jan-18	Y	N
GSV-6	Jan-18	Y	N
GSV-8	Jul-18	N	Y
GSV-11	Jan-18	Y	N
GSV-14	Jul-18	Y	Y
GSV-15	Jul-18	N	Y
GSV-16	Jul-18	N	N
GSV-20	Jul-18	Y	Y

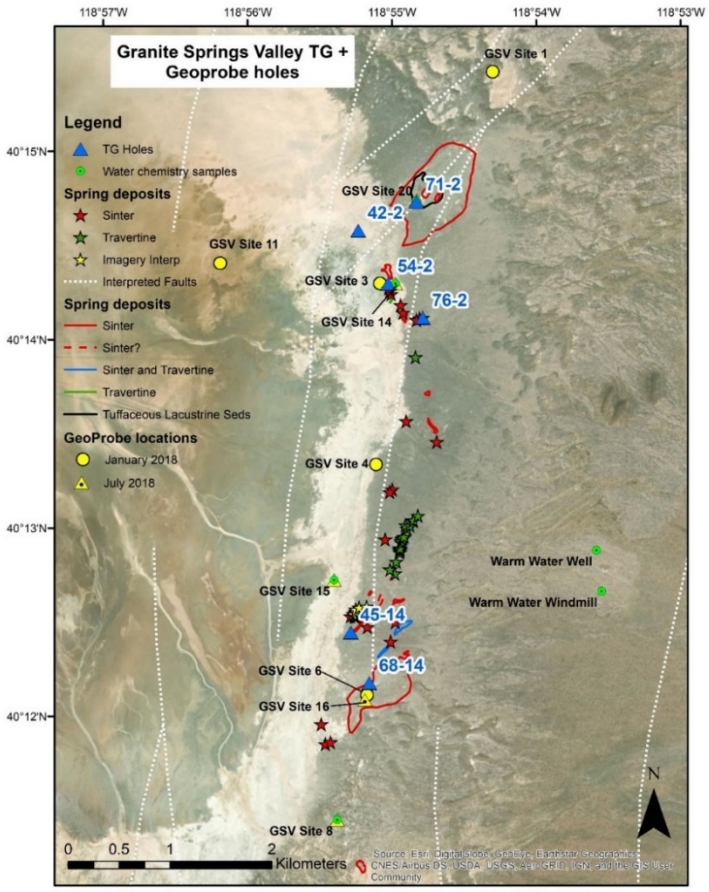

Figure 27: Location of GeoProbe and TG holes drilled in Granite Springs Valley during Phase 3 of the Nevada Geothermal play fairway project.

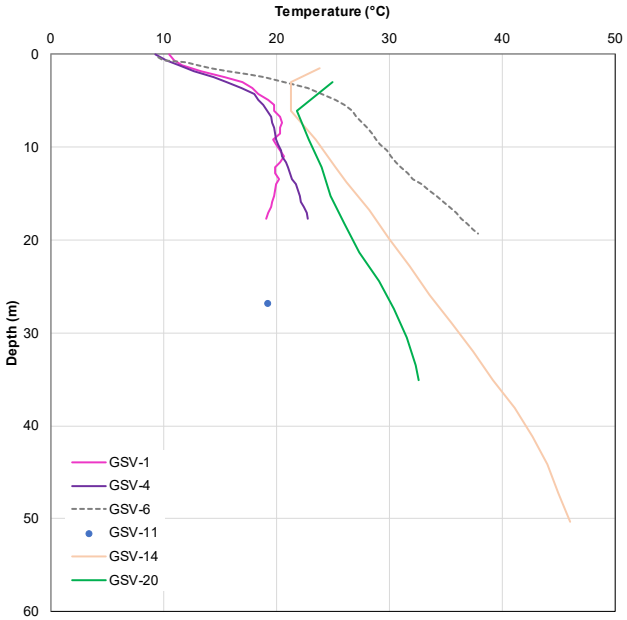

Figure 28: Shallow temperature data obtained from the GeoProbe drilling.

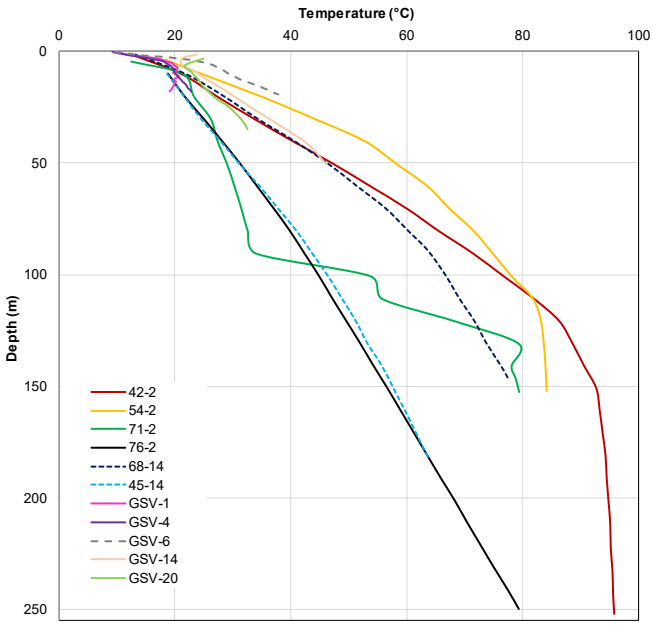

Figure 29: Shallow temperature data obtained from the GeoProbe drilling compared with the deeper TG hole dataset.

Gabbs Valley: Six TG holes were drilled in late May through June 2018 by the U.S. Geological Survey research drilling unit to a depth of ~152 m (500 ft). The holes were distributed roughly across the extent of the shallow-temperature and geophysical anomalies (Figure 30). However, the actual location of the drill holes was somewhat constrained by budgetary and time constraints, ease of access from existing roads, and the nearby boundary of a Wilderness Study Area, where drilling was not allowed.

Six temperature surveys were completed in the holes from June 9, 2018 to April 17, 2019 to ensure that TG profiles had equilibrated (Figure 31). Estimates of the water table depths were used to ensure that the temperature logs were run slowly through the air-filled sections of the TG holes, so that the temperature tool could equilibrate at each depth interval. Holes 65-33 and 87-3 maintained the highest water elevations of 1356 and 1380 m, respectively. The water elevations in holes 41-1, 85-3, 31-2, and 52-2 all settled to within 1312 to 1297 m (Figure 31) by the final survey, and this may correspond to the local elevation of the water table through the area. The proposed water table elevations are slightly greater than the water table elevation of 1284 m reported in agricultural wells at a nearby ranch in the northwestern part of the study area (well logs sourced from http://water.nv.gov/), which is compatible with the location of the TG holes in a topographically higher part of the valley up hydrologic gradient from the ranch.

Holes 31-2 and 52-2 yielded the greatest maximum temperatures with bottom-hole values of 114.5°C and 124.9°C, respectively. Both of these wells exhibit relatively linear, high temperature gradients, extending from the surface down to isothermal zones at near boiling temperatures about 20 m above the inferred water table (Figure 31). The high temperature gradient continues 5-10 m below the water table and then rolls over to relatively low temperature gradients before becoming isothermal in the lower 20 m of each hole. Holes 87-3, 41-1, and 85-3 are cooler than 31-2 and 52-2, but all have anomalously high temperature gradients ranging from 190 to 400°C/km and reach temperatures of 47.6 to 79.2°C. Holes 87-3 and 85-3 exhibit linear temperature gradients from 20-30 m depth to TD (Figure 31). Hole 41-1 exhibits a slightly steeper temperature gradient below the inferred water table. Hole 65-33 has a temperature gradient of 57°C/km, which is within background temperature gradients for the Great Basin region (Coolbaugh et al., 2005). Overall, these TG holes captured the peak of the thermal anomaly along a northeast-southwest transect (Figure 30), but the thermal anomaly is not constrained to the northwest or southeast of this transect.

The temperature gradients and MT data permit some first-order interpretations of the geothermal aquifers in southeastern Gabbs Valley. Based on the MT data and apparent depth of the low resistivity

anomaly, it is likely that all TG holes did not penetrate to an inferred clay cap to the geothermal system. The upper isothermal zones (Figure 31) in 31-2 and 52-2 may correspond to perched thermal outflow aquifers connected to a structurally bound aquifer of greater elevation located laterally from these holes. The isothermal zone in the lower 20 m of each of these two holes likely represents mixed water, flowing laterally through a permeable zone in basin-fill sediments (e.g., coarse sandstone or gravel) near the inferred clay cap.

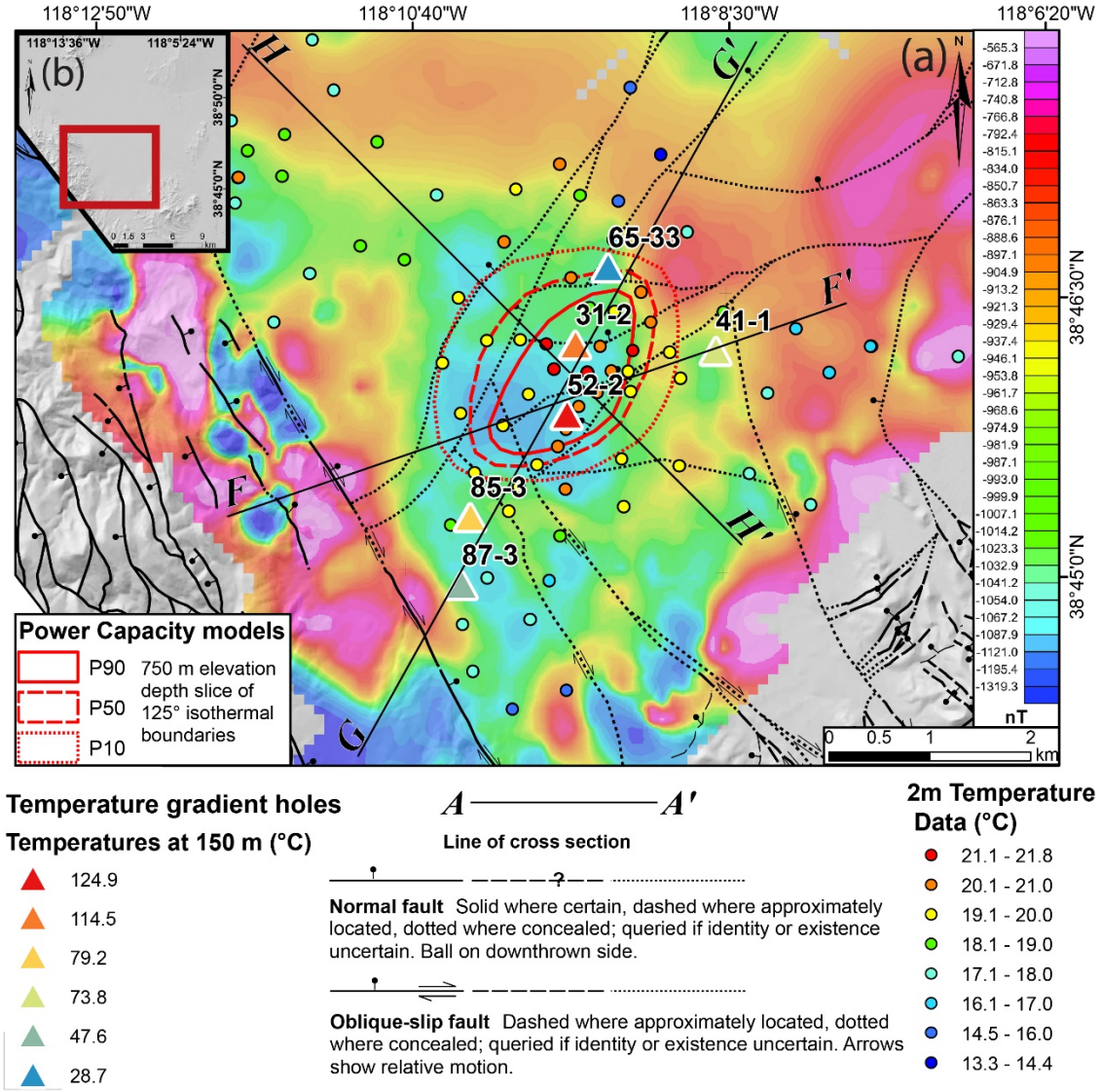

Figure 30. (a) Map view of thermal anomaly area with 2-m temperature survey data, TG hole locations, projected depth slice (750 m) of power capacity models, and cross section profiles, all overlain on the magnetic survey. Location of TG holes (colored triangles) with respect to the favorable structural setting (red dashed ellipse) and inferred faults (black lines). Warmer colored triangles indicate higher bottom-hole temperatures at 152 m. Cross sections F-F' through H-H' and conceptual resource capacity models (Task 32). The 750 m depth slice of the 125°C isotherm in the P90, P50, and P10 models is projected to the surface and shown as red dotted, dashed, and solid polygons, respectively. Basemap is reduced to pole magnetic map of study area overlain on DEM hillshade. Warmer colors indicate relatively higher magnetic values (nT) than cooler colors. **(b)** General study area showing location of map as red polygon.

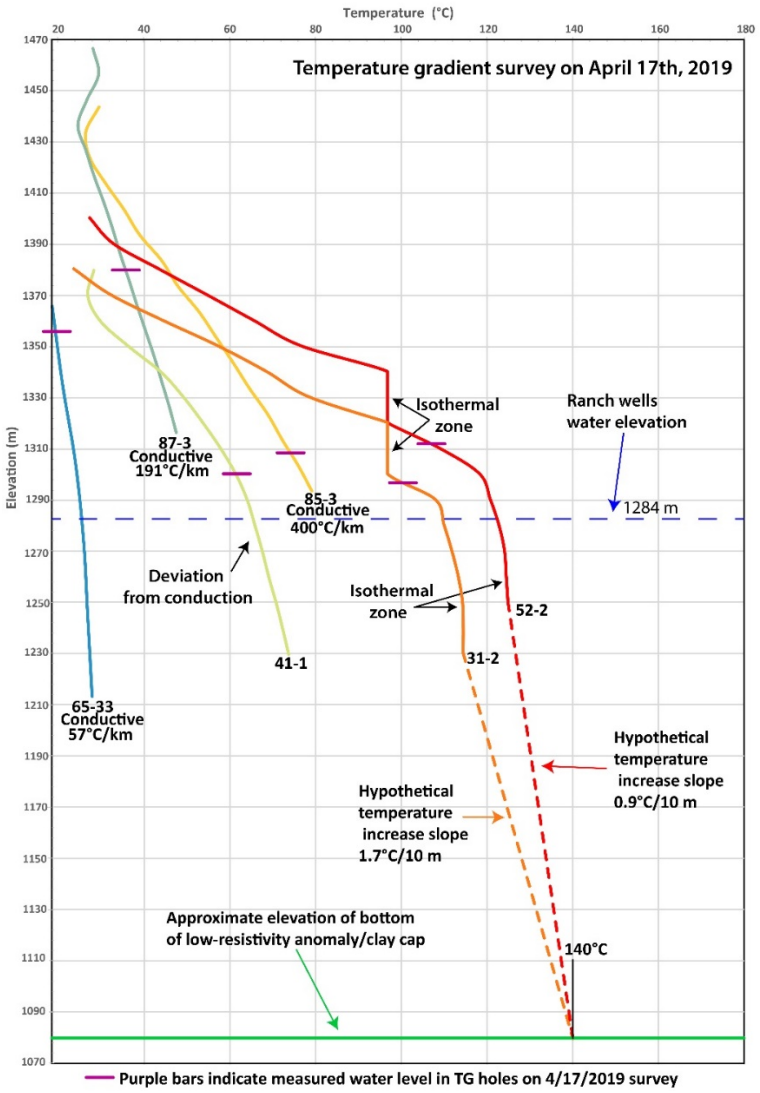

Figure 31. Temperature-gradient data for southeastern Gabbs Valley. Final temperature-gradients shown here were measured on April 17, 2019, approximately 10 months after drilling. Temperature (°C) vs. depth (m) graph with drill-hole names and annotated interpretations. For wells displaying conductive gradients, the calculated linear gradient is extended to 1 km to yield a °C/km estimation for reference, which is listed below the well name. Measured water levels in TG holes on the April 17, 2019 survey shown as purple bars on temperature gradient graphs for each of the holes. Dashed blue line shows measured static water elevation of 1284 m in agricultural wells at the ranch in the lower part of the valley. Temperature gradients for holes 31-2 and 52-2 are projected below the completed depth of drilling as dashed lines to a temperature of 150°C at the approximate elevation of the base of the low-resistivity anomaly (1080 m) to show potential for the median (P50) resource capacity estimate (see discussion in Task 32).

Granite Springs Valley: Six TG holes were drilled in Granite Springs Valley between November 2018 and February 2019, from ~150 to 250 m total depth. The locations of the wells were targeted on the basis of the GeoProbe results (measured temperatures and geothermometry estimates from the fluid samples described in Task 28), local geology (presence of paleo-sinter deposits), and interpreted structural framework (fault locations and basin geometry developed from the geological and geophysical datasets). Four wells were proposed for the northern focus area, given the more promising geothermometry estimates, as well as proximity to the intersection of several blind faults that may host more fracture permeability (Figure 32).

Two wells were drilled in the southern focus area. Although geothermometry estimates are slightly lower (~20°C) for this location, extensive paleo-sinter deposits suggest past geothermal fluid upflow. All wells were logged multiple times over a period of ~12 months to capture the thermal recovery after drilling and return to equilibrium conditions. The logging was done using a hand-winched wireline cable with a platinum resistance temperature device (RTD).

The results show that all wells, with the exception of well 76-2, experienced temperature recovery (increases) through time (Figure 33), although most appear to attain thermal equilibrium within 2 months of drilling (i.e. the temperature profiles show minimal changes after this time). Comparison of all logs together reveal that the warmest temperatures were encountered in well 42-2 in the northern focus area (Figure 34).

Four of the six TG holes show evidence of hydrothermal fluid movement: wells 42-2, 54-2, 71-2, and 68-14. Well 42-2 in the northern focus area in GSV records the highest subsurface temperatures of ~96°C and has an isothermal profile in the lower 100 m of the hole (Figure 33a) that is interpreted to reflect geothermal fluid upflow. Well 54-2 shares a similar character (Figure 33b), with a short isothermal section at the bottom of the hole that also suggests geothermal fluid upflow, although at a lower temperature than in well 42-2 (~85 °C). Well 71-2 shows some variability in subsurface temperatures with depth and also includes a small temperature reversal (Figure 33c). The upper portion of this temperature log (top 90 m) records the lowest geothermal gradient of all wells. This may reflect lateral flow of cold, shallow groundwater that depresses the isotherms in this area. However, this well is up hydrologic gradient to well 42-2, and the temperature profile in well 42-2 shows no evidence of this possible shallow cold, groundwater flow. A northeast-striking fault is interpreted to pass between well 71-2 and 42-2. It is possible that this fault could be a hydrologic barrier to shallow fluid flow, and shallow groundwater is diverted to the north or south. Alternatively, the section of lowest geothermal gradient may reflect background gradients in Granite Springs Valley that have not been influenced by either convective or conductive heat transfer from geothermal fluid upflow. Below this 90 m thick interval, temperatures rapidly increase to a maximum of ~80 °C at 150 m depth. This temperature is close to the maximum temperatures measured in wells 42-2 and 54-2, and thus may reflect a contribution from the same upflow source. The minor temperature reversal at the base of the well may suggest intersection with a narrow outflow plume of the geothermal fluid. This temperature reversal appears to be a robust feature of the data, given that it is measured in multiple logging runs over the >12 month period. Geothermal fluids could be flowing up the fault that lies directly to the west of well 71-2, with some leakage up-dip or along the fault to produce the thermal anomalies in 71-2, with the majority of the fluid flowing basin-ward to the west (as encountered in 42-2). Alternatively, another thermal outflow plume could be responsible for the temperature reversal (of unknown source).

The curved temperature profile measured in TG hole 68-14 (Figure 33f) also suggests hydrothermal influence, given its deviation from a straight, conductive profile and similarity to the profile in TG hole 54-2. TG holes 76-2 and 45-14 show conduction-dominated profiles (i.e. ~ constant geothermal gradients), suggesting minimal permeability (Figures 33d, 33e, and 34). However, the calculated geothermal gradients across the short depth interval (<250 m) of both profiles are high (>220 °C/km), which is much greater than typical background geothermal gradients in the Great Basin (~40 - 60 °C/km). One interpretation is that these areas are impermeable, but proximal to geothermal upflow locations and subject to conductive heating by these convective upflows.

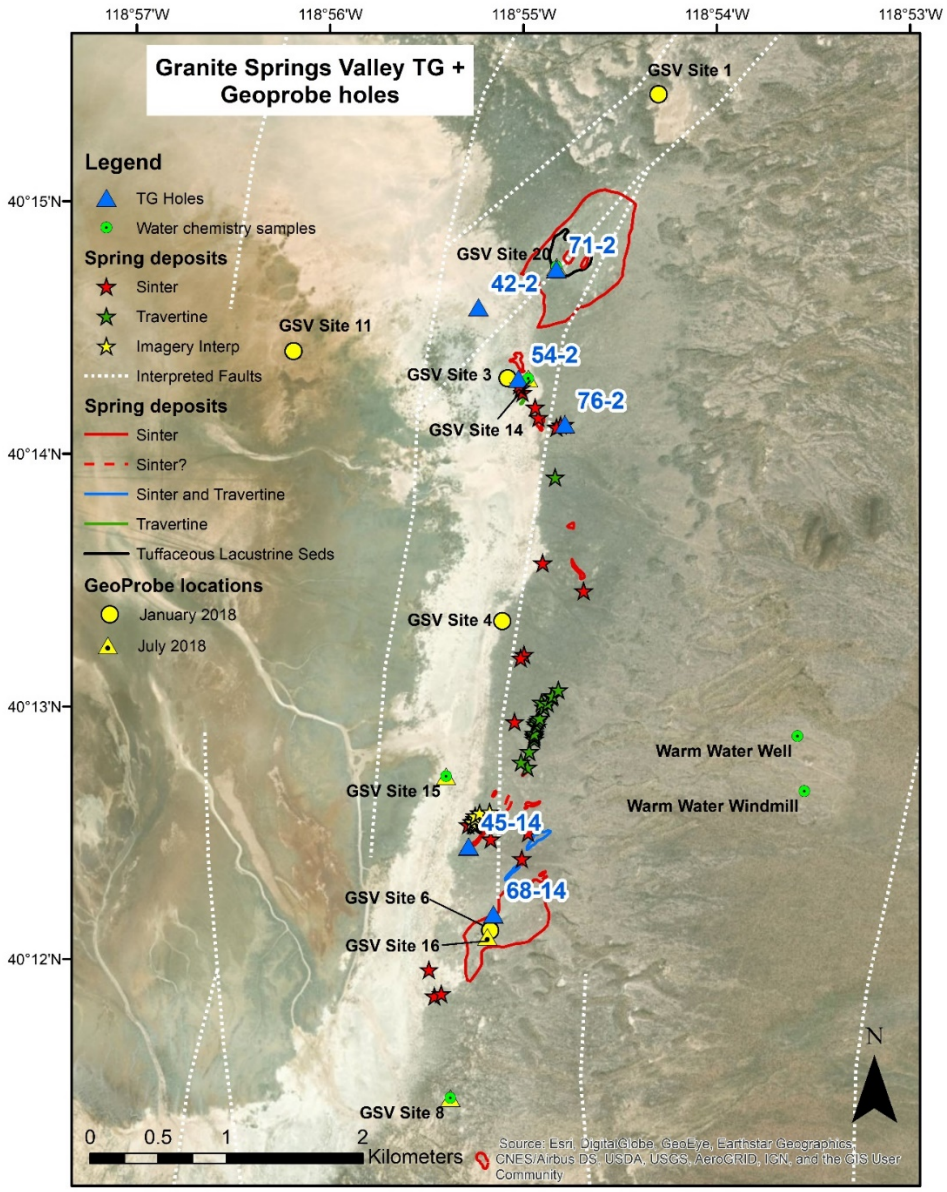

Figure 32: Location of thermal gradient (TG) holes drilled in Granite Springs Valley during Phase 3 of the Nevada play fairway project.

In summary, the TG drilling program successfully identified multiple thermal anomalies in Granite Springs Valley and obtained a maximum measured temperature of 96°C at 250 m depth. The temperature log profiles demonstrate convincing indications of hydrothermal fluid flow (including upflow). However, the precise locations of geothermal upflow are not well constrained. Temperature logs collected from wells drilled proximal to one another show some notable differences (particularly well 71-2), suggesting geological complexity (which could be related to the inferred complex fault intersections in this northern area). Further work to constrain the conceptual model of the resource is required, including refining geological cross sections and populating these with known and inferred isotherm distributions.

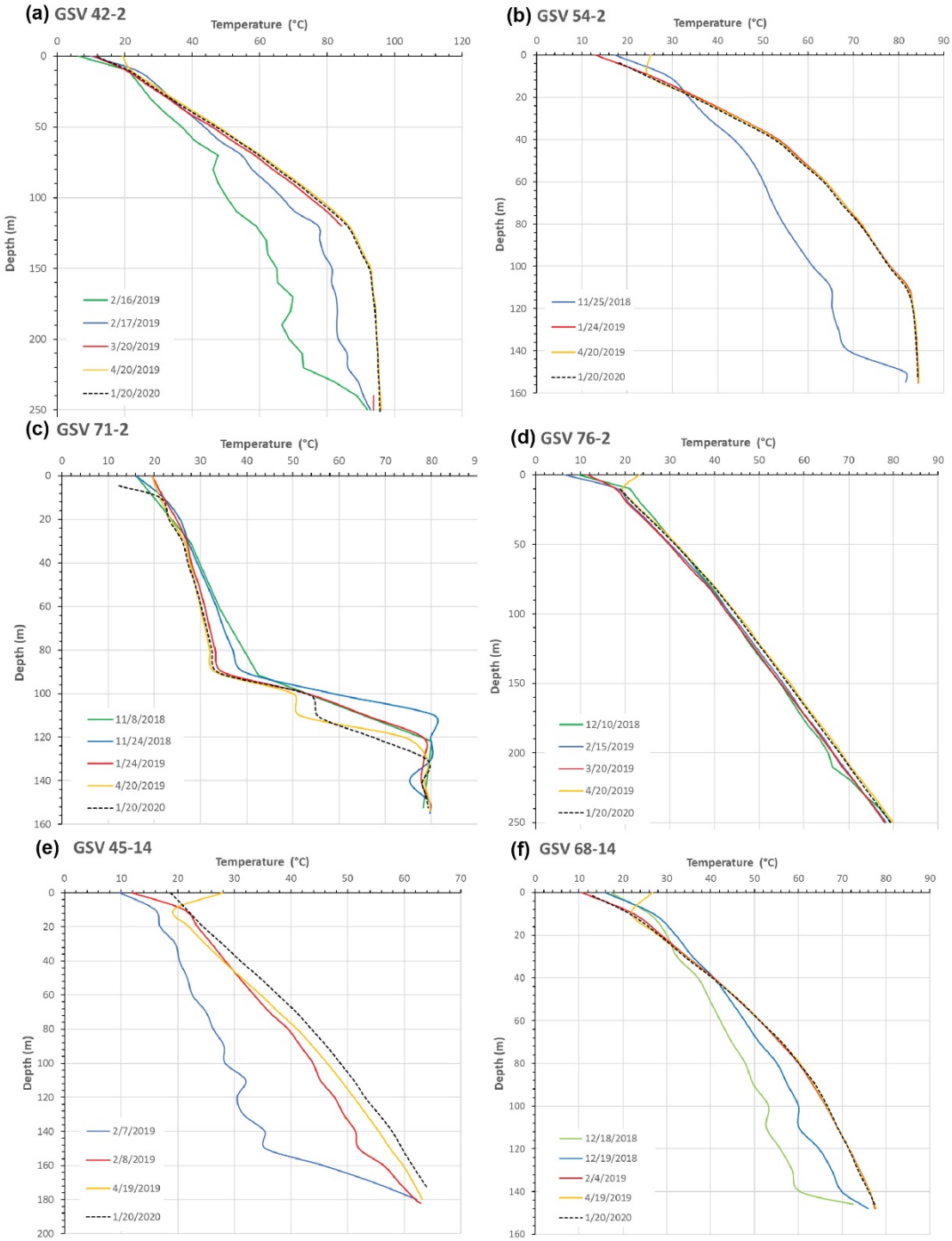

Figure 33: Temperature logs collected from TG holes in northern Granite Springs Valleys. (a) TG hole 42-2 in the northern focus area. (b) TG hole 54-2 in northern focus area. (c) TG hole 71-2 in northern focus area). (d) TG hole 76-2 in northern focus area. (e) TG hole 45-14 in the southern focus area. (f) TG hole 68-14 in southern focus area.

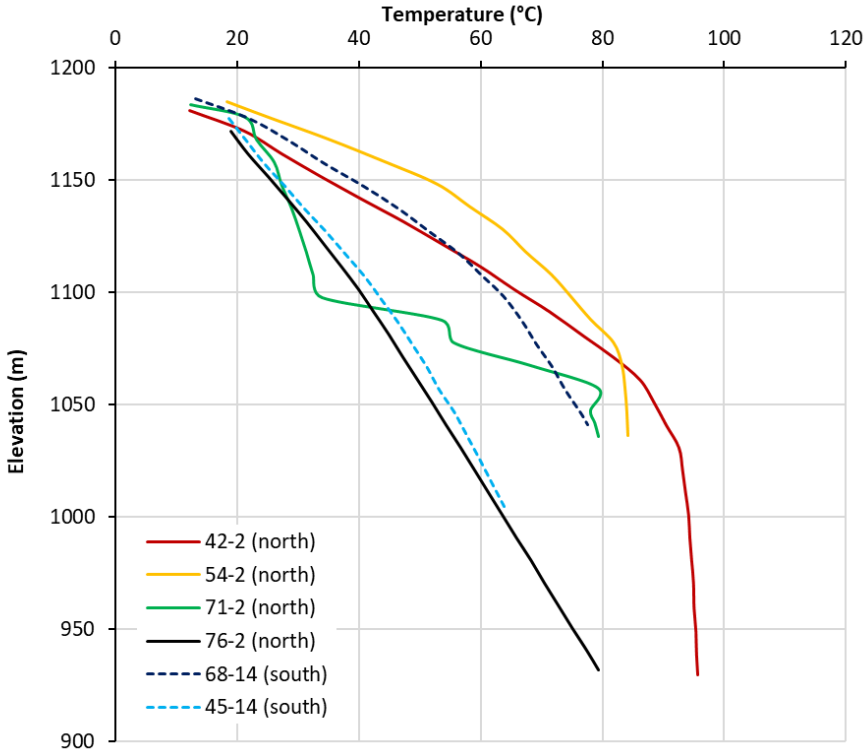

Figure 34: Most recent temperature logs collected in the six TG holes at Granite Springs Valley (logging date was January 20, 2020). Profiles are plotted against elevation; southern profiles are dashed.

Task 28.0. Geochemical Analyses/Fluid Sampling: Six GeoProbe water samples @ 100-200 ft (31-62 m) at up to three sites will be analyzed for major and trace element chemistry. Geothermometry will be calculated from the geochemical data. Water samples will be evaluated in the context of existing water data obtained in Phases 1 and 2 of the project to assess geothermometers and possible fluid relationships. **Milestones 28.1 (**Acquisition of as many as 18 new geochemical samples from up to three sites) and **28.2** (Geochemical overview of as many as ~18 new samples from three sites, including synthesizing new data with those data collected in Phases 1 and 2) were completed for Granite Springs Valley but were not be possible for any other sites.

Gabbs Valley: Because GeoProbe drilling could not be conducted at Gabbs Valley due to a deep water table and presence of coarse alluvium, water samples were not obtained at this site for geochemical analyses. Funding and time constraints did not allow for consideration of a third site.

Granite Springs Valley: Four new water samples were collected from four GeoProbe holes (Sites 8, 14, 15 and 20) that were drilled in Granite Springs Valley in early July 2018. Water samples were not collected from the new GeoProbe hole at Site 16, as no fluids were intersected (the GeoProbe intersected a hard, impenetrable layer at shallow depth). All fluid samples contained substantial suspended sediment load and required double filtering, involving first using an electric vacuum-pump system with a 5 µm filter size, followed by hand-filtering through a 0.45 µm filter. At each site, three sub-samples were collected: 1) one bottle for anion analyses (250 mL), 2) a bottle (250 mL) for cation analyses (acidified with HNO_3 to a pH of 2), and 3) bottle (125 mL) for stable isotopes ($\delta^{18}O$ and δD).

The chemical composition of the four samples varies, with total dissolved solids ranging from ~780 mg/L (Site 14), up to a high of ~24,000 mg/L at Site 15 (Table 5). However, the samples are all classified as alkali-chloride fluids (Figure 35). The only other samples with a similar composition were previously collected from two warm water wells ('Warm Water Well', and 'Windmill Well') (Figures 35 and 36),

which are located only a few kilometers from the GeoProbe sites. All other fluids previously reviewed and compiled in the broader Granite Springs Valley region for Phases 1 and 2 of the play fairway project are dominantly bicarbonate fluids, which is typically associated with shallow groundwater (Figure 35). These bicarbonate fluids are also lower in total dissolved solids (Figure 36). The four new fluids have stable isotope compositions that are similar to other samples collected from springs and wells in the region (Figure 37). The slight offset from the Global Meteoric Water Line likely reflects a combination of water-rock interaction and possible evaporation effects.

Geothermometry estimates for the GeoProbe water samples indicate some variability, especially among the cation geothermometers (Table 6). Such variability is relatively common given that the cation relationships are empirically derived using field data from a range of locations (e.g., including New Zealand and Iceland), which may have different reservoir mineral assemblages and/or higher-temperature geothermal systems than Granite Springs Valley and the Great Basin. Given this variability, the SiO_2 results are considered to be more reliable. The highest estimated temperature using the quartz (conductive) geothermometry relationship is associated with Site 20 (126°C), followed by Site 14 (101°C). This is consistent with the largest mapped areas of paleo-sinter deposition around Site 20 (Figure 38).

Table 5: Geochemical results for new water samples collected from GeoProbe wells in GSV.

Sample name	pH	Li	Na	K	Ca	Mg	SiO_2	B	Cl	F	SO_4	HCO_3	CO_3	Cond.	TDS	$\delta^{18}O$	δD	Charge balance
Unit		mg/L	mg/L	mg/L	mg/L	mg/L	mg/L	mg/L	mg/L	mg/L	mg/L	mg/L	mg/L	umhos/cm	mg/L	(‰)	(‰)	
GSV Site 8	9.53	<0.1[a]	1600	11	1.3	<0.5[a]	42	3.4	1400	15	250	370	290	7500	3200	-15.3	-128	6.7%
GSV Site 14	8.73	0.54	260	3.1	19	<0.5[a]	49	1.4	350	6.1	56	22	10	1600	780	-15.6	-129	1.6%
GSV Site 15	8.6	1.5	14000	110	3.8	1.4	34	1.4	14000	5	2800	2900	320	64000	24000	-13.7	-121	9.0%
GSV Site 20	9.05	0.45	280	5.7	6.8	<0.5[a]	81	1.4	330	11	53	31	32	1600	800	-15.6	-128	0.8%

a = detection limit

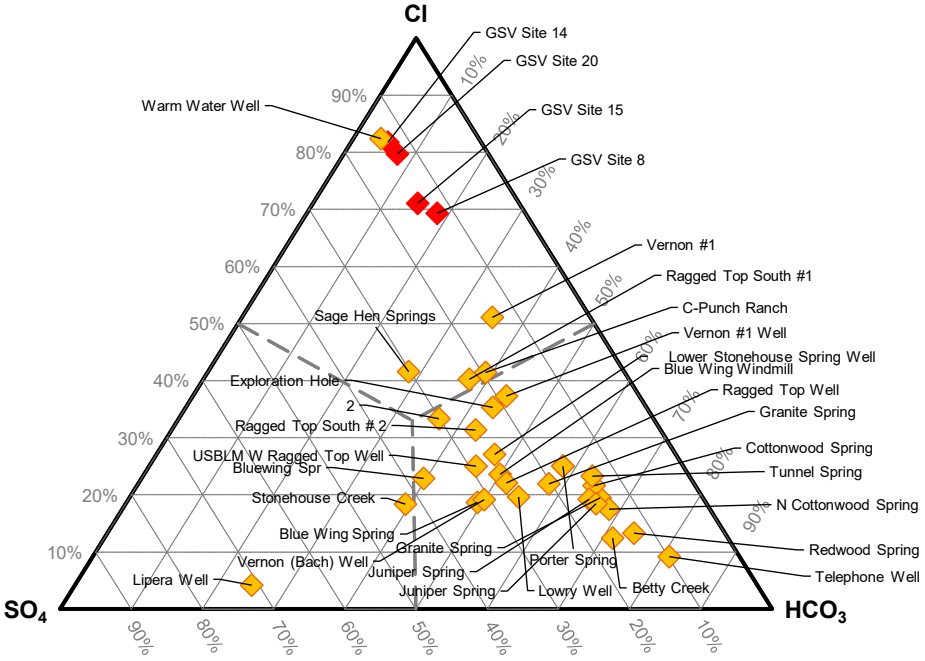

Figure 35: Chemical composition of fluids samples from new Geoprobe holes in GSV (red symbols), as well as samples from other wells and springs in the valley evaluated in Phases 1 and 2 of the Nevada Geothermal Play Fairway project.

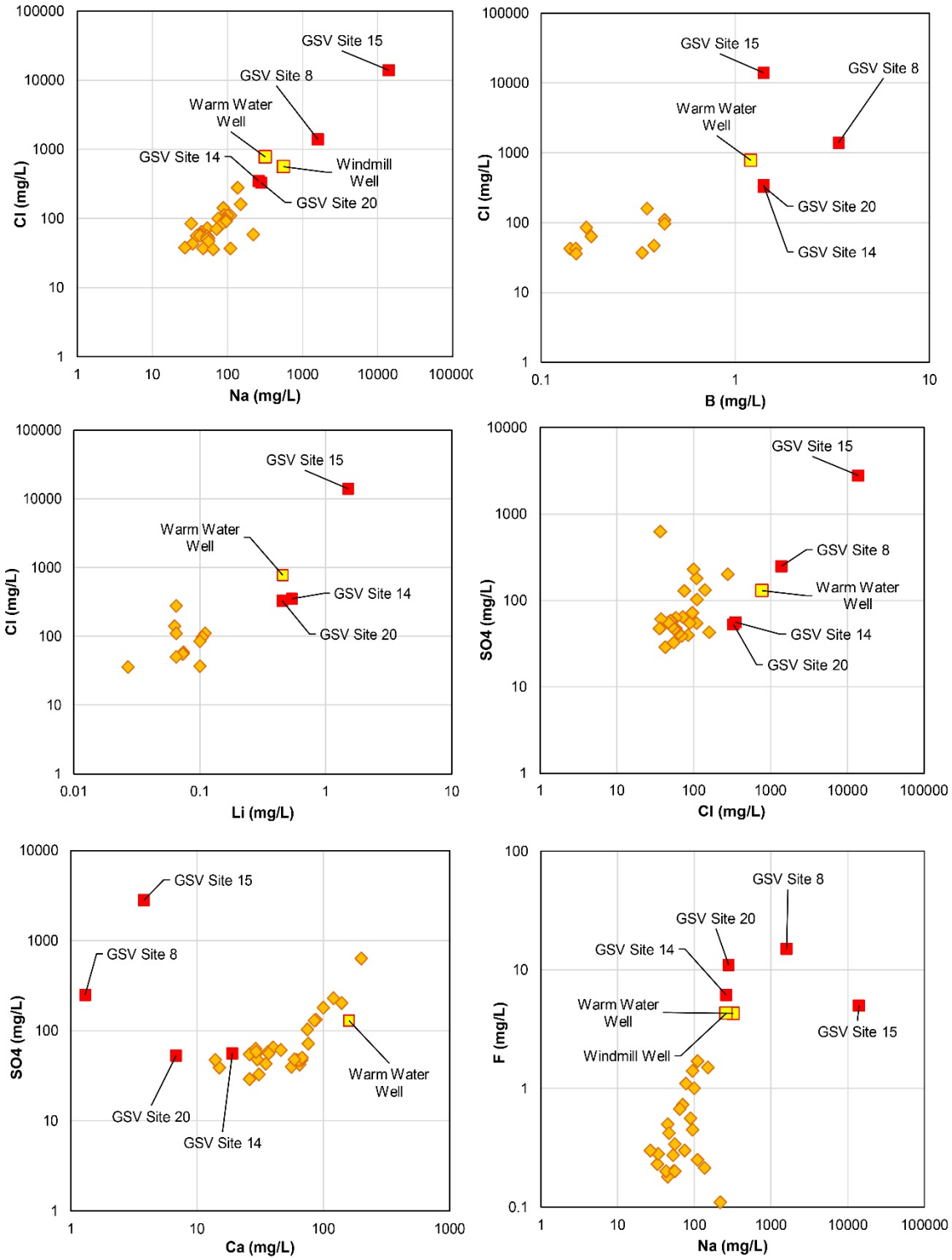

Figure 36: Chemical composition of fluids samples from new Geoprobe holes in GSV (red symbols), the two well samples that are located nearby (yellow symbols), and samples from other wells and springs in the valley evaluated in Phases 1 and 2 of the Nevada Geothermal Play Fairway project (orange symbols). Sample from the Windmill Well has an incomplete chemical analysis and is thus not shown on all plots. Note logarithmic axes for all plots.

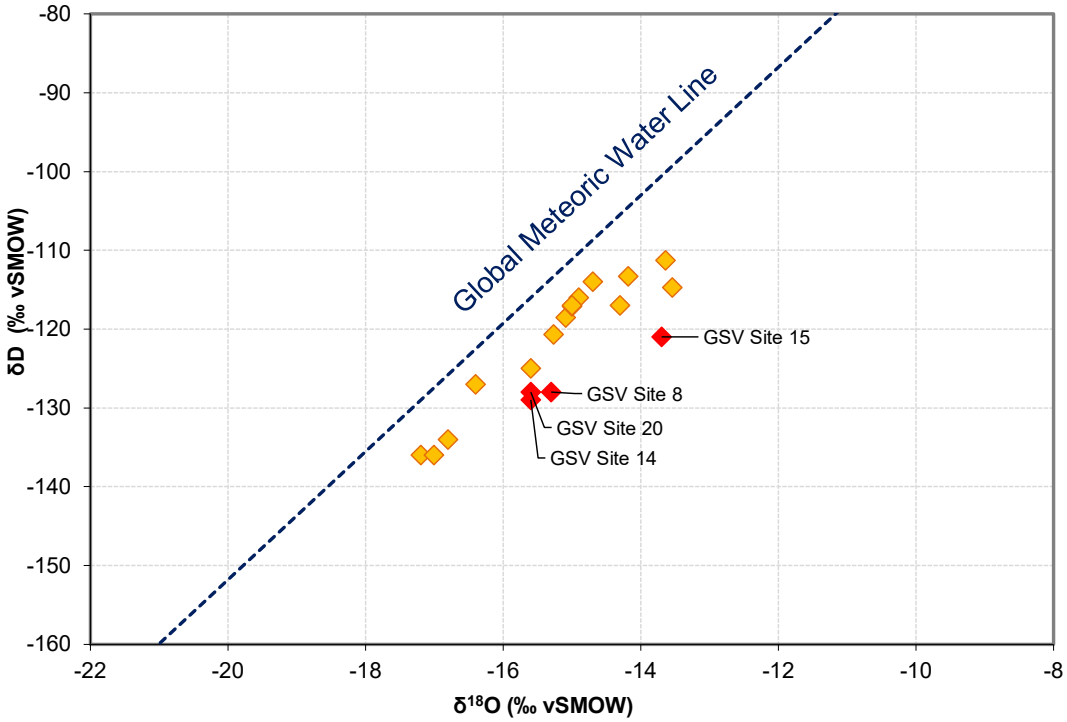

Figure 37: Stable isotope ($\delta^{18}O$ and δ D) characteristics of fluids samples from new Geoprobe holes in GSV, compared with existing data from other wells and springs in the region evaluated in Phases 1 and 2 of the Nevada Geothermal Play Fairway project.

Table 6: Geothermometry estimates for GeoProbe sites 8 through 20 in Granite Springs Valley, and the two well samples that are nearby (see Figure 38 for map location). The amount of variability in the results is not unusual. The quartz conductive results are generally the most reliable.

Sample Name	**Chalcedony conductive**	**Quartz conductive**	**Na-K-Ca**	**Na/K**	**Na/K**	**Na/K**	**Na/K**	**K/Mg**
Reference	*Fournier, 1977*	*Fournier & Potter, 1982*	*Fournier & Truesdell, 1973*	*Fournier 1979*	*Truesdell 1976*	*Giggenbach 1988*	*Arnorsson et al. 1983*	*Giggenbach 1988*
GSV Site 8	63.4	94.3	112.5	60.7	10.2	82.1	22.5	108.1
GSV Site 14	70.9	101.3	71.9	84.1	34.5	105.2	46.7	75.0
GSV Site 15	53.6	85.2	141.0	66.1	15.7	87.4	28.0	167.3
GSV Site 20	97.9	125.9	121.7	110.2	62.6	130.8	74.4	90.2
Warm Water Well	76.7	106.7	90.5	183.4	146.2	200.8	155.6	91.8
Windmill Well	75.8	105.8	89.6	178.6	140.6	196.3	150.2	92.5

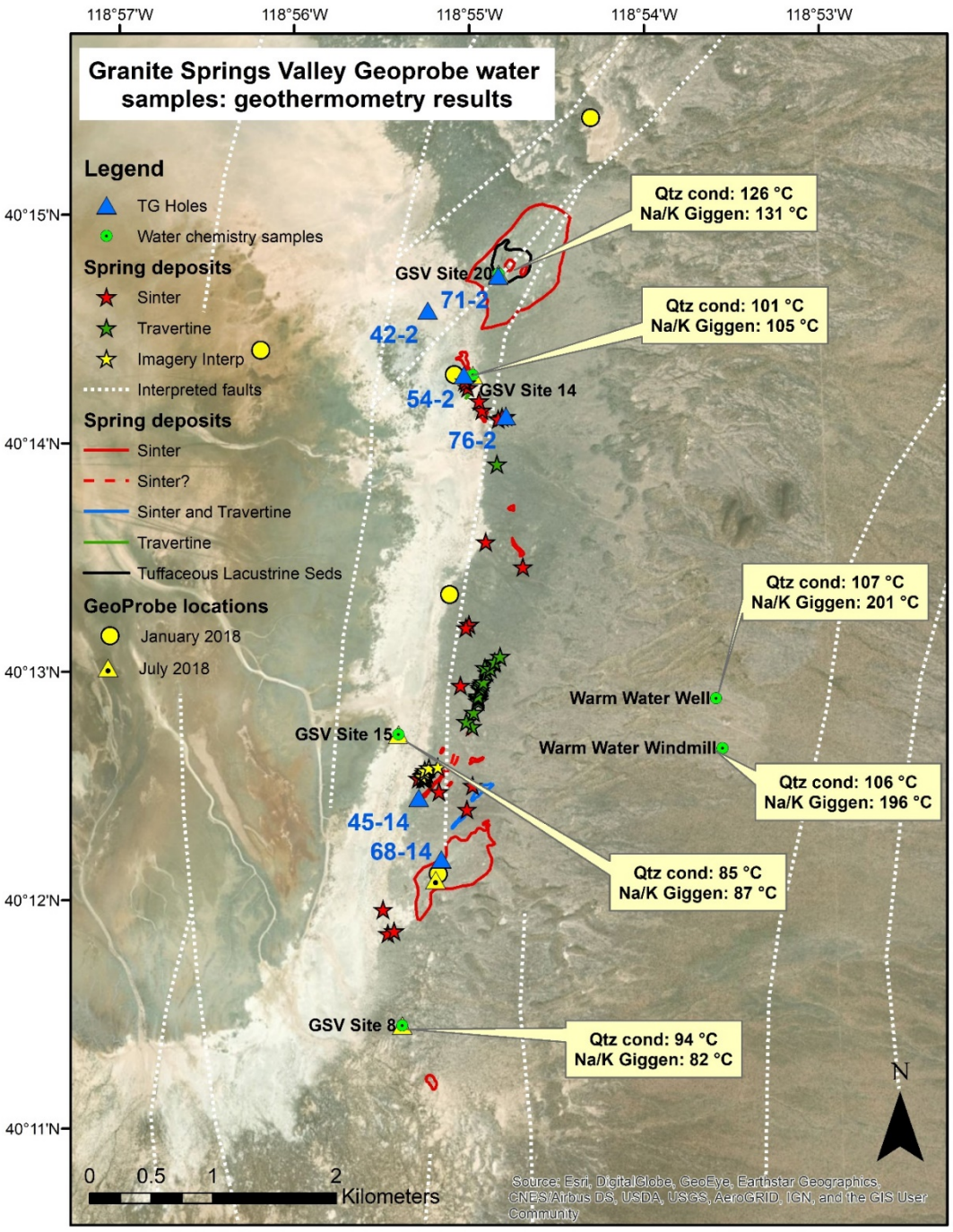

Figure 38: Location of Geoprobe holes in Granite Springs Valley and geothermometry summaries for the alkali-chloride fluids that were encountered in these holes. Geothermometry estimates for two nearby wells are also shown for comparison (Warm Water Well, and Windmill Well): these are also alkali-chloride fluids.

Task 29.0. Potential Fields Geophysical Surveys: A combination of detailed ground magnetics and gravity surveys will provide control on building and then testing 3D geological models of two of the detailed study areas. These areas are located in basins such that potential field geophysics will be key to defining primary elements of the structural and stratigraphic framework. We will use standard 3D modeling techniques focused on first developing detailed 2D cross-sections that provide the framework for the 3D

models. Therefore, 2D ground magnetics (up to 1500 km total) will be collected in combination with closely spaced gravity stations along lines perpendicular to structural grain in each area. The combination of ground magnetic and gravity, also supplemented by direct density and magnetic susceptibility measurements of samples from representative stratigraphic units, will enable detailed cross-sections to be constructed with these data and forward/inverse modeled. Together, these cross-sections will be integrated with surface mapping and available drill-hole data to build or refine 3D geological models. Gravity data will also be collected at 300 m spacing over the study areas so that the geologic model can be forward/inverse modeled. The detailed 2D models will ensure that the 3D model fits relatively closely with the geophysics. The 3D inversions and forward modeling will screen the model for inconsistencies for all areas between the 2D cross-sections. In total, up to 1000 new gravity stations will be collected between the two areas. The potential field geophysical surveys will be carried out by the USGS under supervision of UNR, and USGS personnel and will be funded directly by the DOE.

Overview of Potential Field Surveys: The detailed geophysical surveys during Phase 3 were focused entirely on Gabbs Valley and Granite Springs Valley (Table 3). Geophysical field work involved gravity and magnetics surveying, outcrop measurements, and rock property sample collection for laboratory analysis of magnetic remanence, density, and magnetic susceptibility. Specific accomplishments regarding these surveys are described below. All major milestones for this task were accomplished without variance and on schedule. These included:

- **Milestones: 29.1** – Completed acquisition of new ground magnetic data for two sites.
- **Milestone 29.2** – Interpretation of existing magnetic data for two sites.
- **Milestone 29.3** – Completed acquisition of new gravity data for two sites.
- **Milestone 29.4** – Forward and inverse modeling of gravity data for two sites.
- **Milestone 29.5** – Interpretation of existing gravity data for two sites.

Gabbs Valley: Three field sessions for gravity and magnetic surveying were conducted in southeastern Gabbs Valley. This included collection and processing of 480 new gravity stations and 300 line-km of ground magnetic data. In addition, 51 rock property samples were acquired. Laboratory work included sample preparation and analyses of these samples for magnetic remanence, density, and magnetic susceptibility (quantities used to constrain potential field modeling). An additional 18 samples from two paleomagnetic sites were processed and measured for magnetic remanence, density, and magnetic susceptibility. Data processing included reducing/re-reducing and merging new and existing gravity and magnetic data, including regional data and datasets acquired from UNR and Ormat. This included reprocessing and merging of 728 Ormat gravity points, 286 UNR (Zonge) gravity stations, and ~145 line-km of Ormat ground magnetic data with USGS data. These datasets were used to generate gravity (e.g., complete Bouguer and isostatic residual) and magnetic maps of the area (Figures 22, 23, and 30), which in turn facilitated 2D and 3D modeling efforts. Various filtered and derivative maps, such as maximum horizontal gravity gradient and pseudogravity, were utilized to identify subsurface faults. Inversions of gravity were also used to derive a depth to Mesozoic basement map (i.e., interpretation of pre-Cenozoic crystalline basement surface). These data were subsequently used to develop joint gravity and magnetic 2D forward models along seven profiles across the study area and to constrain 3D models (Task 31). Additionally, inversions of magnetic data were tested for subsurface alteration.

Granite Springs Valley: Three field sessions for gravity and magnetic surveying were conducted in northern Granite Springs Valley. This included collection and processing of 666 new gravity stations and 581 line-km of ground magnetic data. In addition, 20 rock property samples were acquired. Laboratory work included sample preparation and analyses of the 20 samples for magnetic remanence, density, and magnetic susceptibility (quantities used to constrain potential field modeling). Additional samples from two paleomagnetic sites were processed and measured for magnetic remanence, density, and magnetic susceptibility. Data processing included reducing/re-reducing and merging new and existing gravity and

magnetic data, including regional data. For example, 1,118 UNR gravity stations from Granite Springs Valley were merged with the newly acquired data. These datasets were used to generate gravity (e.g., complete Bouguer and isostatic residual) and magnetic maps of the area (Figures 6D, 25B, and 39), which in turn facilitated 2D and 3D modeling efforts. Various filtered and derivative maps, such as maximum horizontal gravity gradient and pseudogravity, were utilized to identify subsurface faults. Inversions of gravity also were used to produce a map depicting depth to Mesozoic basement. These data were also used to develop joint gravity and magnetic 2D forward models along 11 profiles across the study area and to constrain 3D models (Task 31). Additionally, inversions of magnetic data were tested for subsurface alteration and magnetic bodies (e.g., intrusions). Airborne and ground magnetic data were also merged to generate grids for 3D modeling.

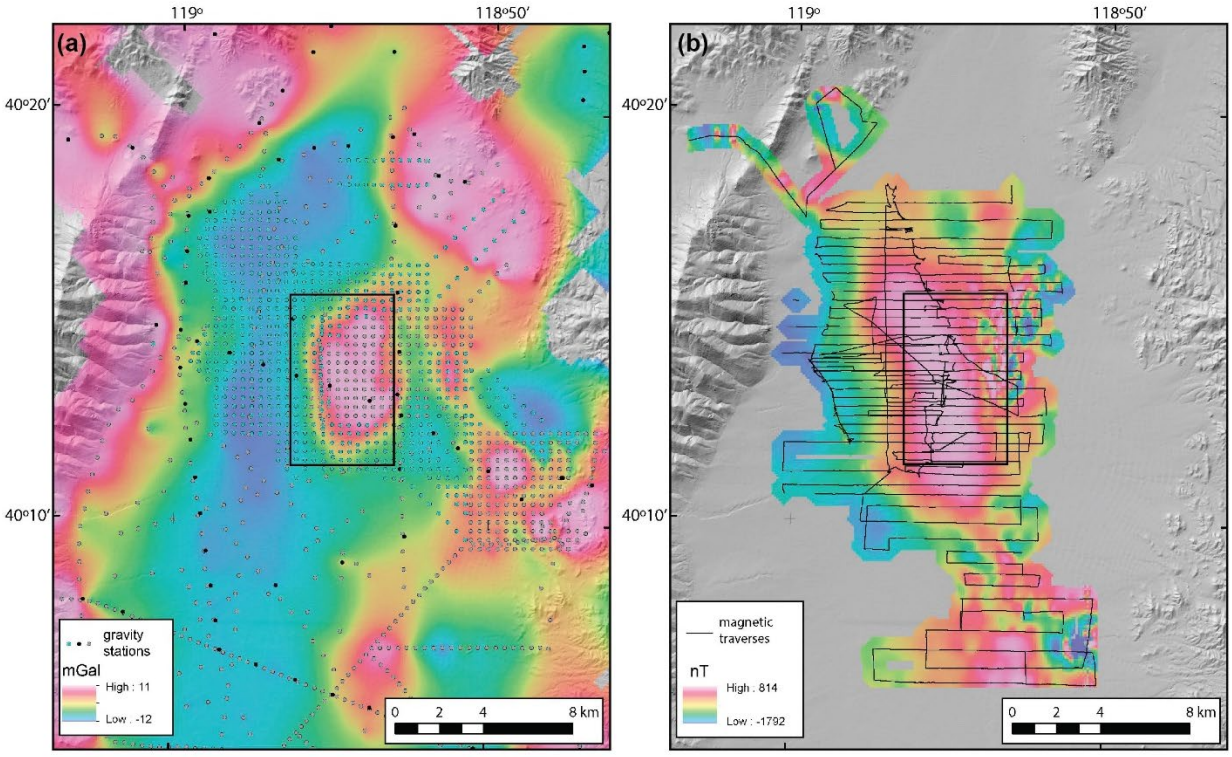

Figure 39. Potential field data, northern Granite Springs Valley. Black box encompasses area shown in Figure 25 and corresponds to approximate location of hidden geothermal system. GeoProbe boreholes and TG wells were drilled in this area. (a) Isostatic residual gravity. (b) Reduced-to-pole magnetic data.

Geological Investigations: In addition to the geophysical surveys, new geologic data were collected and/or compiled for three sites during Phase 3: 1) southeastern Gabbs, 2) northern Granite Springs Valley, and 3) Crescent Valley (Figure 1), with the aim of supplementing previous geologic studies completed in earlier phases of this project and complementing the geophysical surveys to better constrain the structural and stratigraphic controls on geothermal activity. Significant efforts were directed toward Crescent Valley in the early stages of Phase 3, because it represented a third potential site for GeoProbe and/or TG drilling, but only if funds allowed. Ultimately, funding levels did not permit drilling at Crescent Valley, and thus Phase 3 geologic studies there were less involved than at Gabbs or Granite Springs Valleys.

Gabbs Valley: Geological investigations during Phase 3 in southeastern Gabbs Valley included new geologic mapping of >60 km^2, compilation of >400 km^2 of geological mapping completed in this project, generation of a new fault map, construction of multiple detailed cross sections, and identification of several new favorable structural settings for geothermal activity hidden in the subsurface of the basin (Figure 22).

New mapping and structural analysis in Phase 3 included 40 km^2 of reconnaissance mapping of Tertiary volcanic rocks in the Gabbs Valley Range directly south of the valley, ~10 km^2 of detailed mapping of Mesozoic metasedimentary rocks at Mystery Ridge on the west flank of the valley, and ~13 km^2 in the Black Hills/Fissure Ridge area directly northwest of the valley. This work elucidated the structural framework of the area and potential structural controls on the thermal anomaly. For example, the metasedimentary rocks at Mystery Ridge and plutonic rocks at Fissure Ridge likely underlie the thermal anomaly and may therefore host a geothermal reservoir in this area. Thus, the physical and structural characteristics of these units are particularly important. The geological data was fully synthesized with the geophysical data to produce several detailed cross sections, which formed the basis for the 3D modeling efforts. All geologic, geophysical, geochemical, and drilling data were integrated into a GIS database. As discussed in earlier sections of this report, several collocated features, including intersecting gravity gradients, magnetic low, low resistivity anomaly, and a thermal anomaly defined by both TG wells and 2-m temperature data (Figures 8, 23 and 30), indicate a hidden geothermal system in southeastern Gabbs Valley (Craig, 2018; Faulds et al., 2018). Much of the geologic work and data synthesis for southern Gabbs Valley was completed by M.S. student Jason Craig, who successfully defended his thesis in December 2018 (Craig, 2018). Several papers and presentations were given at various venues on the Gabbs Valley project (Craig et al., 2017; Faulds et al., 2018). In addition, we led a field trip to Gabbs Valley for the 2018 GRC Annual Meeting, with ~20 participants.

Granite Springs Valley: Geological investigations during Phase 3 consisted of new surficial geologic mapping of Quaternary paleogeothermal features in the Adobe Flat area, including deposits of sinter, silicified sands, and travertine (Figure 25). An attempt was made to carbon date one of these deposits, but not enough material was available to yield an accurate date. All geologic, geophysical, and geochemical datasets were integrated into a GIS database, which guided selection of sites for GeoProbe and TG drilling. The gravity data and distribution of both the paleogeothermal deposits and warm wells suggest that the thermal anomaly on the east side of Adobe Flat occupies a complex fault termination with multiple fault splays at the south end of a major west-dipping normal fault zone that continues northward along the west flank of the Seven Troughs Range. The hottest wells with the most favorable geochemistry occur in a small dimple or slight right step within a north-northeast-trending gravity gradient (Figure 25B and 39A), suggesting that upwelling fluids may be focused in a small stepover in the broader horse-tailing fault termination. However, completion of a suite of detailed cross sections for this site, with iterations to incorporate geophysical constraints, was not completed due to multi-month delays in drilling related in part to the government shutdown in November-January 2018-2019 and limited budgets. Key results for Granite Springs Valley were presented, however, at the 2019 Stanford Geothermal Workshop (Faulds et al., 2019).

Crescent Valley: Crescent Valley represented a possible third drilling location if funds were available after drilling was completed in Gabbs and Granite Springs Valleys. Detailed mapping of six step-overs was completed along the Cortez Range front (McConville, 2018), three of which were previously identified in Phase 2 and three smaller ones identified in Phase 3 (Figures 13 and 40). Other work completed in Phase 3 included: 1) logging of ~9 km of well cuttings, 2) analysis of 24 temperature profiles of mineral wells to map temperature contours across the basin, 3) analysis of fault kinematic data, 4) analysis of four silica deposits via XRD, 5) a new 31 station 2-m temperature survey (Figure 41), and 6) conversion of four previously interpreted seismic reflection profiles from time to depth based on available velocity models. Most of this work was completed by M.S. student Emma McConville, who successfully defended her thesis in August 2018 (McConville, 2018). The XRD analysis showed that there is only one sinter (opal-A) deposit located at the Hand-Me-Down Creek hot spring. The remainder of the samples are composed of alpha quartz, and thus they are older than the sinter deposit. The 2-m data revealed a statistically significant temperature anomaly ~1 km west of Hand-Me-Down Creek hot spring (Figure 41). Two elevated (~1°C above background) temperatures were recorded near the Crescent Valley fault along the west flank of the Cortez Mountains. One is in the northernmost step-over and fault intersection ("E" in Figure 41), and the other is in a small left step-over in the Crescent Valley fault at the base of an altered fault scarp. The stress

inversion, based on 31 measurements of fault surfaces, was used to define the regional stress field (Figure 42), which was incorporated in slip and dilation tendency analyses to assess which faults are most likely to channel geothermal fluids. In addition, several detailed cross sections were prepared for Crescent Valley based on interpretations of seismic reflection, gravity, and well data. A new geologic map for Crescent Valley was completed showing locations of paleo-geothermal features, geothermal wells, subsurface faults, and favorable structural settings for geothermal activity (McConville, 2018). All available geologic and geophysical data were synthesized into a conceptual structural model for the Crescent basin, including detailed models for the Hot Springs Point and Hand-Me-Down Creek geothermal systems. All of these datasets were incorporated into a revised play fairway analysis for the Crescent basin, including ranking of individual favorable structural settings. The step-over in the Crescent Valley fault zone at Hand-Me-Down Creek ranked the highest in the area. Potential new drilling targets were selected at the Hand-Me-Down Creek site for future work (McConville, 2018).

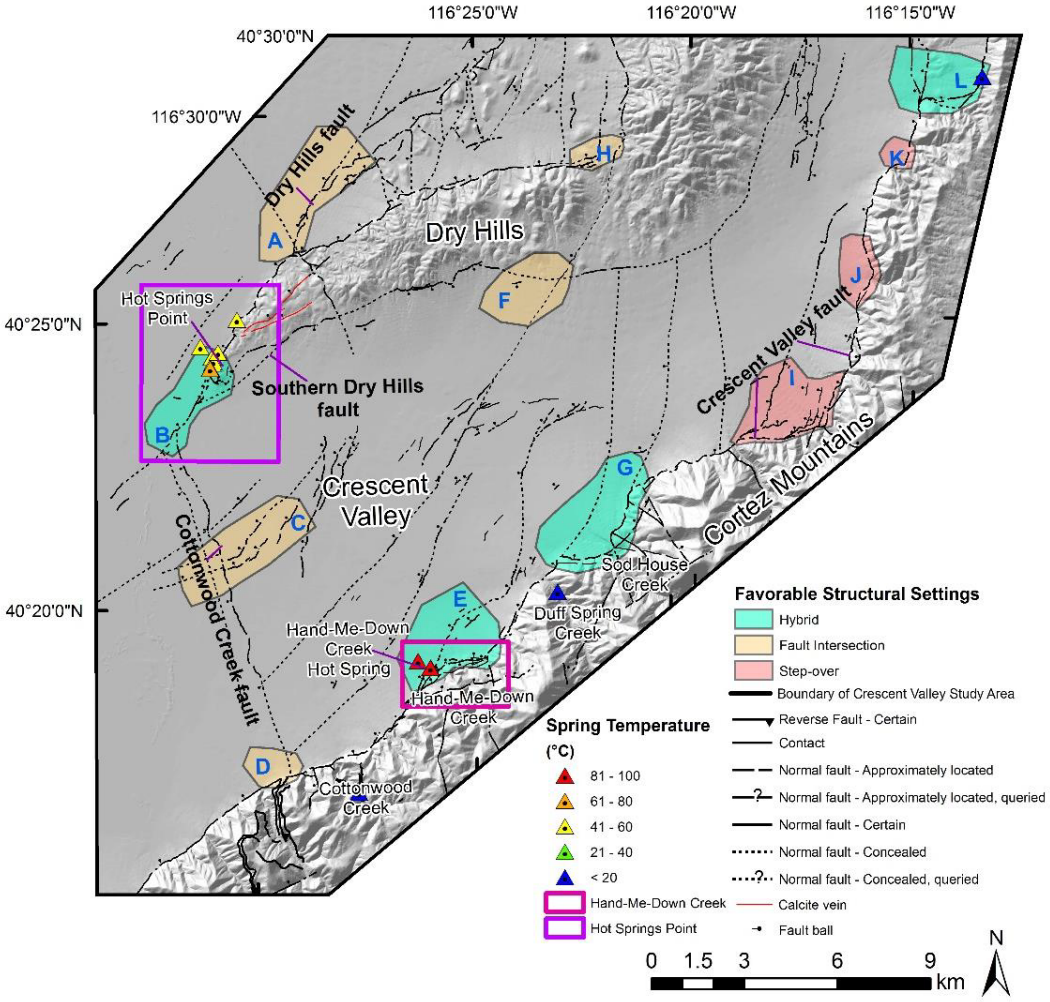

Figure 40. DEM hillshade map of Crescent Valley showing the location, type, and geometry of favorable structural settings (from McConville, 2018). Favorable structural settings include hybrid systems (two or more favorable structural settings) shown in turquoise (B, E, G, L), fault intersections shown in orange (A, C, D, F, H), and fault step-overs (relay ramps) shown in red (I, J, K). Black lines are faults with fault balls on the hanging wall. Springs are represented by triangles and are colored based on temperatures, where warm colors correspond to higher temperatures and cool colors correspond to cooler temperatures. Purple box encompasses the geothermal system at Hot Springs Point, and the pink box denotes the system in the Hand-Me-Down Creek area.

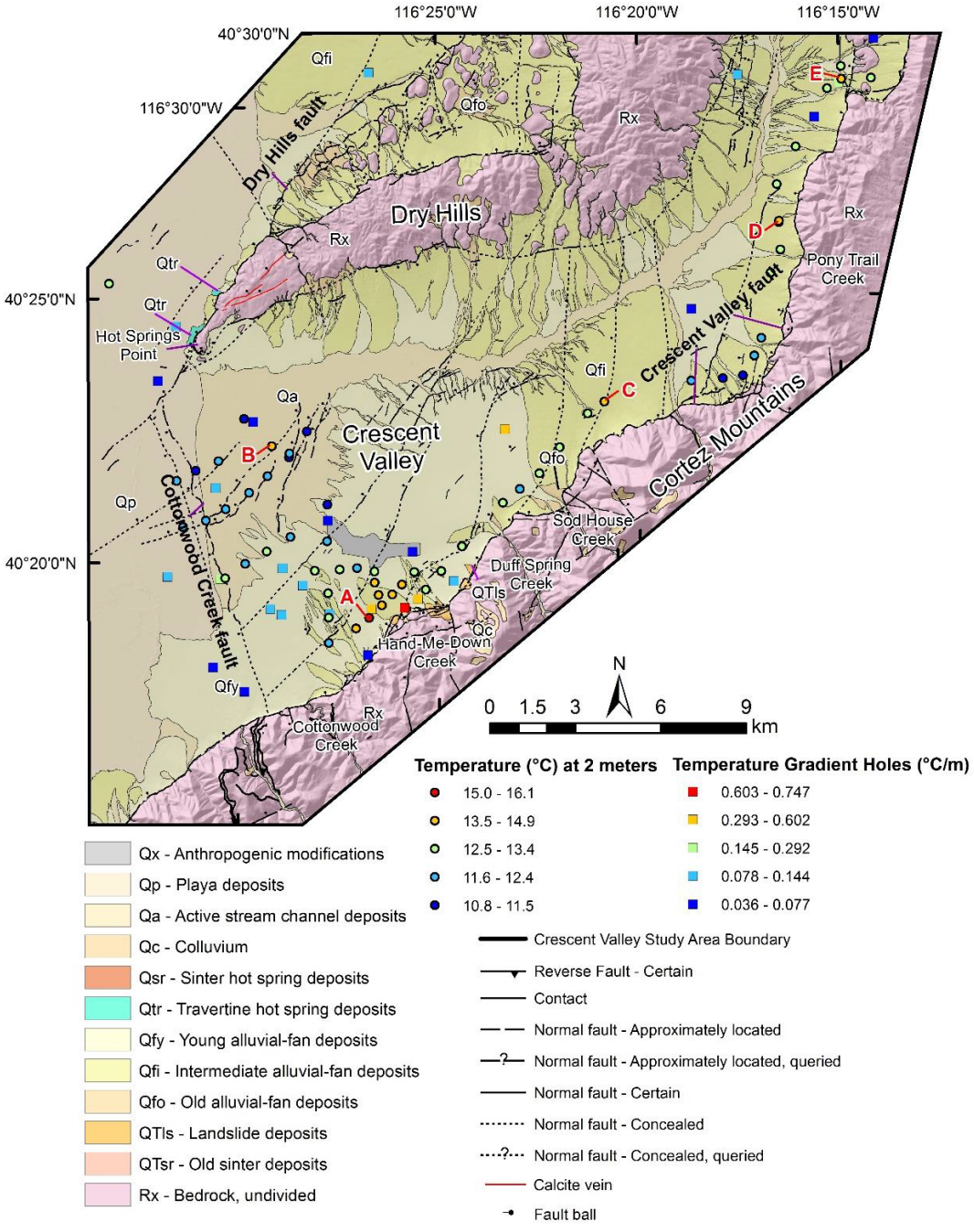

Figure 41. Temperatures at 2 m below the surface in Crescent Valley (from McConville, 2018). DEM hillshade overlain by simplified geologic map. Circles represent 2-m temperature stations and are colored by temperature. Squares represent temperature gradient holes and are colored by geothermal gradient. Anomalous and warm 2-m locations are labeled A, B, C, D, and E.

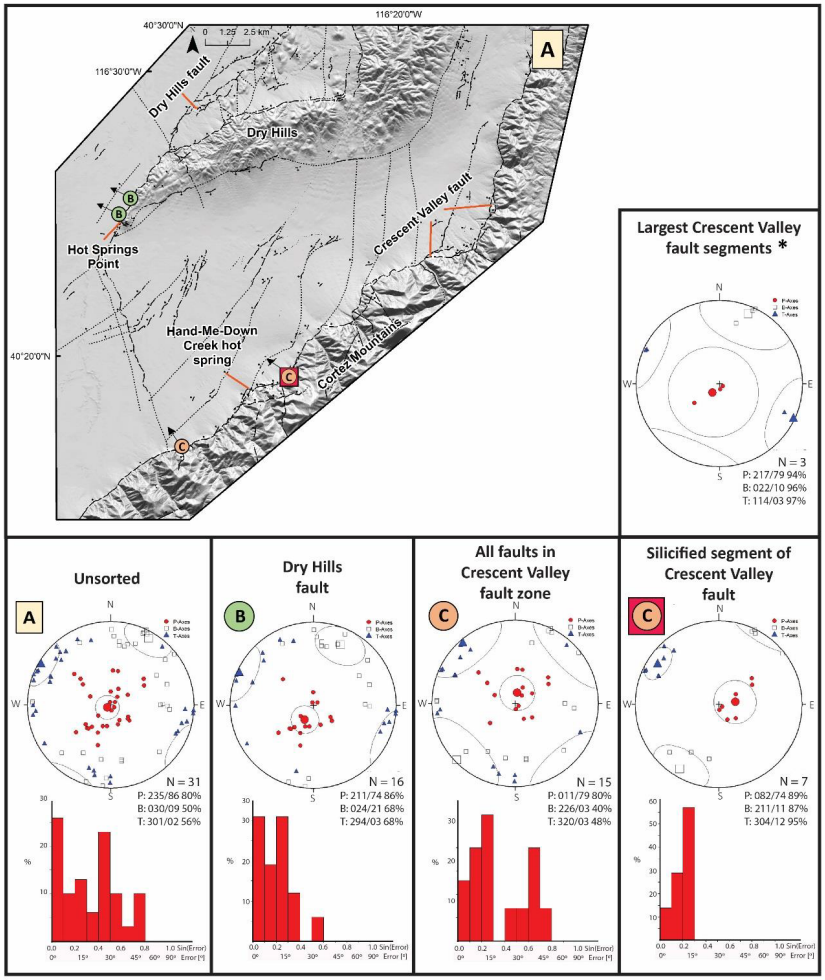

Figure 42. Spatial distribution of fault kinematic data from McConville (2018). A. DEM hillshade with fault map. Locations of measured kinematic data are represented with letters and colored circles and squares. Arrows indicate the trend of slickenlines at each site. Lower-hemisphere, stereographic projections of stress directions correspond to locations on the map. Red circles indicate the compressive axis (P), white squares indicate the intermediate axis (B), and blue triangles indicate tension axis (T). Contoured circles are 99% confidence, and the histograms for areas with more than four kinematic indicators show the distribution of angles between the predicted trend and plunge and the measured trend and plunge of kinematic indicators. * Results from three of the best developed Crescent Valley fault surfaces. N = number of measurements.

Task 30.0. Magnetotelluric Surveys: Up to 50 broadband MT survey stations will be collected in total at two sites in a layout primarily designed for 2D inversions. The goal of the MT models will be to identify low resistivity hydrothermal clay caps and moderately low resistivity reservoirs. The geologic models, water table, and information relevant to fossil alteration will be used to consider multiple interpretations of key low resistivity features. The MT surveys will be carried out by the USGS under the supervision of UNR, and USGS personnel and will be funded directly by DOE.

The detailed MT surveys during Phase 3 focused entirely on Gabbs Valley and Granite Springs Valley. Specific accomplishments regarding these surveys are described below. All major milestones for this task were accomplished without variance (Table 3). These included: **Milestones: 30.1 –** Completed acquisition of new MT data for two sites – and **30.2** – Interpretation of MT data for two sites and integration of these data with other datasets.

***Gabbs Valley**:* One field session for MT surveying was carried out, with a total of 24 MT stations collected by the USGS using ZEN data loggers, ANT-4 induction coils, and Borin Ag-AgCl electrodes. Data were recorded for 20 hours and processed using the bounded influence robust processing code developed by Chave and Thompson (2004), where synchronous stations were used as remote references. The data were inverted using ModEM (Kelbert et al., 2014) on NASA's supercomputer Pleiades. Results indicate several low-resistivity anomalies in the study area (Figure 43). The largest low-resistivity anomaly has a semi-ellipsoidal geometry that is ~10 km^2, trends northeast, and ranges from 100-1000 m in depth. This low-resistivity anomaly is located in the southeastern part of the basin and is collocated with conspicuous gravity gradients and the 2 km^2 magnetic-low (Figure 30). Detailed MT methods and results used in this study are further discussed in Peacock et al. (2018). TG well locations were selected based on the collocation of these features.

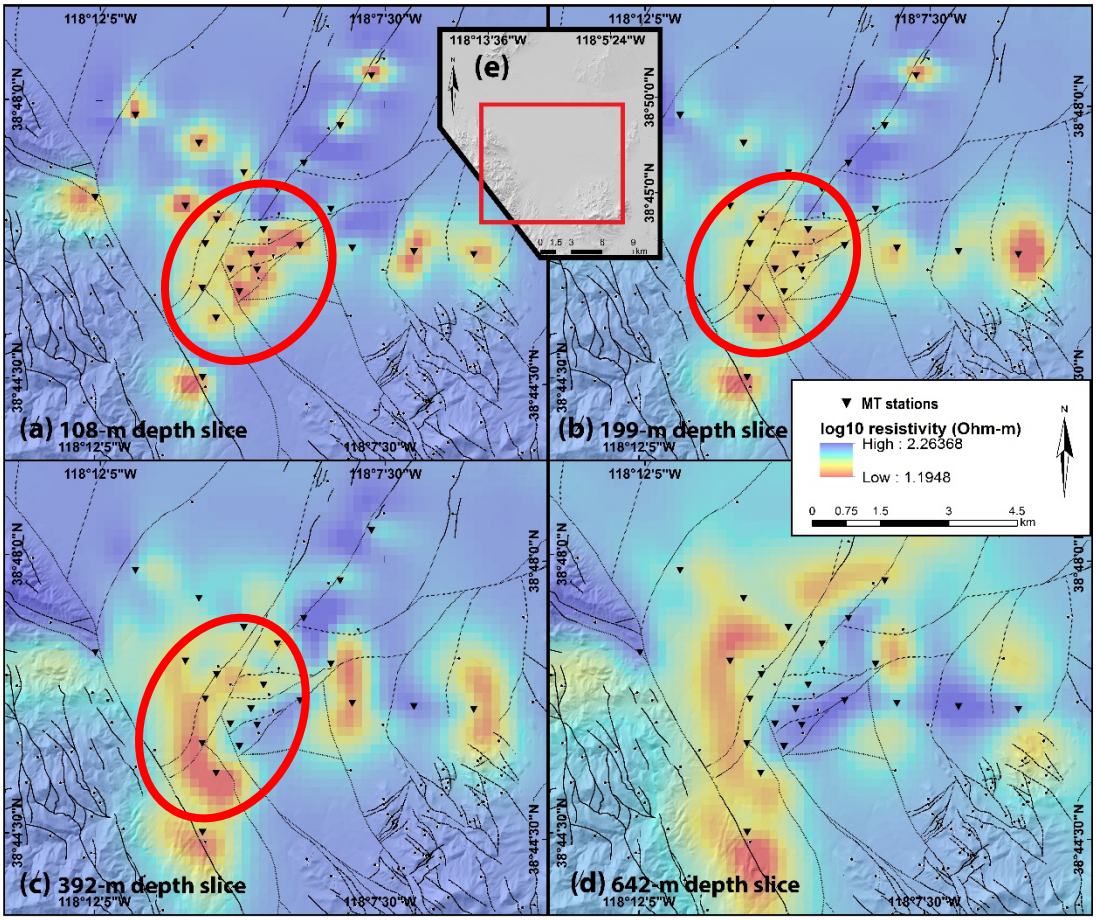

Figure 43. MT resistivity depth profiles. Warmer colors indicate areas with relatively low-resistivity values (Ohm-m). MT station locations are shown as inverted triangles. Mapped faults are black lines. Basemap is DEM topographic hillshade. Red ellipses encompass low resistivity anomaly associated with inferred blind geothermal system. **(a)** Resistivity depth slice at 108-m. **(b)** 199-m resistivity depth slice. **(c)** 392-m resistivity depth slice. **(d)** 642-m resistivity depth slice. **(e)** General study area showing location of maps as red polygon.

Granite Springs Valley: One field session for MT surveying was carried out, with 24 MT stations collected. The MT data at Granite Springs Valley showed broad low resistivity anomalies associated with a depocenter of thick conductive sediments in the Adobe Flat area (Figure 44), which masked any potential hydrothermal signature in the targeted area along the eastern margin of the basin. Thus, the MT data in Granite Springs

Valley were not as helpful compared to Gabbs Valley for selecting TG drilling sites but still useful for developing conceptual models of the area.

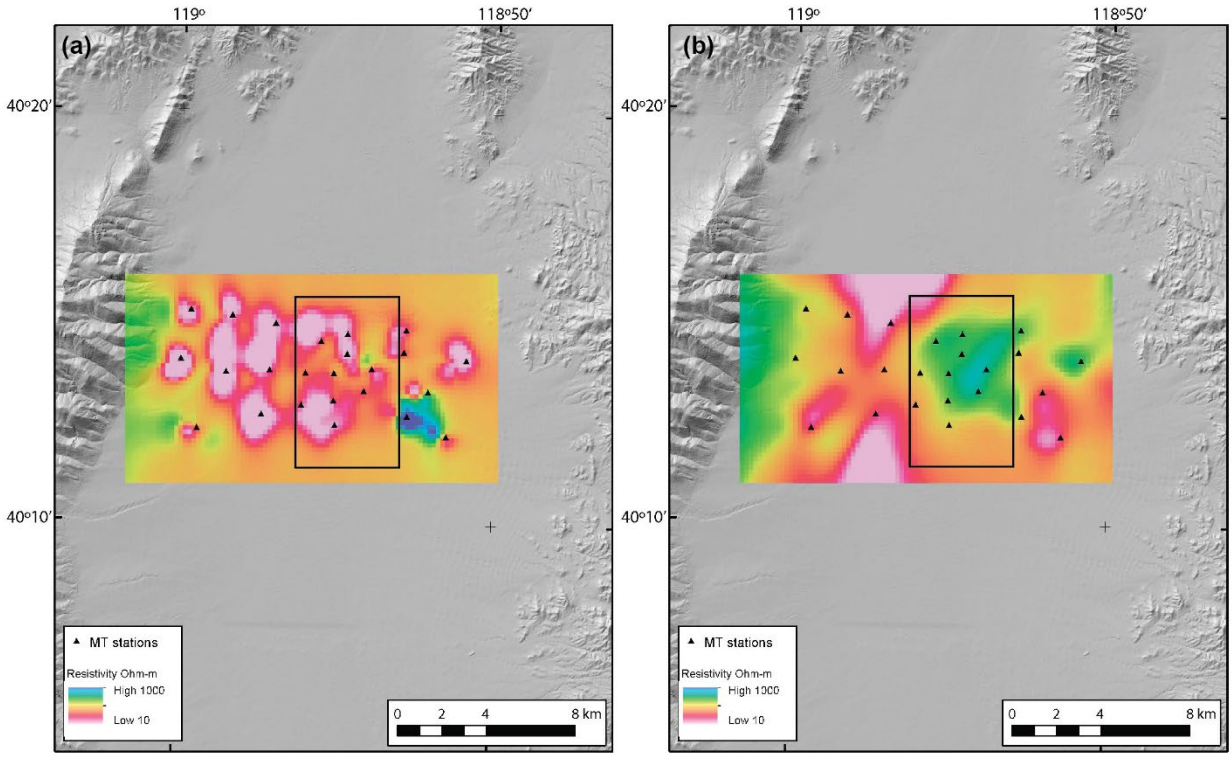

Figure 44. Representative MT depth slices from northern Granite Springs Valley. Black box encompasses area shown in Figure 25 and corresponds to approximate location of hidden geothermal system. GeoProbe boreholes and TG wells were drilled in this area. (a) MT data at 199 m depth. (b) MT data at 1,124 m depth. Unlike Gabbs Valley, there is not a distinct low resistivity anomaly at this location, although conductive basin-fill sediments in the Granite Springs basin may mask any anomaly associated with the geothermal system.

Task 31.0. 3D Modeling: To further constrain subsurface geologic geometries and drilling targets, the preliminary 3D geologic map for Granite Springs Valley built in Phase 2 will be iteratively updated with new data collected in Phase 3. Also, a new 3D geologic map will be constructed for Gabbs Valley, where 3D modeling was not carried out in Phase 2. Detailed 3D models facilitate targeting of geothermal reservoirs. Based on the 3D mapped structural and stratigraphic geometries, the potential for structurally controlled permeability in the subsurface will be analyzed based on the distribution of three proxies for permeability: 1) the stress state on faults, 2) the distribution and density of structural discontinuities, and 3) the host rock lithology. The spatial co-location of highly favorability areas, as defined by each of the permeability proxies, will help to define discrete deep drilling targets that have a high likelihood for permeability and also provide a framework from which to co-evaluate MT models, temperature data, and develop and evaluate conceptual models of reservoirs. The 3D modeling will be carried out by the USGS with significant input from UNR, with funding to the USGS directly through DOE.

The 3D modeling during Phase 3 focused on Gabbs Valley and involved production of a 3D geologic map as well as 3D gravity inversion and modeling. Specific accomplishments regarding this work are discussed below. **Milestone 31.1 (**New 3D models for 2-3 study areas; Table 3) was fully accomplished for Gabbs Valley and partially completed for Granite Springs Valley.

Gabbs Valley – 3D geologic mapping and 3D gravity inversion modeling: A 3D geologic map of southeastern Gabbs Valley was constructed using established methods (Moeck et al., 2010; Jolie et al., 2015; Siler et al., 2016a, 2019). The 3D map was based on geologic mapping and associated geologic cross-sections (Craig et al., 2017; Craig, 2018), gravity and magnetic anomaly maps, gravity and magnetic maximum horizontal gradient data, and 2D forward models of gravity and magnetic data (Earney et al., 2018). The southern Gabbs Valley 3D geologic map is centered on the six 150 m-deep TG holes (Faulds et al., 2018), spans 169 km^2 (13 km x 13 km), and extends from the land surface to 2 km depth. The 3D geologic map contains ninety-eight fault surfaces and five geologic units (Figure 45).

To further constrain the 3D geologic structure of southeastern Gabbs Valley, 3D gravity inversion modeling was performed based on the results from the initial 3D geologic map. Advanced 3D geophysical modeling methods (e.g., Witter et al., 2016) were utilized to reduce uncertainty in the construction of geothermal conceptual models. The aim of the work was to perform geophysical inversion modeling of gravity data, guided by rock density measurements, as a test of 3D geological models built for the Gabbs project. Specifically, for areas of the 3D geological model that were found to conflict with the gravity measurements, adjustments to the model were made to bring the two into agreement. This process of updating the 3D geological model, so that it becomes quantitatively consistent with the measured gravity data, is a means to reduce uncertainty in the final 3D geologic representation of the subsurface.

The workflow performed in the 3D gravity inversion modeling was as follows: 1) the stratigraphic surfaces from the 3D geologic map were exported and used to bound the rock units in the 3D inversion model; 2) a density model was generated based on rock units from the 3D geologic map and populated with initial density values based on density measurements, literature density values, and density values calculated during 2D forward modeling of gravity data; 3) the 3D gravity inversion was performed, allowing the starting density values in each rock unit to vary within realistic limits (500 kg/m^3 in this case) until the gravity response from the density model was within the measurement error of the gravity measurements; 4) the density model was examined relative to the 3D geologic map; and 5) changes to the 3D stratigraphic surfaces were made to maximize within-geologic-unit density homogeneity.

The 3D gravity inversion modeling revealed stacked high- or low-density anomalies at several locations in the model (Figure 46). This suggests that the stratigraphic surfaces were either too high or too low, which resulted in the inversion algorithm using anomalously high- or low-density values to fit the gravity data. The stratigraphic surfaces were adjusted accordingly, and the gravity was re-inverted. Three iterations of adjustment to the 3D geologic model and gravity re-inversion were performed. The resultant 3D geologic map, which is consistent with geologic mapping and cross-sections, gravity and magnetic anomaly maps, 2D gravity and magnetic modeling, and 3D gravity inversion modeling, is an incredibly well constrained representation of the subsurface structure in southeastern Gabbs Valley, especially for a study area with no subsurface geologic data (e.g., deeper wells or seismic reflection data). A more detailed description of the 3D inversion modeling methods and results is presented in Siler et al. (2020).

The 3D geologic map constrains the 3D geometry of the displacement transfer zone that we interpret to be the primary control of subvertical permeability and geothermal upwelling in the system. The displacement transfer zone corresponds to the area of intersection and interaction between two fault systems: 1) the Petrified Springs fault and related northwest-striking strike-slip and oblique-slip faults, and 2) predominantly northeast-striking normal faults. At the location of highest measured temperatures, as high as 124° at 150 m depth, these two fault systems bound an uplifted structural block in which the metamorphic basement rocks (Trvc in the 3D geologic map) are within ~475 m of the surface, more than 2 km higher than they are in the deepest parts of the adjacent basins (Figure 45). These details of the fault system and geologic structure depicted in the 3D geologic map provide critical constraints for future exploration and allow the construction of conceptual models of geothermal processes that can be tested with future exploration and drilling.

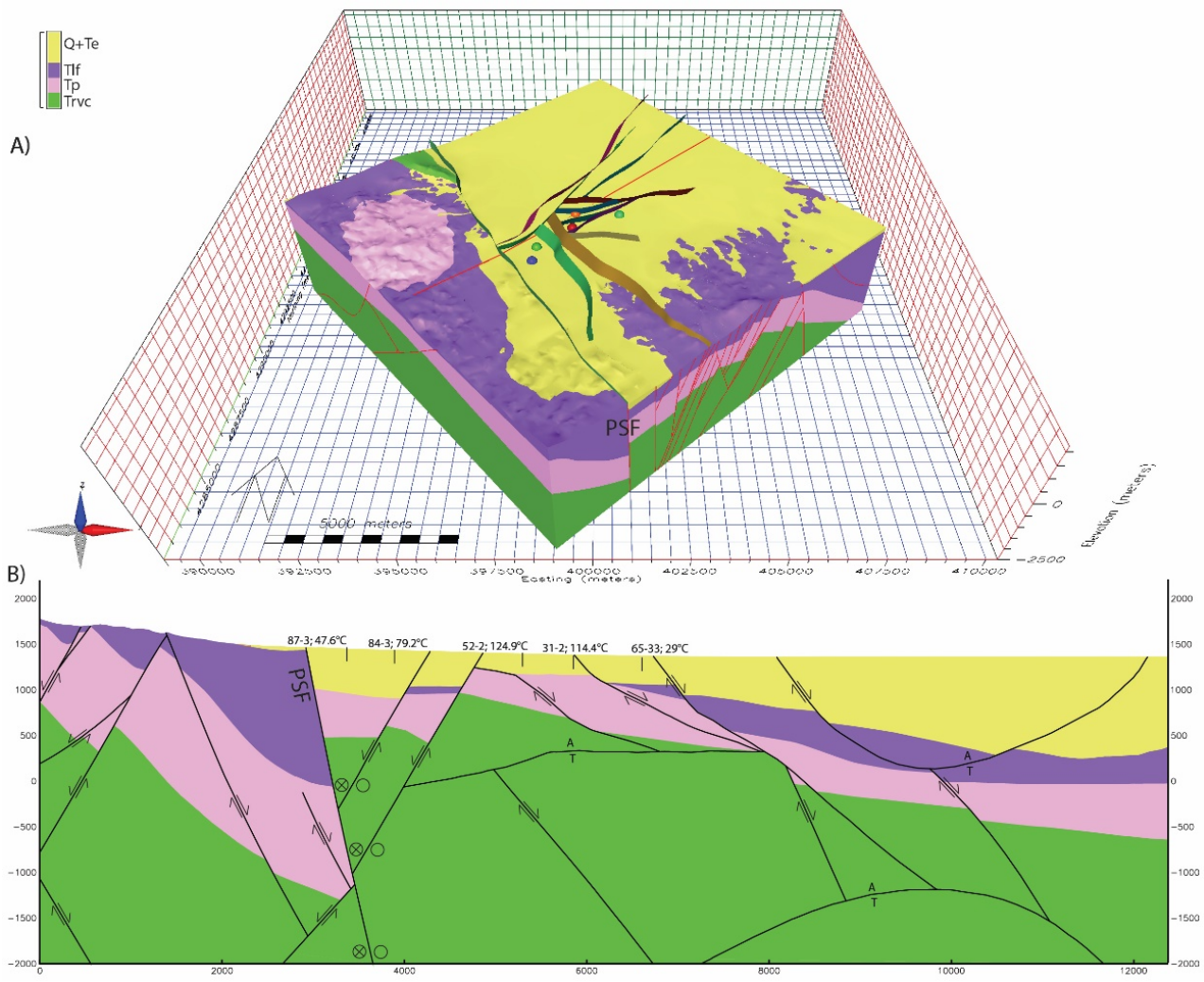

Figure 45. 3D geologic map of southeastern Gabbs Valley, A) perspective view looking north, and B) cross-section B-B'. Section line is shown as a red line on the surface of the 3D map. The eleven faults that constitute the dense fault intersection zone are shown extending above the topographic surface in A). The locations of the six temperature gradient wells are shown as hemispheres and are colored according to their maximum temperature (warm colors for warmer wells). The two hottest wells are the red and orange hemispheres. On B) all six temperature gradient wells are projected to the section and labeled according to their measured temperature. Crossed circles and open circles on strike-slip and oblique-slip faults indicate the direction of movement: crossed-circle away, open circle toward. A and T denote direction of movement for normal faults that are sub-parallel to the cross-section: A for away, T for toward.

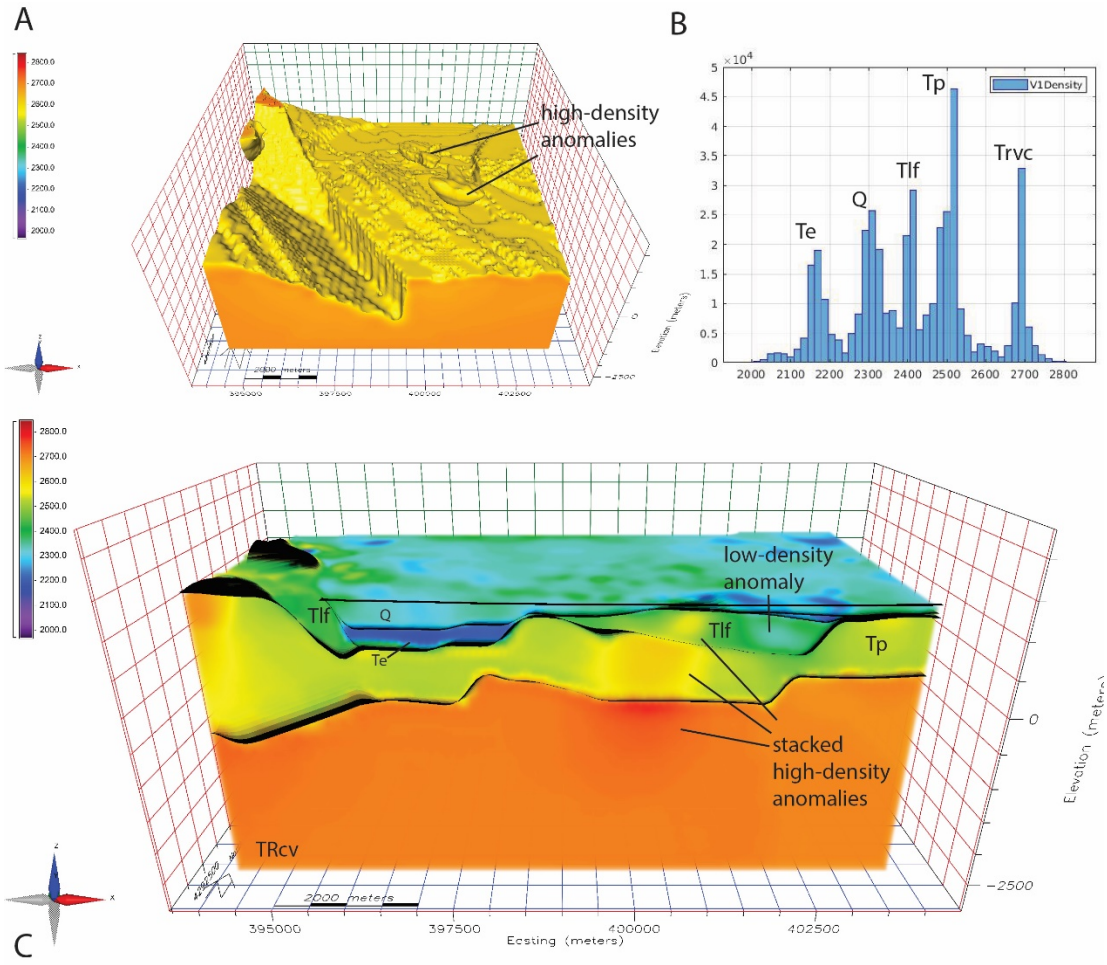

Figure 46. A) and C) show 3D perspective views looking north at the initial density model. Density in the color scale is in kg/m^3. A) Densities lower than 2600 kg/m^3 (i.e. lower than densities typical for basement rocks) have been removed revealing anomalous regions of relatively high-density material within lower density, overlying geologic unit(s). B) Histogram of the density values for the density model. X-axis values are density in kg/m^3. The five peaks are labeled by the median density for each unit. C) E-W cross section through the 3D density model cutting through one set of high-density anomalies. Relatively higher densities than the median (2700 kg/m^3 ~orange is the median for Trvc; 2510 kg/m^3 ~pale green is the median for Tp) in the Trvc and Tp are needed to fit the gravity measurements. In the Tlf unit, both densities lower and higher than the median (2410 kg/m^3 ~dark green is the median) are needed to fit the gravity measurements.

Gabbs Valley – Fault intersection density, and 3-D stress modeling southern Gabbs Valley: Using the detailed 3D geometry of the southern Gabbs Valley fault system, we calculated the spatial distribution of three 3D geologic characteristics inferred to control geothermal upwelling in the area. The three characteristics are slip tendency, dilation tendency, and fault intersection density. Slip and dilation tendency were calculated based on published methods (Morris et al., 1996; Ferrill et al., 1999) using the 3D geometry of each fault and a representative 3D stress model based on regional stress data and stress magnitudes measured in geothermal fields in western Nevada. The stress directions used were Shmin ≈ 124°, Shmax ≈ 34°, and Sv = vertical. Different stress models were used for normal faults, oblique-slip faults, and strike-slip faults (distinguished based on fault mapping by Craig, 2018). For normal faults (Shmin<Shmax<Sv), a linear increase with depth for each of the principal stresses from the surface to values of Shmin= 20.7 Mpa, Shmax = 27.6 Mpa and Sv = 34.5 Mpa at 1.5 km depth was used. Similarly, for strike-slip faults

(Shmin<Sv<Shmax) a linear increase with depth for a stress model with values of Shmin= 20.7 Mpa, Shmax = 34.5 Mpa and Sv = 27.6 Mpa at 1.5 km depth and for oblique-slip faults (Shimn<Shmax≈Sv) stress values of Shmin= 20.7 Mpa, Shmax = 34.5 Mpa and Sv = 34.5 Mpa at 1.5 km depth. These stress models are consistent with values measured in other geothermal fields in western Nevada at geothermal reservoir depths (Hickman et al., 1998; Hickman and Davatzes, 2010; Blake and Davatzes, 2011; Jolie et al., 2015) though not directly measured at Gabbs Valley. Fault intersection density is calculated as the 3D density of lines of fault intersection per unit volume.

There are eleven faults that we interpret to be the primary constituents of the displacement transfer zone and the likely controls of geothermal activity (Figure 45). The NE-striking, steeply dipping faults and fault segments have the highest dilation tendency; similarly, the NNE- to NE-striking faults and fault segments have the highest slip tendency (Figures 47a, b). This suggests that these faults are the most likely faults to remain critically stressed and serve as fluid flow conduits. The highest density of fault intersections between the eleven primary faults is directly adjacent to the two hottest temperature gradient wells, 52-2 and 31-2 (Figure 47c d). This dense zone of intersection plunges moderately WNW, suggesting that the geothermal upwelling from depth may be emanating from the WNW.

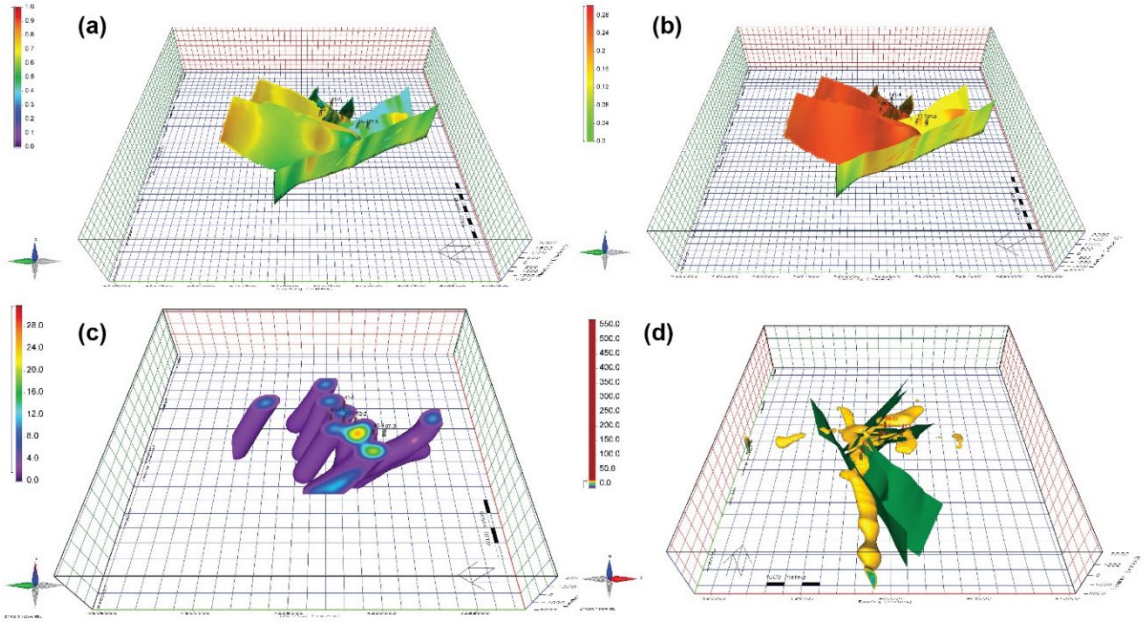

Figure 47. (a) 3-D perspective view looking east at dilation tendency on the 11 southeastern Gabbs Valley faults interpreted as likely fluid flow controls. Warm colors for high dilation tendency, and cool colors for low dilation tendency. The NE-striking faults and fault segments have the highest dilation tendency. TG wells 52-2 and 31-2 have measured temperatures of 124.9°C and 114.4°C at 150 m. (b) 3D perspective view looking east at slip tendency on 11 faults. Warm colors for high slip tendency, and cool colors for low slip tendency. The NNE- to NE-striking faults and fault segments have the highest slip tendency. (c) 3D perspective view looking east at the calculated fault intersection density for the 11 primary faults at Gabbs Valley. Warm colors for high fault intersection density, cool colors for low intersection density. The highest density of fault intersections occurs directly adjacent and to the west of the two hottest temperature gradient wells (52-2 and 31-2) and plunges to the WNW. (d) 3D perspective looking north at faults interpreted as the primary controls on geothermal upwelling and the lowest resistivity values (0-15 ohm-m) in the MT inversion model. An inferred clay cap can be seen in the vicinity and to the NW of the TG wells. In addition to the clay cap, a clear spatial correlation between faults and low resistivity values suggest a hydrothermal alteration signal as well as possible clay gouge, or other fault related damage signal in the MT data.

Granite Springs Valley: Time and budgetary constraints precluded completion of the 3D geologic model for Granite Springs Valley, but nonetheless significant advances were made. The budgetary challenges resulted from the greater than anticipated expense in permitting, planning, and managing the drilling operations. The timing constraints for completing the modeling resulted from delays in drilling and the government shutdown from November 2018 to January 2019. Once on track, other commitments limited contributions from key personnel, particularly at UNR. However, a new, smaller footprint 3D map area was chosen compared to that developed in Phase 2 of the project. This smaller area was more focused on the likely location of the geothermal resource rather than the entire basin. It is centered on the area containing the paleogeothermal deposits and TG holes (Figures 25 and 38). Results from 2D potential field profile models were imported into the 3D work space. 3D faults and Mesozoic basement were built based on the potential field results (Figure 48). It was found that additional work was needed to fully integrate the potential field and seismic reflection data to construct new and refine existing cross sections. This work could not be completed prior to the end of the project.

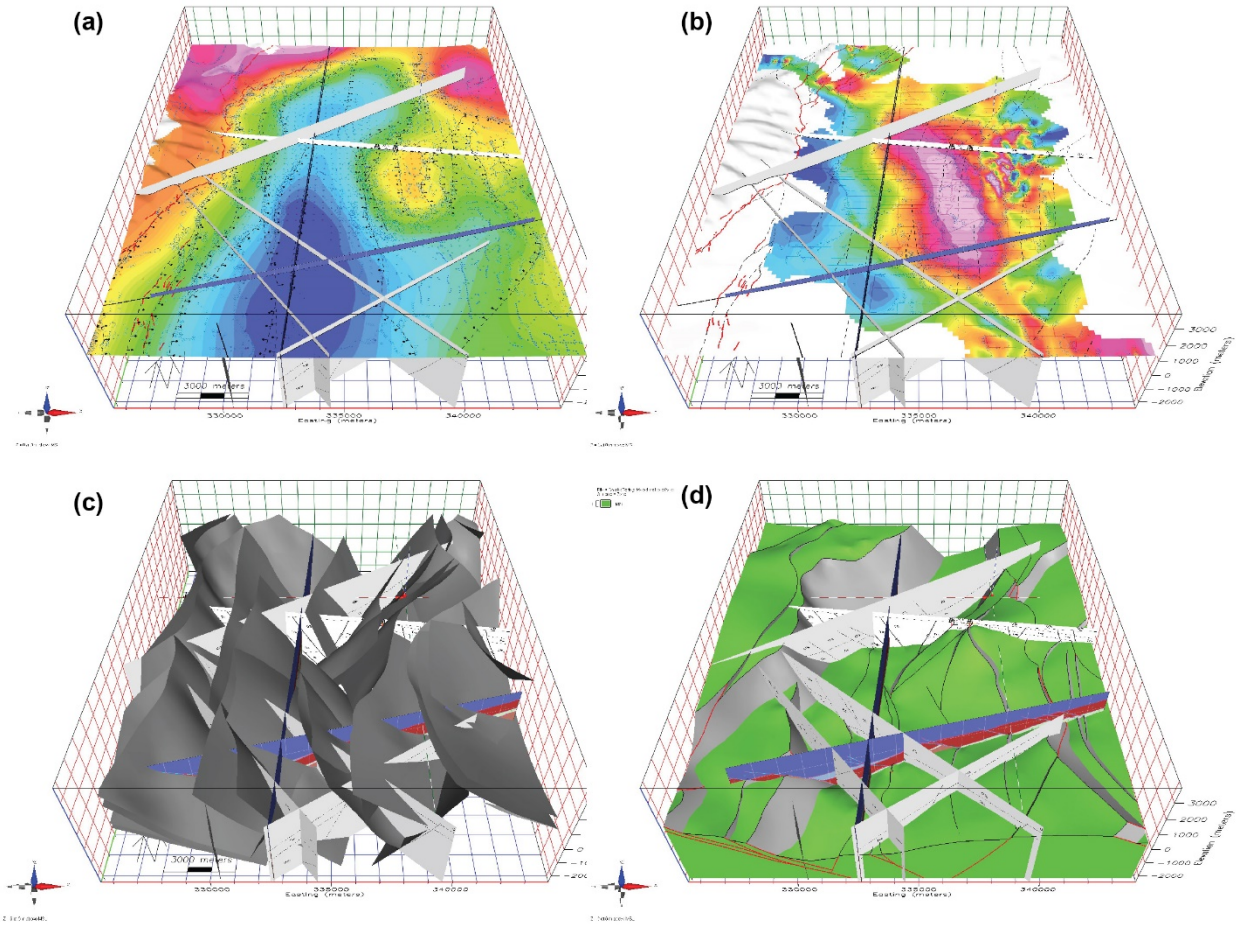

Figure 48. 3D views of the geothermal prospect in northern Granite Springs Valley (all look north). This smaller footprint 3D map is centered on a gravity high that lies directly east of the fault zone that controls the geothermal activity along which the TG holes were drilled (Figure 25). (a) Complete Bouguer gravity grid showing the seismic reflection profiles and cross-sections. (b) Magnetic reduced-to-pole grid with the seismic profiles and cross-sections. (c) 3D faults from the preliminary 3D map. (d) 3D basement surface from the preliminary 3D map.

Task 32.0. Conceptual Models and Resource Capacity Estimates: The final stage of Phase 3 will be to synthesize all the data, including the 3D geologic map data, MT models, temperature data, and geochemistry to develop conceptual models for each area. These conceptual models will follow established outlined methodology in which all data will be integrated and assessed thermodynamically to develop a range of conceptual models for reservoir geometry, size, and temperature. These conceptual models will provide several key final parts to this project. 1) Characterization of the structural and stratigraphic framework hosting the reservoir such that these data can be viewed relative to both the play fairway analysis input data and play fairway results for the rest of the Nevada study area. 2) Selecting deep drill targets to test the value of the play fairway study to identify power capable resources and provide a framework for selecting deep drill targets. 3) These models will provide a framework for calculating a range of potential power capacity estimates in MWe using a lognormal probability density function. Ultimately, deep wells will need to be drilled and tested to confirm the power capacity estimates, but using industry-standard methods for calculating resource capacity provides initial context for the results of this play fairway study.

The conceptual modeling and resource capacity estimates focused on Gabbs Valley. Specific accomplishments regarding this work are discussed below. Specific milestones included **32.1** (Revised and refined conceptual models), **32.2** (Selection of potential deep drilling targets for geothermal reservoirs), and **32.3** (Resource capacity estimates). We had originally anticipated completing these milestones for 2-3 areas, but time constraints, unanticipated costs and time needed for drilling operations, and delays in drilling limited full completion of these tasks to Gabbs Valley, with partial completion in Granite Springs Valley (Faulds et al., 2019) and Crescent Valley (McConville, 2018). Only Gabbs Valley is discussed in this report.

Gabbs Valley: The results of the TG drilling provide direct evidence of a newly discovered blind geothermal system in southeastern Gabbs Valley (Figures 30 and 31). All available datasets were synthesized to generate conceptual resource models (Figure 49) of the geothermal system, which were subsequently used for power capacity estimations (Craig, 2018; Craig et al, in prep). Conceptual resource models of the geothermal system provide general constraints on reservoir geometry, hydrothermal upflow/outflow pathways, and spatial distribution of subsurface temperatures. Key model inputs for southeastern Gabbs Valley include the following:

- Temperature data: Temperature data from six TG holes along a nearly 4 km long northeast-southwest transect that spans the thermal anomaly, with a maximum recorded temperature of ~125°C at 152 m depth (Figures 30 and 31).
- MT data: The approximate thickness of an inferred clay cap is based on the configuration of a low resistivity anomaly gleaned from MT data. The ~10 km^2 low-resistivity anomaly (Figures 23C and 43) probably results from smectite-dominated argillic alteration in the system and is generally centered on the TG thermal anomaly. The domal-shaped MT conductor is mostly distributed between depths of 250-750 m (Figures 43 and 49) in Tertiary volcanic and sedimentary rocks. It is important to note that this relatively impermeable clay cap may be the primary reason that the geothermal system in southeastern Gabbs Valley is blind with no surface hot springs or steam vents.
- Temperature projections: Given the thickness of the clay cap, temperatures at 300 m below the surface may reach 130 to 142°C (Figure 31). Given broad analogs across the Great Basin region, reservoir temperatures may reach upwards of 175 to 180 °C.
- Gravity data and structural setting: Intersecting gravity gradients indicate a complex fault intersection and area of tightly spaced faults in southeastern Gabbs Valley in the south-central part of the study area, which marks a particularly favorable part of the displacement transfer zone for geothermal activity (Area A in Figure 22). Fracture density and associated locally elevated permeability is likely enhanced at and proximal to fault intersections (Figures 47C and 49).

- Magnetic data: The 2 km^2 magnetic low (Figures 30 and 49) may define part of the spatial extent of hydrothermal alteration in volcanic stratigraphy and possibly constrains the zone of net upflow and/or outflow of fluids in this system over time.
- Slip and dilation tendency analysis indicating that the north-northeast- to northeast-striking, normal faults are best oriented to host fluid flow (Figures 23D and 47A, B).
- Inferred permeability: Permeability in the metasedimentary Mesozoic basement is likely relatively low. Thus, upflow in the basement is expected to be narrowly focused along faults and/or fault intersections until fluid flow reaches more permeable units in the overlying Cenozoic strata.
- Inferred geothermal flow paths and reservoirs: Tertiary volcanic strata dip northeast and are ~250 to 750 m thick in the area drilled, whereas Pliocene-Quaternary sediments are relatively thin. Thermally buoyant fluids may flow up through faults and then up stratigraphic dip from faults into highly fractured tuff and/or permeable sedimentary units along stratigraphically controlled horizons (Figure 49). The Hu-Pwi Rhyodacite (Tp) likely contains highly fractured tuffs adjacent to the fault zones and fault intersections. The Esmeralda Formation (Te), composed of fluviolacustrine siltstones, sandstones, and conglomerates, overlies the Hu-Pwi Rhyodacite in the area of the thermal anomaly. Permeable units within the Esmeralda Formation may serve as shallow reservoirs for some of the hydrothermal fluids, as conglomerates, in particular, can have permeability rivaling open fractures in fault zones.

Synthesis of all datasets generated conservative (P90), median (P50), and optimistic (P10) conceptual resource capacity models (Craig et al., in prep.; Figure 49). The P90 and P10 models represent 90% and 10% confidence, respectively, in total resource capacity. The resource models are representative of the 90, 50, and 10 percentiles of the cumulative distribution function of a graphical compilation of worldwide geothermal field power density versus resource temperatures (Wilmarth and Stimac, 2015). It is worth noting that numerous possible conceptual models for the geothermal system fit the currently existing geologic, geophysical and geochemical data. Three of the most probable conceptual models include: 1) upflow along one or more of the northeasterly striking faults, 2) upflow along one or more fault intersections between northwest-striking and northeast-striking faults, or 3) upflow along both northeasterly striking faults and the intersections with the northwest-striking faults. Our preferred model is the median (P50) resource model (Figures 30 and 49) involving ~150°C upflow along a northeast-striking normal fault that projects to the surface directly southwest of TG hole 52-2 (Figure 30).

The resource models were used in lognormal power density functions to derive power capacity estimates utilizing established methods (Cumming, 2016a, b). A lognormal probability density function for resource capacity in MWe is estimated by multiplying two lognormal power density functions: 1) interpreted resource area in km^2, and 2) power density in MW/km^2. Inputs for each of the three resource capacity models applied progressively increasing values of maximum reservoir temperatures and power densities, ranging from: 1) P90- 135°C max reservoir temperature and power density of 3 MWe/km^2; 2) P50- 150°C max reservoir temperature and power density of 6 MWe/km^2; and 3) P10- 175°C max reservoir temperature with a power density of 12 MWe/km^2. Established reservoir temperatures and power densities of developed geothermal systems in the Great Basin region, which are considered to have a relatively analogous geologic and geophysical expression to the blind system in southeastern Gabbs Valley, were used for the range of inputs (Wilmarth and Stimac, 2015) for the three models. The power density function was applied for the interpreted resource area from the modeled 125°C isothermal temperature at a 750 m elevation depth-slice in each of the models (Figure 30), which is considered to be a structurally favorable, drill-target production zone.

Results yield power capacity estimates of 6 MWe for the P-90 (conservative) model, 16 MWe for the P-50 (median) model, and 38 MWe for the P-10 (optimistic) model. These estimates are reasonable and consistent with the majority of geothermal power plants operating in the Great Basin (Muntean et al., 2018). Future data inputs, particularly additional well data, can refine estimates and provide advanced capacity boundaries for the geothermal energy resource.

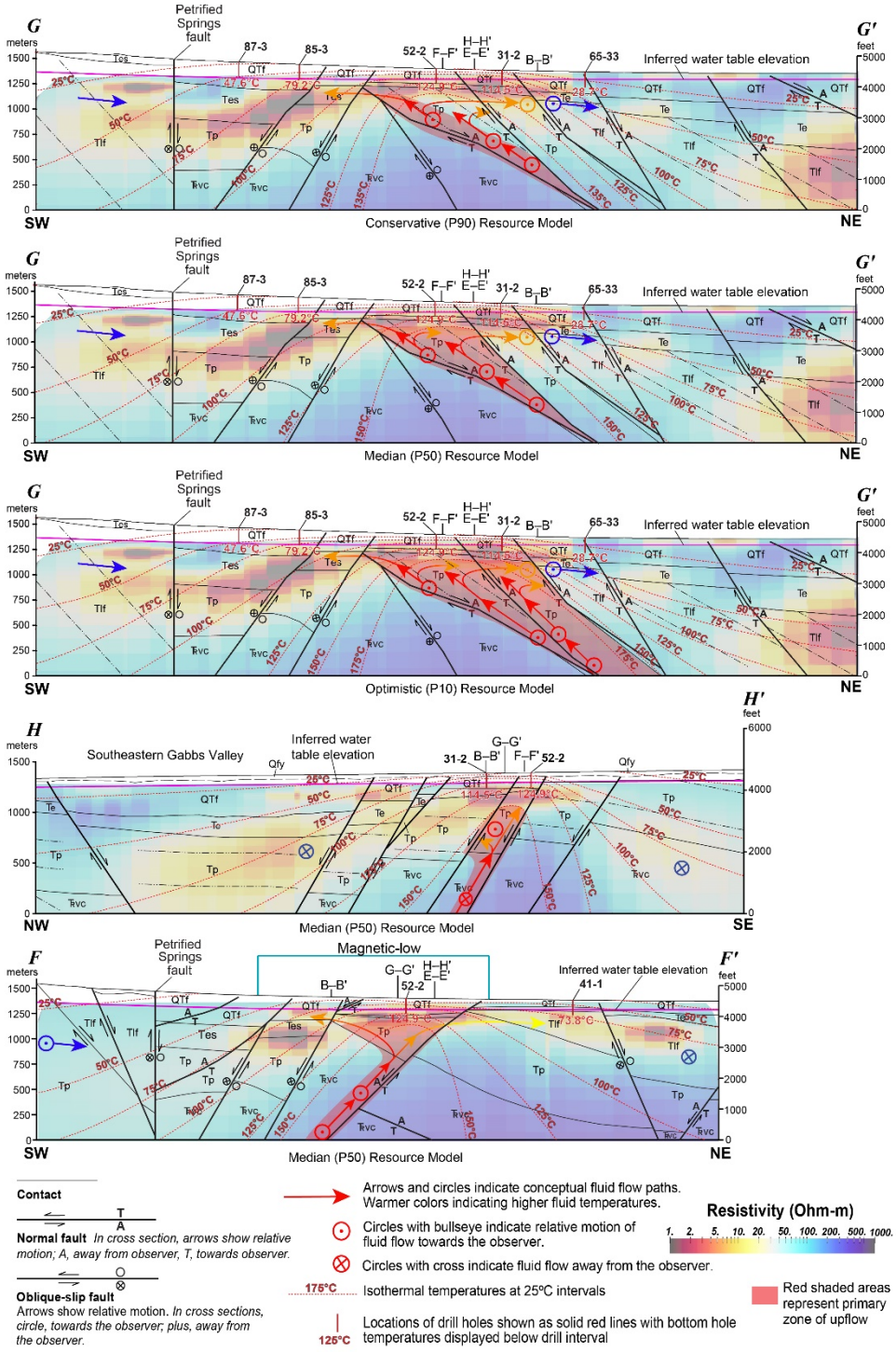

Figure 49. Resource conceptual models (from Craig et al., in prep). Cross section locations shown in Figure 30 (sections not to scale with map). Cross sections display faults and contacts as black lines. The red shaded area is spatial extent of primary zone of upflow. Locations of drill holes are solid red lines. Isothermal temperatures at 25ºC intervals shown as dashed red lines. Inferred water table elevation is pink line, and potential flow paths of hydrothermal fluids are shown as arrows and circles (bullseye indicates relative flow toward observer and cross-circle indicates flow away from observer) overlain on MT data. Warmer colors indicate lower-resistivity vales (Ohm-m) in MT data.

Task 33.0. Final Reporting and Project Review: The purpose of this task is to synthesize results into a final report. All databases, publications, and maps will be uploaded to the NGDS/GDR. A key component of the project review are sections that assess the play fairway analysis and discuss differences in the findings between Phase 1 and Phase 2, including specific modifications to the play fairway analysis made to accommodate the more detailed and localized investigations.

Milestone 33.1 involving creating a final report with illustrations and databases (Table 3) has been satisfied with submittal of this report. Required reporting during the course of this project, including all quarterly narratives and financial summaries, were also completed.

Moreover, the results of this project were presented to the geothermal and scientific community through publication of 18 papers and 10 abstracts. In addition, more than 45 presentations describing the results of this study were given at major conferences, meetings of professional societies, state and federal agencies, and university colloquiums across the U.S. and abroad. This included three keynote addresses. At least nine media reports also resulted from this project, including interviews with California Energy Markets, Bloomberg Environment and Energy, Nevada Face the State (KTVN, Channel 2, Reno), KUNR (Reno public radio), and Outdoor Nevada (Nevada public TV). Links to these interviews are provided in the final section of this report.

CONCLUSIONS AND BROAD OUTCOMES

Geothermal play fairway analysis involves integration of geological, geophysical, and geochemical parameters indicative of geothermal activity to discover new geothermal systems, especially blind systems with no surface hot springs or steam vents. In Phase 1 (Budget Period 1) of the Nevada play fairway project, we incorporated nine parameters to develop a regional geothermal potential map of 96,000 km^2 of the Great Basin region in Nevada (Figure 1). In Phase 2 of this project, we acquired detailed geologic, geophysical, and geochemical data to analyze five particularly promising areas identified on the initial geothermal potential map produced in Phase 1. The play fairway analysis was adapted to a finer-scale to vector into favorable sites for drilling in the detailed study areas (Figures 6E, 8C, 11B, 23, 15B, 19, 20, 21, 22, and 40). More detailed geophysical and geochemical surveys and TG drilling were then conducted at two sites, southeastern Gabbs Valley and northern Granite Springs Valley, in Phase 3 of this project. Results from the TG drilling, including bottom-hole temperature of 96°C to 124°C and related geophysical anomalies (Figures 23, 24, 25, 26, and 30), suggest that blind geothermal systems may exist at both sites, thus providing initial validation of the play fairway analysis methodology.

Although play fairway analysis is easily adaptable to any region or tectonic setting and therefore has broad applicability, the individual weightings of various parameters and general algorithms employed will likely differ in each area depending on local conditions and availability and robustness of datasets. Challenges common to geothermal play fairway analysis include estimating 'weights of influence' for features, incomplete datasets, lack of key datasets, and limited numbers of training sites (Faulds et al., 2020a). Machine learning techniques (Goodfellow et al., 2018) and value of information analysis (Trainor-Guitton et al., 2014) hold significant promise in resolving some of these challenges while also facilitating identification of subtle links between some of the datasets that may indicate hidden geothermal systems.

Specific lessons learned in the course of this project include: 1) initially identified sites commonly include multiple favorable structural settings at a finer scale; 2) promising sites in Cenozoic basins generally cannot be recognized without detailed geophysical surveys; and 3) play fairway analysis should be refined as the exploration program vectors into the most promising sites and finer-scale data are acquired. This requires revision of initial predictions of permeability potential to reflect more detailed analyses and preparation of higher-resolution play fairway maps prior to selecting sites for drilling. In addition, we advise flexibility in terms of the timing, budgeting, and interpreting results in the drilling phase of such a project. As well known in industry, there are many factors that can affect drilling operations, including permitting, weather, equipment repairs, and the inevitable challenges in building complex 3D conceptual

models. Simply managing such operations is a large time commitment that should be factored into similar future projects.

Although final validation of the inferred hidden geothermal systems identified in this study (e.g., southeastern Gabbs Valley and northern Granite Springs Valley) awaits deeper drilling, this project has already significantly impacted geothermal exploration in the Great Basin region as well as assessment of geothermal resources in both the western U.S. and elsewhere. As reported by California Energy Markets, this project helped to stimulate the largest geothermal lease sale in Nevada history in September 2019 (*https://www.newsdata.com/california_energy_markets/southwest/*). Several of the promising areas identified on our geothermal play fairway map (Figure 1) were leased for potential geothermal development. Thus, this project has resulted in broader outcomes, which are helping to kindle interest in assessment and development of geothermal resources in the Great Basin region.

REFERENCES CITED
(blue shading indicates contributions from this project)

Allis, R., J. Moore, B. Blackett, M. Gwynn, S. Kirby, and D. Sprinkel, 2011, The potential for basin-centered geothermal resources in the Great Basin: Geothermal Resources Council Transactions, v. 35, p. 683–688.

Allis, R., B. Blackett, M. Gwynn, C. Hardwick, J. Moore, C. Morgan, D. Schelling, and D.A. Sprinkel, 2012, Stratigraphic reservoirs in the Great Basin : The bridge to development of enhanced geothermal systems in the U.S.: Geothermal Resources Council Transactions, v. 36, p. 351-358.

Allis, R., and Moore, J, 2014, Can deep stratigraphic reservoirs sustain 100 MW power plants: Geothermal Resources Council Transactions, v. 38, p. 1009-1016.

Allis, R., M. Gwynn, C. Hardwich, G. Mines and J. Moore, 2015, Will stratigraphic reservoirs provide the next big increase in U.S. geothermal power generation?: Geothermal Resources Council Transactions, v. 39, p. 389-398.

Arnorsson, S., Gunnlaugsson, E., and Svavarsson, H., 1983, The chemistry of geothermal waters in Iceland. III. Chemical geothermometry in geothermal investigations: Geochimica et Cosmochimica Acta, v. 47, p. 567-577.

Bell, J.W., and Ramelli, A.R., 2007, Active faults and neotectonics at geothermal sites in the western Basin and Range: Preliminary results: GRC Transactions, v. 31, p. 375-378.

Bell, J.W., and Ramelli, A.R., 2009, Active fault controls at high-temperature geothermal sites: Prospecting for new faults: Geothermal Resources Council Transactions, v. 33, p. 425–429.

Benoit, D., 2008, The Adobe Valley thermal anomaly and geology (revised): Unpublished report, 6 p.

Blackwell, D., Wisian K, Benoit D, Gollan B., 1999, Structure of the Dixie Valley Geothermal System, a "Typical" Basin and Range Geothermal system, From Thermal and Gravity Data: Geothermal Resources Council Transactions, v. 23, p. 525-531.

Blake, K., and Davatzes, N.C., 2011, Crustal stress heterogeneity in the vicinity of Coso geothermal field, CA: Proceedings, Thirty-Fifth Workshop on Geothermal Reservoir Engineering, Stanford University. p. 914–924.

Blewitt, G., Coolbaugh, M.F., Sawatzky, D., Holt, W.E., Davis, J.L., Bennett, R.A., 2003, Targeting of potential geothermal resources in the Great Basin from regional to basin-scale relationship between geodetic strain and geological structures: Geothermal Resources Council Transactions, v. 27, p. 3-7.

Blewitt, G., Hammond, W.C., Kreemer, C., 2005, Relating geothermal resources to Great Basin tectonics using GPS: Geothermal Resources Council Transactions, v. 29, p. 331–335.

Caskey, S.J., Wesnousky, S.G, Zhang, P., and Slemmons, D.B., 1996, Surface faulting of the 1954 Fairview Peak (Ms 7.2) and Dixie Valley (Ms 6.8) earthquakes, central Nevada: Bulletin of the Seismological Society of America, v. 86, no. 3, p. 761-787.

Chave, A.D., Thomson, D.J., 2004, Bounded influence magnetotelluric response function estimation: Geophysical Journal International, v. 157, p. 988-1006.

Chovanec, Y.M., 2003, Geothermal analysis of Schellbourne, East-Central Nevada, Steptoe Valley [M.S. Thesis]: University of Texas at Arlington, 138 p.

Coolbaugh, M.F., Zehner, R., Kreemer, C., Blackwell, D., Oppliger, G., 2005, A map of geothermal potential for the Great Basin, USA: recognition of multiple geothermal environments: Geothermal Resources Council Transactions, v. 29, p. 223-228.

Coolbaugh, M.F., Raines, G.L., and Zehner, R.E., 2007, Assessment of exploration bias in data-driven predictive models and the estimation of undiscovered resources: Natural Resources Research, v. 16, no. 2, p. 199-207.

Craig, J.W., Faulds, J.E., Shevenell, L.A., and Hinz, N.H., 2017, Discovery and analysis of a potential blind geothermal system in southern Gabbs Valley, western Nevada: Geothermal Resources Council Transactions, v. 41, in press.

Craig, J.W., 2018. Discovery and Analysis of a Blind Geothermal System in Southeastern Gabbs Valley, Western Nevada, [M.S. Thesis]: University of Nevada, Reno, 110 p.

Craig, J.W., Faulds, J.E., Hinz, N.H., Earney, T.E., Schermerhorn, W.D., Glen, J.M., Peacock, J., Coolbaugh, M.F., Siler, D.L., and Deoreo, S.B., in final preparation, Discovery and analysis of a blind geothermal system in southeastern Gabbs Valley, western Nevada, USA: to be submitted to Geothermics.

Cumming, W., 2009, Geothermal resource conceptual models using surface exploration data: Proceedings: 34th Workshop on Geothermal Reservoir Engineering, Stanford University, Stanford, CA, 6 p.

Cumming, W., 2016a, Resource capacity estimation using lognormal power density from producing fields and area from resource conceptual models; advantages, pitfalls and remedies: Proceedings: 41st Workshop on Geothermal Reservoir Engineering, Stanford University, Stanford, CA, 7 p.

Cumming, W., 2016b, Resource conceptual models of volcano-hosted geothermal reservoirs for exploration well targeting and resource capacity assessment: construction, pitfalls and remedies: Geothermal Resources Council Transactions, v. 40.

Curewitz, D. and Karson, J.A., 1997, Structural settings of hydrothermal outflow: fracture permeability maintained by fault propagation and interaction: Journal of Volcanology and Geothermal Research, v. 79, p. 149-168.

Desormier, W.L., 1985, Fireball Ridge geothermal prospect, Churchill County, Nevada: Department of Energy Report, 107 p.

Doust, H., 2010, The exploration play: What do we mean by it?: American Association of Petroleum Geologists Bulletin, v. 94, p. 1657-1672.

Earney, T.E., Schermerhorn, W.D., Glen, J.M., Peacock, J., Craig, J.W., Faulds, J.E., Hinz, N.H., Siler, D.L., 2018. Geophysical Investigations of a Blind Geothermal System in Southern Gabbs Valley, Nevada. Geothermal Resources Council Transactions 42, 14.

Faulds, J.E., Coolbaugh, M., Blewitt, G., and Henry, C.D., 2004, Why is Nevada in hot water? Structural controls and tectonic model of geothermal systems in the northwestern Great Basin: Geothermal Resources Council Transactions, p. 649-654.

Faulds, J.E., Coolbaugh, M.F., Vice, G.S., and Edwards, M.L., 2006, Characterizing structural controls of geothermal fields in the northwestern Great Basin: A progress report: Geothermal Resources Council Transactions, v. 30, p. 69-76.

Faulds, J.E., and Henry, C.D., 2008, Tectonic influences on the spatial and temporal evolution of the Walker Lane: An incipient transform fault along the evolving Pacific – North American plate boundary, *in* Spencer, J.E., and Titley, S.R., eds., Circum-Pacific Tectonics, Geologic Evolution, and Ore Deposits: Tucson, Arizona Geological Society, Digest 22, p. 437-470.

Faulds, J.E., Coolbaugh, M.F., Benoit, D., Oppliger, G., Perkins, M., Moeck, I., and Drakos, P., 2010, Structural controls of geothermal activity in the northern Hot Springs Mountains, western Nevada: The tale of three geothermal systems (Brady's, Desert Perk, and Desert Queen): Geothermal Resources Council Transactions, v. 34, p. 675-683.

Faulds, J.E., Coolbaugh, M.F., Hinz, N.H., Cashman, P.H., and Kratt, C., Dering, G., Edwards, J., Mayhew, B., and McLachlan, H., 2011, Assessment of favorable structural settings of geothermal systems in the Great Basin, western USA: Geothermal Resources Council Transactions, v. 35, p. 777-784.

Faulds, J.E., Hinz, N.H., Dering, G.M., Drew, D.L., 2013, The hybrid model – the most accommodating structural setting for geothermal power generation in the Great Basin, western USA: Geothermal Resources Council Transactions, v. 37, p. 3-10.

Faulds, N.H., and Hinz, N.H., 2015, Favorable tectonic and structural settings of geothermal settings in the Great Basin Region, western USA: Proxies for discovering blind geothermal systems: Proceedings, World Geothermal Congress 2015, Melbourne, Australia, 6 p.

Faulds, J.E., Hinz, N.H., Coolbaugh, M.F., Shevenell, L.A., Siler, D.L., dePolo, C.M., Hammond, W.C., Kreemer, C., Oppliger, G., Wannamaker, P.E., Queen, J.H., and Visser, C.F., 2015a, Integrated geologic and geophysical approach for establishing geothermal play fairways and discovering blind geothermal systems in the Great Basin region, western USA: A progress report: Geothermal Resources Council Transactions, v. 39, p. 691-700.

Faulds, J.E., Hinz, N.H., Coolbaugh, M.F., Shevenell, L.A., Siler, D.L., dePolo, C.M., Hammond, W.C., Kreemer, C., Oppliger, G., Wannamaker, P.E., Queen, J.H., and Visser, C.F., 2015b, Discovering blind geothermal systems in the Great Basin region: An integrated geologic and geophysical approach for establishing geothermal play fairways: Final report submitted to the Department of Energy (DE-EE0006731), 106 p.

Faulds, J. E., Hinz, N.H., Coolbaugh, M. F., Shevenell, L. A., and Siler D. L, 2016a, The Nevada play fairway project — Phase II: Initial search for new viable geothermal systems in the Great Basin region, western USA: Geothermal Resources Council Transactions, v. 40, p. 535-540.

Faulds, J.E., Hinz, N.H., Coolbaugh, M.F., Shevenell, L.A., and Siler, D.L., 2016b, Methodologies and strategies for harnessing the vast geothermal potential of Nevada and the Great Basin region: A summary of recent studies and advances: American Association of Petroleum Geologists, Pacific Section and Rocky Mountain Section Joint Meeting, Las Vegas, Nevada, October 2-5.

Faulds, J.E., Hinz, N.H., Coolbaugh, M.F., Siler, D.L., Shevenell, L.A., Queen, J.H., dePolo, C.M., Hammond, W.C., and Kreemer, C., 2016c, Discovering geothermal systems in the Great Basin region: an integrated geologic, geochemical, and geophysical approach for establishing geothermal play fairways: Proceedings, 41st Workshop on Geothermal Reservoir Engineering, Stanford University, Stanford, CA, 15 p.

Faulds, J. E., Hinz, N.H., Coolbaugh, M. F., Shevenell, L. A., Sadowski, A.J., Shevenell, L.A., McConville, E., Craig, J., Sladek, C., and Siler D. L, 2017a, Progress report on the Nevada play fairway project: Integrated geological, geochemical, and geophysical analyses of possible new geothermal systems in the Great Basin region: Proceedings, 42nd Workshop on Geothermal Reservoir Engineering, Stanford University, Stanford, California, February 13-15, 2017, SGP-TR-212, 11 p.

Faulds, J.E., Hinz, N., Sadowski, A., McConville, E., Craig, J., Bourdeau-Hernikl, J., Shevenell, L., Coolbaugh, M., Siler, D., Hardwick, C., and Queen, J., 2017b, Discovering blind geothermal systems in the Great Basin region: An integrated geologic and geophysical approach for establishing geothermal play fairways: Final report for budget period 2 (DE-EE0006731): Department of Energy, 30 p.

Faulds, J.E., Craig, J.W., Coolbaugh, M.F., Hinz, N.H., Glen, J.M., Deoreo, S., 2018, Searching for blind geothermal systems utilizing play fairway analysis, western Nevada: Geothermal Resources Council Bulletin, v. 47, p. 34-42.

Faulds, J.E., Hinz, N.H., Coolbaugh, M.F., Ramelli, A., Glen, J.M, Ayling, B.A., Wannamaker, P.E., Deoreo, S.B., Siler, D.L., and Craig, J.W., 2019, Vectoring into potential blind geothermal systems in the Granite Springs Valley area, western Nevada: Application of the play fairway analysis at multiple scales: Proceedings 44th Workshop on Geothermal Reservoir Engineering, Stanford University, Stanford, California, SGP-TR-214, p. 74-84.

Faulds, J.E., Brown, S., Coolbaugh, M., DeAngelo, J., Queen, J.H., Treitel, S., Fehler, M., Mlawsky, E., Glen, J.M., Lindsey, C., Burns, E., Smith, C.M., Gu, C., and Ayling, B.A., 2020a, Preliminary report on applications of machine learning techniques to the Nevada geothermal play fairway analysis:

Proceedings 45th Workshop on Geothermal Reservoir Engineering Stanford University, SGP-TR-216, 6 p.

Faulds, J.E., Sadowski, A.J., Coolbaugh, M.F., and Siler, D.L., 2020b, Geothermal play fairway analysis of the Sou Hills, northern Nevada: A major Quaternary accommodation zone in the Great Basin region: Geothermal Resources Council Transactions, v. 44, p 542-556.

Ferrill, D.A., Winterle, J., Wittmeyer, G., Sims, D., Colton, S., Armstrong, A., Horowitz, A.S., Meyers, W.B., and Simons, F.F., 1999, Stressed rock strains groundwater at Yucca Mountain, Nevada: GSA Today, v. 9, p. 2–9.

Fonseca, J., 1988, The Sou Hills: A barrier to faulting in the central Nevada seismic belt: Journal of Geophysical Research, v. **93**, p. 475-489.

Forson, C., Czajkowski, J. L., Norman, D. K., Swyer, M. W., Cladouhos, T.T. and Davatzes N., 2016, Summary of phase 1 and plans for phase 2 of the Washington state geothermal play-fairway analysis: Geothermal Resources Council Transactions, v. 40, p. 541-550.

Fournier, R.O., 1977, Chemical geothermometers and mixing models for geothermal systems: Geothermics, v. 5, p. 41-50.

Fournier, R.O., 1979, A revised equation for the Na/K geothermometer: Geothermal Resources Council Transactions, v. 3, p. 221-224.

Fournier, R.O., and Truesdell, A.H., 1973, An empirical Na-K-Ca geothermometer for natural waters: Geochimica et Cosmochimica Acta, v. 37, no. 5, p. 1255-1275.

Fournier, R.O., and Potter, R.W., 1982, A revised and expanded silica (quartz) geothermometer: Geothermal Resources Council Bulletin, v. 11, no. (10), p. 3–12.

Friedrich, A.M., Lee, J., Wernicke, B.P., and Sieh, K., 2004, Geologic context of geodetic data across a Basin and Range normal fault, Crescent Valley, Nevada: Tectonics, v. 23, TC2015.

Fritz, W.H., 1968, Geologic map and sections of the southern Cherry Creek and northern Egan Ranges, White Pine County, Nevada: Nevada Bureau of Mines and Geology Map 35, scale 1:62,500.

Giggenbach, W.F., 1988, Geothermal Solute Equilibria: Derivation of Na-K-Mg-Ca Geoindicators: Geochimica et Cosmochimica Acta, v. 52, p. 2749-2765.

Goodfellow, I., Bengio, Y., and Courville, A., 2018, Deep Learning, MIT Press, e-book, http://www.deeplearningbook.org.

Gwynn, M., Allis, R., Sprinkel, D., Blackett, R., and Hardwick, C., 2014, Geothermal potential in the basins of northeastern Nevada: Geothermal Resources Council Transactions, v. 38, p. 1029-1039.

Hammond, W.C., Kreemer, C., Blewitt, G., 2009, Geodetic constraints on contemporary deformation in the Northern Walker Lane: 3, Central Nevada seismic belt postseismic relaxation: in Oldow, J.S., and Cashman, P.H., eds., Late Cenozoic Structure and Evolution of the Great Basin – Sierra Nevada Transition: Geological Society of America Special Paper 447, p.33-54, doi: 10.1130/2009.2447(03)

Hickman, S.H., Barton, C.A., Zoback, M.D., Morin, R., Sass, J.H., and Benoit, R., 1997, In-situ stress and fracture permeability along the Stillwater fault zone, Dixie Valley, Nevada: International Journal of Rock Mechanics and Mining Sciences Abstracts, v. 34, no. 3–4, Paper No. 126.

Hickman, S., Zoback, M.D., Benoit, W.R., 1998. Tectonic controls on reservoir permeability in the Dixie Valley, Nevada, geothermal field. Proceedings, Twenty-Third Workshop on Geothermal Reservoir Engineering, Stanford University. 291–298.

Hickman, S.H., and Davatzes, N.C., 2010, In-situ Stress and Fracture Characterization for Planning of an EGS Stimulation in the Desert Peak Geothermal Field, Nevada, *in* Proceedings, Thirty-Fifth Workshop on Geothermal Reservoir Engineering, Stanford University, v. 35, p. 13.

Hinz, N.H., Faulds, J.E. and Stroup, C., 2011, Stratigraphic and structural framework of the Reese River geothermal area, Lander County, Nevada: A new conceptual structural model: Geothermal Resources Council Transactions, v. 35, p. 827-832.

Hinz, N., Faulds, J., Siler, D., 2013, Developing systematic workflow from field work to quantitative 3D modeling for successful exploration of structurally controlled geothermal systems: GRC Transactions, v. 37, p. 275-280.

Hinz, N.H., Faulds, J.E., Coolbaugh, M.F., 2014, Association of fault terminations with fluid flow in the Salt Wells geothermal field, Nevada, USA: Geothermal Resources Council Transactions, v. 38, p. 3–10.

Hinz, N.H., Coolbaugh, M.F., Faulds, J.E., Siler, D.L., and Dering, G., 2015, Building the Next Generation of Regional Geothermal Potential Maps: Examples from the Great Basin Region, Western USA, *in* Proceedings of the World Geothermal Congress, 6 p.

Hinz, N.H., Faulds, J.E., and Coolbaugh, M.F., 2017, Fault-hosted geothermal resources in the Great Basin region, USA: Evolution of structural-tectonic characterization over the past four decades: Geological Society of America Abstracts with Programs, v. 49, no. 4, doi: 10.1130/abs/2017CD-293057.

Hinz, N.H., Faulds, J.E., Coolbaugh, M.F., Hardwick, C., Gwynn, M., Queen, J., and Ayling, B., 2020, Play fairway analysis of Steptoe Valley, Nevada: Integrating geology, geochemistry, geophysics, and heat flow modeling in the search for blind resources: Geothermal Resources Council Transactions, v. 44, p. 593-612.

Hose, R.K., Blake, M.C., Jr., and Smith, R.M., 1976, Geology and mineral resources of White Pine County: Nevada Bureau of Mines and Geology Bulletin 85, scale 1:250,000, 113 pages.

Hulen, J.B., 2007, Unpublished geologic, alteration, and temperature-gradient maps for the northern Fireball Ridge area, western Nevada: Ormat (internal report).

Jolie, E., Moeck, I., Faulds, J.E., 2015. Quantitative structural–geological exploration of fault-controlled geothermal systems—A case study from the Basin-and-Range Province, Nevada (USA): Geothermics v. 54, p. 54–67. https://doi.org/10.1016/j.geothermics.2014.10.003

Kelbert, A., Meqbel, N., Egbert, G.D., Kush, T., 2014, ModEM: A modular system for inversion of electromagnetic geophysical data: Computers and Geoscience, v. 66, p. 40-53.

Kirby, S.M., 2012. "Summary of Compiled Permeability with Depth Measurements for Basin Fill, Igneous, Carbonate, and Siliciclastic Rocks in the Great Basin and Adjoining Regions." Utah Geological Survey Open-File Report 602, 9 p.

Koehler, R.D., and Wesnousky, S.G., 2011, Late Pleistocene regional extension rate derived from earthquake geology of late Quaternary faults across Great Basin, Nevada between 38.5 and 40 N latitude, Geological Society of America Bulletin, v. 123, no. 3-4, p. 631–650, doi: 10.1130/B30111.1.

Kreemer, C., Hammond, W.C., Blewitt, G., Holland, A.A., and Bennett, R.A., 2012, A geodetic strain rate model for the Pacific-North American plate boundary, western USA: NBMG Map 178, scale 1:1.500,000, 1 sheet.

Lautze N.C., Thomas D., Hinz N., Ito G., Frazer N., Waller D., 2017, Play fairway analysis of geothermal resources across the state of Hawai'i: 1. Geological, geophysical, and geochemical datasets: Geothermics, v. 70, p. 376–392, doi: 10.1016/j.geothermics.2017.02.001.

McConville, E.G., 2018, Detailed analysis of geothermal potential in Crescent Valley, north-central Nevada [M.S. Thesis]: University of Nevada, Reno, 122 p.

McConville, E.G., Faulds, J.E., Coolbaugh, M.F., Shevenell, L., Siler, D.L, Bourdeau-Hernikl, J., 2017, A play fairway approach to geothermal exploration in Crescent Valley, Nevada: Geothermal Resources Council Transactions, v. 41, in press.

Moeck, I., Hinz, N., Faulds, J.E., Bell, J.W., Kell-hills, A., Louie, J., 2010. 3D Geological mapping as a new method in geothermal exploration: A case study from central Nevada. Geothermal Resources Council Transactions, v. 34, p. 807–812.

Morris, A., Ferrill, D.A., and Henderson, D.B., 1996, Slip-tendency analysis and fault reactivation: Geology, v. 24, p. 275–278.

Muntean, J.L., Davis, D.A., and Ayling, B., 2018, The Nevada mineral industry 2017: Nevada Bureau of Mines and Geology Special Publication MI-2017, 212 p.

Nordquist, J., and Delwiche, B., 2013, The McGinness Hills geothermal project: Geothermal Resources Council Transactions, v. 37, p. 57-63.

Payne, J., J. Bell, W. Calvin and K. Spinks, 2011, Active fault structure and potential high temperature geothermal systems: Lidar analysis of the Gabbs Valley, Nevada, fault system: Geothermal Resources Council Transactions, v. 35, p. 961-966.

Payne, J., 2013, Characterization of a blind geothermal prospect through LiDAR analysis and shallow temperature survey, Gabbs Valley, Nye and Mineral Co., NV [M.S. Thesis]: University of Nevada, Reno.

Richards, M., and Blackwell, D., 2002, A difficult search: Why Basin and Range systems are hard to find: Geothermal Resources Council Bulletin, v. 31, p. 143-146.

Shervais, J.S., Glen, J.M., Nielson, D., Garg, S., Dobson, P., Gasperikova, E., Sonnenthal, E., Visser, C., Liberty, L.M., DeAngelo, J., Siler, D., Varriale, J., and Evans, J.P., 2016, Geothermal play fairway analysis of the Snake River Plain: Phase 1, Proceedings, 41st Workshop on Geothermal Reservoir Engineering, Stanford University, SGP-TR-209, 7 p.

Shevenell, L., and M. Coolbaugh, 2011, A new method of evaluation of chemical geothermometers for calculating reservoir temperatures from thermal springs in Nevada: Geothermal Resources Council Transactions, v. 35, p. 657-661.

Siler, D.L., Mayhew, B., and Faulds, J.E., 2012, Three-Dimensional Geologic Characterization of Geothermal Systems: Astor Pass, Nevada, USA: Geothermal Resources Council Transactions, v. 36, p. 783–786.

Siler, D.L., Faulds, J.E., Mayhew, B., and Mcnamara, D.D., 2016a, Analysis of the favorability for geothermal fluid flow in 3D: Astor Pass geothermal prospect, Great Basin, northwestern Nevada, USA: Geothermics, v. 60, p. 1–12, doi: 10.1016/j.geothermics.2015.11.002.

Siler, D.L., Hinz, N.H., Faulds, J.E., and Queen, J., 2016b, 3D Analysis of geothermal fluid flow favorability: Brady's, Nevada, USA: The 41st Workshop on Geothermal Reservoir Engineering, Stanford University, v. 41, 10 p.

Siler, D.L., Zhanga, Y., Spycher, N.F., Dobson, P.F., McClain, J.S., Gasperikova, E., Zierenberg, R.A., Schiffman, P., Ferguson, C., Fowler, A., and Cantwell, C., 2017, Play-fairway analysis for geothermal resources and exploration risk in the Modoc Plateau region: Geothermics, v. 69, p. 15-33.

Siler, D.L., Hinz, N.H., and Faulds, J.E., 2018, Stress concentrations at structural discontinuities in active fault zones in the western United States: Implications for permeability and fluid flow in geothermal fields: Geological Society of America Bulletin, v. 130, no. 7-8, p. 1273-1288; https://doi.org/10.1130/B31729.1.

Siler, D.L., Faulds, J.E., Hinz, N.H., Dering, G.M., Edwards, J.H., Mayhew, B., 2019. Three-dimensional geologic mapping to assess geothermal potential: examples from Nevada and Oregon. Geothermal Energy 7, 2. https://doi.org/10.1186/s40517-018-0117-0

Siler, D.L., Witter, J.B., Craig, J.W., Faulds, J.E., Glen, J.M.G., Earney, T.E., Schermerhorn, W.D., Peacock, J., Fournier, D., and the Nevada Play-Fairway Team, 2020*. Using 3D gravity inversion modeling to iteratively refine 3D geologic maps: An example from Southern Gabbs Valley, geothermal field, Nevada, USA. Proceedings, World Geothermal Congress, Reykjavik, Iceland. *WGC meeting cancelled so paper may be deferred to publication in 2021.

Sladek, C., and Coolbaugh, M., 2013, Development of online map of 2 meter temperatures and methods for normalizing 2 meter temperature data for comparison and initial analysis: Geothermal Resources Council Transactions, v. 37, p. 333-336.

Spycher, N, L. Pfeiffer, S. Finsterle and E. Sonnenthal, 2016, GeoT user's guide: A computer program for multicomponent geothermometry and geochemical speciation , version 2.1: LBNL Report, Rev. 1, June 6, 2016, 42 p.

Stewart, J.H., 1988, Tectonics of the Walker Lane belt, western Great Basin: Mesozoic and Cenozoic deformation in a zone of shear, *in* Ernst, W. G., ed., Metamorphism and crustal evolution of the western United States: Prentice Hall, Englewood Cliffs, New Jersey, p. 681-713.

Trainor-Guitton, W.J., Hoversten, G.M., Ramirez, A., Roberts, J., Juliusson, E., Key, K., and Mellors, R., 2014, The value of spatial information for determining well placement : A geothermal example: Geophysics, v. 79, p. W27–W4.

Truesdell, A.H., and R.O. Fournier, 1976, Calculation of deep temperatures in geothermal systems from the chemistry of boiling spring waters of mixed origin: Proceedings of the Second United Nations symposium on the development and use of geothermal resources, p. 837-844.

Ussher, G., 2000, Understanding the resistivities observed in geothermal systems: Proceedings: World Geothermal Congress 2000, Kyushu-Tohoku, Japan, May 28-June 10, 6 p.

U.S. Department of Energy, 2019, GeoVision: Harnessing the heat beneath our feet, 218 p.

Wallace, R.E., 1984, Fault scarps formed during the earthquakes of October 2, 1915, in Pleasant Valley, Nevada, and some tectonic implications: U.S. Geological Survey Professional Paper 1274-A, 33 p.

Wannamaker, P., Maris, V., Sainsbury, J., and Iovenitti, J., 2013, Intersecting fault trends and crustal-scale fluid pathways below the Dixie Valley geothermal area, Nevada, inferred from 3D magnetotelluric surveying, Proceedings 38th Workshop on Geothermal Reservoir Engineering, SGP-TR-198, 6 p.

Wannamaker, P.E., Moore, J.N., Pankow, K.L., Simmons, S.D., Nash, G.D., Maris, V., Trow, A.J., and Hardwick, C.L., 2017, Phase II of play fairway analysis for the eastern Great Basin extensional regime, Utah: Status of Indications: Geothermal Resources Council Transactions, v. 41, 15 p.

Wannamaker, P., Faulds, J., Kennedy, B.M., Maris, V., Siler, D., Ulrich, C., and Moore, J., 2019, Integrating magnetotellurics, soil gas geochemistry, and structural analysis to identify hidden, high enthalpy, extensional geothermal systems: Proceedings 44th Workshop on Geothermal Reservoir Engineering, Stanford University, Stanford, California, SGP-TR-214, p. 191-209.

Watt, J.T., Glen, J.M.G, John, D.A., Ponce, D.A., 2007, Three-dimensional geologic model of the northern Nevada rift and the Beowawe geothermal system, north-central Nevada: Geosphere, v.3, p.667-682.

Wesnousky, S.G., Barron, A.D., Briggs, R.W., Caskey, S.J., Kumar, S., and Owen, L., 2005, Paleoseismic transect across the northern Great Basin: Journal of Geophysical Research, v. 110, B05408.

Williams, C., Reed, M., Galanis, S.P., and DeAngelo, J., 2007, The USGS National Geothermal Resource Assessment: An Update: GRC Transactions, v. 31, p. 99-104.

Williams, C.F., Reed, M.J., DeAngelo, J., and Galanis, S.P. Jr., 2009, Quantifying the undiscovered geothermal resources of the United States: Geothermal Resources Council Transactions, v. 33, p. 995-1002.

Wilmarth, M. and Stimac, J., 2015, Power density in geothermal fields: Proceedings, World Geothermal Congress, Melbourne, Australia, 7 p.

Witter, J.B., Siler, D.L., Faulds, J.E., and Hinz, N.H., 2016, 3D Geophysical inversion modelling of gravity data to test the 3D geological model of the Bradys geothermal area, Nevada, USA: Geothermal Energy, v. 4, no. 14, 21 p.

PRODUCTS FROM NEVADA PLAY FAIRWAY ANALYSIS PROJECT

Published Papers

*Faulds, J.E., and Hinz, N.H., 2015, Favorable tectonic and structural settings of geothermal systems in the Great Basin region, western USA: Proxies for discovering blind geothermal systems: Proceedings World Geothermal Congress, Melbourne, Australia, 19-25 April 2015, 6 p.

*Hinz, N.H., Coolbaugh, M.F, Faulds, J.E., Siler, D.L., and Dering, G.M., 2015, Building the next generation of regional geothermal potential maps: Examples from the Great Basin region, western USA: Proceedings, World Geothermal Congress 2015, Melbourne, Australia, 7 p.

*Siler, D.L., Faulds, J.E., and Hinz, N.H., 2015, Regional and local geothermal potential evaluation: Examples from the Great Basin, USA, Iceland, and East Africa: Proceedings, World Geothermal Congress 2015, Melbourne, Australia, 6 p.

Faulds, J.E., Hinz, N.H., Coolbaugh, M.F., Shevenell, L.A., Siler, D.L., dePolo, C.M., Hammond, W.C., Kreemer, C., Oppliger, G., Wannamaker, P.E., Queen, J.H., and Visser, C.F., 2015, Integrated geologic and geophysical approach for establishing geothermal play fairways and discovering blind geothermal systems in the Great Basin region, western USA: A progress report: Geothermal Resources Council Transactions, v. 39, p. 691-700.

Hinz, N.H., Coolbaugh, M.F., and Faulds, J.E., 2015, White Pine County Renewable Energy Feasibility Study and Resource Assessment: Nevada Bureau of Mines and Geology Report 55, 21 p.

Faulds, J. E., Hinz, N.H., Coolbaugh, M. F., Shevenell, L. A., and Siler D. L, 2016, The Nevada play fairway project — Phase II: Initial search for new viable geothermal systems in the Great Basin region, western USA: Geothermal Resources Council Transactions, v. 40, p. 535-540.

Faulds, J.E., Hinz, N.H., Coolbaugh, M.F., Siler, D.L., Shevenell, L.A., Queen, J.H., dePolo, C.M., Hammond, W.C., and Kreemer, C., 2016, Discovering geothermal systems in the Great Basin region: an integrated geologic, geochemical, and geophysical approach for establishing geothermal play fairways: Proceedings, 41st Workshop on Geothermal Reservoir Engineering, Stanford University, Stanford, CA, Feb. 22-24, 15 p.

Hinz, N.H., Coolbaugh, M., Faulds, J.E., Shevenell, L., and Stelling, P., 2016, Regional quantitative play fairway analysis: Methodology, global examples, and application for the East African Rift System: Proceedings, 6th African Rift Geothermal Conference, Addis Ababa, Ethiopia, 2nd – 4th November, 2016, 12 p.

Faulds, J.E., Hinz, N.H., Coolbaugh, M.F., Sadowski, A.J., Shevenell, L.A., McConville, E.G., Craig, J.W., Siler, D.L., Sladek, C., and Siler, D.L., 2017, Progress report on the Nevada play fairway project: Integrated geological, geochemical, and geophysical analyses of possible new geothermal systems in the Great Basin region: Proceedings, 42nd Workshop on Geothermal Reservoir Engineering, Stanford University, Stanford, CA, Feb. 13-15, SGP-TR-212, 11 p.

Faulds, J.E., Hinz, N.H., Coolbaugh, M.F., Shevenell, L.A., 2017, Discovering New Geothermal Systems in the Great Basin Region, Western USA: An Integrated Approach for Establishing Geothermal Play Fairways: Proceedings 39th New Zealand Geothermal Workshop, 21 - 25 November 2017, Rotorua, New Zealand, 7 p. [keynote paper].

Craig, J.W., Faulds, J.E., Shevenell, L. A., Hinz, N.H., 2017, Discovery and analysis of a potential blind geothermal system in southern Gabbs Valley, western Nevada: Geothermal Resources Council Transactions, v. 41, p. 2258-2264.

McConville, E.G., Faulds, J.E., Hinz, N.H, Ramelli, A.R., Coolbaugh M.F., Shevenell L., Siler, D.L., Bourdeau-Hernikl, J., 2017, A play fairway approach to geothermal exploration in Crescent Valley, Nevada: Geothermal Resources Transactions, v. 41, p. 1213-1221.

Faulds, J.E., Craig, J.W., Hinz, N.H., Coolbaugh, M.F., Glen, J.M, Earney, T.E., Schermerhorn, W.D., Peacock, J., Deoreo, S.B., and Siler, D.L., 2018, Discovery of a blind geothermal system in southern Gabbs Valley, western Nevada, through application of the play fairway analysis at multiple scales: Geothermal Resources Council Transactions, v. 42, p. 452-465.

Earney, T.E., Schermerhorn, W.D., Glen, J.M., Peacock, J., Craig, J.W., Faulds, J.E., Hinz, N.H., and Siler, D., 2018, Geophysical investigations of a potential blind geothermal system in southern Gabbs Valley, Nevada: Geothermal Resources Council Transactions, v. 42, p. 1369-1382.

Faulds, J.E., Craig, J.W., Coolbaugh, M.F., Hinz, N.H., Glen, J.M., Deoreo, S., 2018, Searching for blind geothermal systems utilizing play fairway analysis, western Nevada: Geothermal Resources Council Bulletin, v. 47, p. 34-42. [Byline or breaking news article]

Peacock, J.R., Glen, J.M.G., Ritzinger, B., Earney, T., Schermerhorn, W., Siler, D.L., Anderson, M., 2018. Geophysical Imaging of Geothermal Systems Spanning Various Geologic Settings. Geothermal Resources Council Transactions 42, 10.

Faulds, J.E., Hinz, N.H., Coolbaugh, M.F., Ramelli, A., Glen, J.M, Ayling, B.A., Wannamaker, P.E., Deoreo, S.B., Siler, D.L., and Craig, J.W., 2019, Vectoring into potential blind geothermal systems in the Granite Springs Valley area, western Nevada: Application of the play fairway analysis at multiple scales: Proceedings 44th Workshop on Geothermal Reservoir Engineering, Stanford University, Stanford, California, SGP-TR-214, p. 74-84.

Faulds, J.E., Sadowski, A.J., Coolbaugh, M.F., and Siler, D.L., 2020, Geothermal play fairway analysis of the Sou Hills, northern Nevada: A major Quaternary accommodation zone in the Great Basin region: Geothermal Resources Council Transactions, v. 44, p 542-556.

Hinz, N.H., Faulds, J.E., Coolbaugh, M.F., Hardwick, C., Gwynn, M., Queen, J., and Ayling, B., 2020, Play fairway analysis of Steptoe Valley, Nevada: Integrating geology, geochemistry, geophysics, and heat flow modeling in the search for blind resources: Geothermal Resources Council Transactions, v. 44, p. 593-612.

Siler, D.L., Witter, J.B., Craig, J.W., Faulds, J.E., Glen, J.M., Earney, T.E., Schermerhorn, W.D., Peacock, J.R., Fournier, D., and the Nevada Play-Fairway Team, 2020, Using 3D gravity inversion modeling to iteratively refine 3D geologic maps: An example from southern Gabbs Valley, NV geothermal field: Geothermal Resources Council Transactions, V. 44, p. 638-656.

Faulds, J.E., Hinz, N.H., Coolbaugh, M.F., Craig, J.W., Glen, J.M., Ayling, B.F., Sadowski, A.J., Siler, D.L, and Deoreo, S., 2021, The Nevada geothermal play fairway project: Exploring for blind geothermal systems through integrated geological, geochemical, and geophysical analyses: Proceedings World Geothermal Congress 2020, Reykjavik, Iceland, in press.

*Not directly funded by this project, but initial results and concepts from this project were incorporated into presentations.

Completed Theses

McConville, Emma G., 2018 (August), Detailed analysis of geothermal potential in Crescent Valley, north-central Nevada [M.S. Thesis]: University of Nevada, Reno, 122 p.

Craig, Jason W., 2018 (December), Discovery and analysis of a blind geothermal system in southeastern Gabbs Valley, western Nevada [M.S. Thesis]: University of Nevada, Reno, 111 p.

Abstracts

Faulds, J.E., Hinz, N.H., Siler, D.L., Coolbaugh, M.F., Dering, G., Edwards, J., Anderson, R.B., Forson, C., and Sadowski, A.J., 2015, Detailed conventional and innovative 3D geologic maps of geothermal systems in the Great Basin region, western USA: Critical cost-effective tools for geothermal exploration: Geological Society of America Abstracts with Programs, v. 47, no. 7, p. 407.

Faulds, J.E., Coolbaugh, M.F., and Hinz, N.H., 2015, Favorable structural settings of active geothermal and young epithermal systems in the Great Basin region: Implications for exploration strategies: Geological Society of Nevada 2015 Symposium Volume.

Hinz, N.H., Faulds, J.E., and Siler, D.L., 2015, Exploration of structurally controlled geothermal systems – Systematic workflow from field work to 3D modeling and drill targeting: Implications for epithermal mineral exploration: Geological Society of Nevada 2015 Symposium Volume.

Faulds, J.E., Hinz, N.H., Coolbaugh, M.F., Shevenell, L.A., and Siler, D.L., 2016, Methodologies and strategies for harnessing the vast geothermal potential of Nevada and the Great Basin region: A summary of recent studies and advances: American Association of Petroleum Geologists, Pacific Section and Rocky Mountain Section Joint Meeting, Las Vegas, Nevada, October 2-5.

Faulds, J.E., Hinz, N.H., Shevenell, L.A., Coolbaugh, M.F., Siler, D.L., and Hardwick, C., 2017, Geothermal exploration for conventional hydrothermal systems with applications to sedimentary hosted systems: Proceedings – Unlocking the Energy Elephant: A SedHeat Workshop, 2 p.

Faulds, J.E., Hinz, N.H., Coolbaugh, M.F., Shevenell, L., Sadowski, A.J., Ramelli, A.R., Siler, D.L, Craig, J.W., and McConville, E.G., 2017, The Nevada play fairway project: An integrated approach to discovering new geothermal systems in the Great Basin region: Geological Society of America Abstracts with Programs. Vol. 49, no. 6, doi: 10.1130/abs/2017AM-307875.

Faulds, J.E., Hinz, N.H., Coolbaugh, M.F., Siler, D.L., and Shevenell, L.A., 2017, Multi-faceted approach for harnessing the vast geothermal potential of Nevada and the Great Basin region, western USA: A summary of recent studies and advances, in Jónsdóttir, B. and Hersir, G.P., eds., Book of Abstracts, IMAGE (Integrated Methods for Advanced Geothermal Exploration) Final Conference – Novel Approaches for Geothermal Exploration, ÍSOR- Iceland GeoSurvey, p. 16.

Hinz, N.H., Faulds, J.E., and Coolbaugh, M.F., 2017, Fault-hosted geothermal resources in the Great Basin region, USA – Evolution of structural-tectonic characterization over the past four decades: Geological Society of America Abstracts with Programs, v. 49, no. 4, Paper No. 23-7.

Siler, D.L., Hinz, N.H., and Faulds, J.E., 2017. Permeability generation and maintenance at structural discontinuities: A perspective from geothermal fields: Geological Society of America Abstracts with Programs, v. 49, no. 6. doi: 10.1130/abs/2017AM-301051.

Faulds, J.E., Hinz, N.H., Coolbaugh, M.F., and Siler, D.L., 2019, Applications of structural geology to elucidating processes of crustal fluid flow, reducing risks in geothermal exploration, and facilitating geothermal development in the Great Basin region, Western USA: It's all about permeability: Geological Society of America Abstracts with Programs, v. 51, no. 5, ISSN 0016-7592 doi: 10.1130/abs/2019AM-341182.

Presentations

Faulds, J.E., Favorable structural settings of active geothermal systems in the Great Basin region, western USA: Implications for fluid flow, normal faulting mechanics, and geothermal and epithermal mineral exploration: Geological Society of America Annual Meeting, Vancouver, BC (October 21, 2014).

Faulds, J.E., Why is Nevada in hot water? Geologic setting responsible for Nevada's vast geothermal resources, City of Fallon and Churchill County Breakfast Colloquium, Fallon, Nevada (March 18, 2015).

Faulds, J.E., invited talk, Why is Nevada in hot water? Tectonic and structural controls on geothermal activity in extensional settings: University of California, Davis, geoscience colloquium series, Davis, CA (April 1, 2015).

Faulds, J.E., Favorable tectonic and structural settings of geothermal systems in the Great Basin region, western USA: Proxies for discovering blind geothermal systems: World Geothermal Congress, Melbourne, Australia (April 21, 2015).

Faulds, J.E., required talk, Discovering Blind Geothermal Systems in the Great Basin Region: An Integrated Geologic and Geophysical Approach for Establishing Geothermal Play Fairways: DOE peer review, Denver, Colorado (May 12, 2015).

Faulds, J.E., invited talk, Favorable structural settings of active geothermal and young epithermal systems in the Great Basin region: Implications for exploration strategies: Geological Society of Nevada Symposium, Reno, Nevada (May 18, 2015).

Faulds, J.E., invited talk, Geothermal systems: Geologic origins of a vast energy resources: Presentation for congressional briefing sponsored by American Geoscience Institute in Energy from the Earth, Energy-Land-Water Connections Speaker Series, Washington, DC (September 15, 2015).

Faulds, J.E., invited talk, Nevada is still in hot water: An optimistic view of developing vast geothermal resources in the Great Basin region: Presentation for opening plenary session at Geothermal Resources Council Meeting, Reno, Nevada (September 21, 2015).

Faulds, J.E., Integrated geologic and geophysical approach for establishing geothermal play fairways and discovering blind geothermal systems in the Great Basin region, western USA: Geothermal Resources Council Annual Meeting, Reno, NV (September 23, 2015).

Faulds, J.E., invited talk, Discovering blind geothermal systems in the Great Basin region: An Integrated geologic and geophysical approach for establishing geothermal play fairways: Final Report of DOE funded project presented to DOE panel, Denver, Colorado (October 30, 2015).

Faulds, J.E., Detailed conventional and innovative 3D geologic maps of geothermal systems in the Great Basin region, western USA: Critical cost-effective tools for geothermal exploration: Geological Society of America Annual Meeting, Baltimore, MD (November 2, 2015).

Faulds, J.E., Discovering geothermal systems in the Great Basin region: an integrated geologic, geochemical, and geophysical approach for establishing geothermal play fairways: Stanford Geothermal Workshop, Stanford, California (February 23, 2016).

Faulds, J.E., Methodologies and strategies for harnessing the vast geothermal potential of Nevada and the Great Basin region: A summary of recent studies and advances: American Association of Petroleum Geologists, Pacific Section and Rocky Mountain Section Joint Meeting, Las Vegas, Nevada (October 4, 2016).

Faulds, invited by Mridul Gautam (VPRI at UNR) to provide summary of our geothermal program to Deputy Secretary of Department of Energy (Elizabeth Sherwood-Randall), one of two groups requested from College of Science for the meeting, Reno, NV (October 12, 2016).

Faulds, J.E., The Nevada Play Fairway Project – Phase II: Initial search for new viable geothermal systems in the Great Basin region, western USA: Geothermal Resources Council Annual Meeting, Sacramento, California (October 24, 2016).

Faulds, J.E., invited talk, Geothermal energy: Opportunities and challenges – Contributions from the Nevada Bureau of Mines and Geology: Mackay Board of Directors Meeting, Reno, NV (February 10, 2017).

Faulds, J.E., Progress report on the Nevada play fairway project: Integrated geological, geochemical, and geophysical analyses of possible new geothermal systems in the Great Basin region: Stanford Geothermal Workshop, Stanford, California (February 14, 2017).

Faulds, J.E., invited talk, Progress report on the Nevada play fairway project: Department of Energy sponsored Geothermal Play Fairway Workshop, Menlo Park, California (February 16, 2017).

Faulds, J.E., invited talk, Geothermal exploration for conventional hydrothermal systems with applications to sedimentary hosted systems: NSF funded SEDHEAT Workshop: Unlocking the Energy Elephant, Salt Lake City (March 3, 2017).

Faulds, J.E., invited talk (with multiple contributors), The Nevada Play Fairway project: Integrated geologic, geochemical, and geophysical analyses of possible new geothermal systems in the Great Basin region: Department of Energy Final Report Presentation (June 16, 2017). Based on results of analyses during Phase 2 of the Nevada play fairway project. Report and presentation were than evaluated for Phase 3 funding.

Faulds, J.E., **keynote address**, Multi-faceted approach for harnessing the vast geothermal potential of Nevada and the Great Basin region, western USA: A summary of recent studies and advances: IMAGE (**I**ntegrated **M**ethods for **A**dvanced **G**eothermal **E**xploration) Final Conference – Novel Approaches for Geothermal Exploration, Akureyri, Iceland (October 4, 2017).

Craig, J.W., Faulds, J.E., Shevenell, L. A., Hinz, N.H., *Discovery and analysis of a potential blind geothermal system in southern Gabbs Valley, western Nevada*: Geothermal Resources Council Annual Meeting, Salt Lake City, Utah (October 2017).

McConville, E.G., Faulds, J.E., Hinz, N.H, Ramelli, A.R., Coolbaugh M.F., Shevenell L., Siler, D.L., Bourdeau-Hernikl, J., *A play fairway approach to geothermal exploration in Crescent Valley, Nevada*: Geothermal Resources Council Transactions, Salt Lake City, Utah (October 2017).

Faulds, J.E., invited talk, The Nevada play fairway project: An integrated approach to discovering new geothermal systems in the Great Basin region: Geological Society of America Annual Meeting, Seattle, Washington (October 25, 2017).

Faulds, J.E., invited talk, Discovering blind geothermal systems in the Great Basin region: An integrated geologic and geophysical approach for establishing geothermal play fairways: Department of Energy Peer-Review Meeting, Denver, Colorado (November 15, 2017) – Received outstanding scores in all areas for this project, including perfect scores for 2 out 4 categories.

Faulds, J.E., **keynote address**, Discovering new geothermal systems in the Great Basin region, western USA: An integrated approach for establishing geothermal play fairways: 39th New Zealand Geothermal Workshop, Rotorua, New Zealand (November 23, 2017).

Faulds, J.E., invited talk, *Methodologies and strategies for harnessing the vast geothermal potential of the Great Basin region, western USA: A summary of recent studies and advances:* University of Canterbury Colloquium Series, Christchurch, New Zealand, May 14, 2018.

Faulds, J.E., invited talk, *Potential applications of play fairway analysis methodology to the Ngakuru graben, New Zealand*: GNS Science, Lower Hutt Office, New Zealand, May 22, 2018.

Faulds, J.E., invited talk, *Methodologies and strategies for harnessing the vast geothermal potential of the Great Basin region, western USA: A summary of recent studies and advances*: GNS Science, Lower Hutt Office, New Zealand, May 23, 2018.

Faulds, J.E., invited talk, *Why is Nevada in hot water? Tectonic controls on geothermal activity and strategies for harnessing the vast geothermal potential of the Great Basin region*: University of Wisconsin, Eau Claire, Geoscience Colloquium, September 21, 2018.

Faulds, J.E., invited talk, *Case study, Fallon FORGE project, Nevada* – Presentation in workshop entitled *Evolution of geothermal resources models from surface exploration to field development and reservoir management* (organized by Dr. Jeff Witter) as part of the Geothermal Resources Council Annual Meeting, Reno, October 12, 2018.

Faulds, J.E., *Discovery of a Blind Geothermal System in Southern Gabbs Valley, Western Nevada, through Application of Play Fairway Analysis at Multiple Scales*: Geothermal Resources Council Annual Meeting, Reno, October 17, 2018.

Faulds, J.E., *Vectoring into potential blind geothermal systems in the Granite Springs Valley area, western Nevada: Applications of the play fairway analysis at multiple scales*: Stanford Geothermal Workshop, Stanford, California, February 12, 2019.

Faulds, J.E., invited talk, *Overview of the geothermal play fairway project*: Nevada Governor's Office of Energy, Carson City, February 14, 2019.

Faulds, J.E., invited talk, *Geothermal journeys through New Zealand and Nevada: Similarities and differences in geothermal activity between magmatic and non-magmatic rifts:* University of Nevada, Las Vegas, Geoscience Colloquium Series, Las Vegas, March 13, 2019.

Faulds, J.E., invited talk, *Why is Nevada in Hot Water? Tectonic Controls on Geothermal Activity and Strategies for Harnessing the Geothermal Energy in the Great Basin Region:* University of Wisconsin, Milwaukee, Geoscience Colloquium Series, Milwaukee, April 11, 2019.

Faulds, J.E., invited talk, *Geothermal Potential in the Fallon Range Training Complex (FRTC) Land Withdrawal Areas, Nevada*: Nevada Governor's Office of Energy, Carson City, April 26, 2019.

Faulds, J.E., *The Nevada play fairway project: Lessons learned from integrated geological, geochemical, and geophysical analyses of possible new geothermal systems in the Great Basin region*: Workshop for SegemAR (Argentina Geological Survey) for capacity building on geothermal play fairway analysis, Reno, May 8, 2019.

Faulds, J.E., invited talk, *Methodologies and Strategies for Harnessing the Vast Geothermal Potential of the Great Basin Region, Western USA: A Summary of Recent Studies and Advances*: GFZ Symposium honoring the retirement of Ernst Huenges, Potsdam, Germany, August 20, 2019. Ernst has been the

Director of the Geothermal Division at GFZ since its inception in the early 1990s. I was the U.S. representative chosen to speak at this symposium.

Faulds, J.E., invited talk, *Applications of Structural Geology to Elucidating Processes of Crustal Fluid Flow, Reducing Risks in Geothermal Exploration, and Facilitating Geothermal Development in the Great Basin region, Western USA: It's All about Permeability*: Geological Society of America Annual Meeting, Phoenix, Arizona, September 23, 2019.

Faulds, J.E., invited talk, Nevada is in more hot water: *Technological advances for characterization and development of geothermal systems in the Great Basin region, western U.S.*: Talk given as part of duties for serving on panel on "*Characterization and Management of the Subsurface*" for National Academy of Sciences Committee on Earth Resources, October 8, 2019, Washington, DC.

Faulds, J.E., invited talk (**keynote address**), *Refining exploration strategies for geothermal systems in extensional to transtensional settings: Lessons learned from the Great Basin region, western USA*: Keynote address for Montana Mining and Mineral Symposium, Butte, Montana, October 10, 2019.

Faulds, J.E., *Favorable structural settings in geothermal systems with analogues from extensional and volcanic terranes*: INGEMMET (Peruvian Geological Survey) play fairway analysis project for Department of State grant, Lima, Peru, November 19, 2019.

Faulds, J.E., invited talk, *Favorable structural settings and play fairway analysis of geothermal systems in extensional terranes*: On Behalf of the U.S. Department of Interior, International Technical Assistance Program: Talk given to educate Croatian Hydrocarbon Agency on methods of geothermal assessment and exploration, January 29, 2020, Zagreb, Croatia.

Faulds, J.E., invited talk, *The Nevada Play Fairway Project: Opportunities, Challenges, and Lessons Learned:* Workshop organized by National Renewable Energy Laboratory, Stanford, CA, February 13, 2020.

Faulds, J.E., invited talk, *Geothermal play fairway analysis of the Sou Hills, northern Nevada: A major Quaternary accommodation zone in the Great Basin region*: Geothermal Resources Council Annual Meeting (virtual), Reno, October 8, 2020.

Hinz, N.H., Faulds, J.E., and others, *Play fairway analysis of Steptoe Valley, Nevada: Integrating geology, geochemistry, geophysics, and heat flow modeling in the search for blind resources*: Geothermal Resources Council Annual Meeting (virtual), Reno, October 8, 2020.

Faulds, J.E., invited talk, *Favorable Structural Settings & Exploration Strategies for Geothermal Systems in Rift Basins*: Rifts and Rifted Margins Online Seminar – European Union (virtual), October 19, 2020.

Faulds, J.E., invited talk, *Structural and Geophysical Datasets Critical for Geothermal Exploration and Play Fairway Analysis:* Colombian geothermal training virtual workshop for capacity building in developing nations, Reno, November 12, 2020.

Media Reports

Outdoor Nevada TV Show (PBS): Faulds – Filming and interviews at Gerlach Hot Springs and Fly Ranch geyser for segment on geothermal activity for the *Outdoor Nevada* show (April 30, 2015; show aired in March 2016).

KUNR (Reno public radio station): Faulds – Interview on with UNR Provost Kevin Carman and KUNR general manager, David Stipech, describing NBMG's overall mission, as well as our geothermal research program (February 18, 2016). Interview aired in early March.

Nevada Today article: Article describing the Nevada Play Fairway project (Phase 2 progress and Phase 3 award) was released in August 2017 by Nevada Today, the UNR online publication. https://nbmg.wordpress.com/2017/08/28/drilling-to-begin-in-universitys-great-basin-geothermal-exploration-project/.

Nevada Today article: Article entitled *Nevada in More Hot Water: Geothermal Industry Gets a Boost with Discoveries of 'Blind Systems*' released in Nevada Today, which is the online news outlet for the University of Nevada, Reno. https://www.unr.edu/nevada-today/news/2019/geothermal-success (May 21, 2019) – Success of our geothermal play fairway project was highlighted in this article.

Face the State TV Interview: Interviewed by KTVN, Channel 2, in Reno for segment of Face the State discussing geothermal potential in Nevada: https://www.ktvn.com/clip/14834377/face-the-state-geothermal-energy-in-nevada (May 29, 2019).

Bloomberg Interview: Interviewed by Bloomberg Environment and Energy on our successful geothermal play fairway project and Nevada renewable energy policies (July 2019)**:** https://news.bloomberglaw.com/environment-and-energy/earths-heat-gives-states-another-option-for-clean-energy-goals

California Energy Markets: Article entitled "*Biggest-Ever BLM Geothermal Lease Sale Reaps $638,000 in Nevada"* by Abigail Sawyer, California Energy Markets; September 20, 2019; No. 1557; *https://www.newsdata.com/california_energy_markets/southwest/*. Abigail Sawyer interviewed Jim Faulds for this news story. Summary: "Recent research on geothermal potential in Nevada, improved technology, and increasing interest in carbon-free and renewable energy resources is driving geothermal interest in the state, experts say. Geothermal lease sales continue in the largest-ever offering of parcels on federal lands following a Sept. 17 auction that brought in nearly $638,000 in bids in the state" (September 20, 2019).

Mineral Monday with Garrett Barmore, UNR Keck Museum, Geothermal Energy in Nevada: Video at Steamboat Hot Springs describing geothermal energy in Nevada with John Akerley of Ormat. February 28, 2020, https://vimeo.com/showcase/4949353/video/394804446.

Bloomberg Hello World TV Interview about the Walker Lane fault system: I explain the Walker Lane fault system and resulting geothermal resources in the first part of this Bloomberg TV film. Film is entitled "*A Tesla Co-Founder's Big Battery Fix, and the Fault Cleaving Off California*"**.** Bloomberg describes it as: "Hello World's Ashlee Vance masks up, hops in an RV and heads out to the Nevada desert, where a geologist explains the wonders and horrors of a little-known fault that could push California out to sea. Vance then hangs out at the compound of a Tesla co-founder who has big plans for the world's batteries." Filming was carried out on September 21, 2020, and it was released November 12, 2020. https://www.bloomberg.com/news/videos/2020-11-12/a-tesla-co-founder-s-big-battery-fix-and-the-fault-cleaving-off-california-video